

hep-ph/9602316
CPTH-S422.1295
CRETE-96-13
UFIFT-HEP-96-5
Revised June 1996

THE QUANTUM GRAVITATIONAL BACK-REACTION ON INFLATION

N. C. Tsamis*

*Centre de Physique Théorique, Ecole Polytechnique
Palaiseau 91128, FRANCE*

and

*Theory Group, FO.R.T.H.
Heraklion, Crete 71110, GREECE*

and

R. P. Woodard†

*Department of Physics, University of Florida
Gainesville, FL 32611, USA*

ABSTRACT

We describe our recent calculation of two-loop corrections to the expansion rate of an initially inflating universe on the manifold $T^3 \times \mathfrak{R}$. If correct, our result proves that quantum gravitational effects slow the rate of inflation by an amount which becomes non-perturbatively large at late times. In a preliminary discussion of basic issues we show that the expansion rate is a gauge invariant, and that our ultraviolet regulator does not introduce spurious time dependence. We also derive a sharp bound on the maximum strength of higher loop effects.

* e-mail: tsamis@iesl.forth.gr and tsamis@orphee.polytechnique.fr

† e-mail: woodard@phys.ufl.edu

1. Introduction

The purpose of this paper is to discuss the consistency, methodology and accuracy of a very long calculation in perturbative quantum gravity. Although such an exposition is necessary if the result is to win acceptance, we should best begin by explaining the motivation. This labor was undertaken to check the suggestion [1,2] that corrections from the infrared of quantum gravity may extinguish inflation without the need for a special inflaton field. It will be seen that this is also a proposal for solving the problem of the cosmological constant. In our scheme the cosmological constant is not unnaturally small, it only appears so today on account of screening by infrared effects in quantum gravity. Inflation begins in Hubble-sized patches of the early universe over which the local temperature has fallen enough for the cosmological constant to dominate the stress-energy. After a few e-foldings the temperature of such a patch is sufficiently low to permit long range correlations, and the infrared screening effect begins to build up. This build-up requires a long time because gravitational interactions are naturally weak; they can only become significant through causal and coherent superposition over the past lightcone. Effective screening is therefore delayed until an enormous invariant volume has developed within the past lightcone of the observation point to the onset of inflation. This is why inflation lasts long enough to explain the homogeneity and isotropy of the observed universe.

Note that no fine tuning is necessary for our scheme, nor do we require new matter fields or even new gravitational interactions. Of the phenomenologically viable quanta, our mechanism is unique to gravitons. The other known particles are either massive — which precludes coherent superposition — or else they possess conformal invariance on the classical level — which means they cannot exploit the enormous invariant volume in the past lightcone of a conformally flat, inflating universe.

Note also that causality, and the physically motivated initial condition of coherent inflation over a finite spatial region, preclude sensitivity to global issues such as whether

or not the full de Sitter manifold is used. For convenience we worked on the manifold $T^3 \times \mathfrak{R}$. What we computed is the expectation value of the invariant element in the presence of a homogeneous and isotropic state which is initially free de Sitter vacuum:

$$\langle 0 | g_{\mu\nu}(t, \vec{x}) dx^\mu dx^\nu | 0 \rangle = -dt^2 + a^2(t) d\vec{x} \cdot d\vec{x} . \quad (1.1)$$

Inflation redshifts the temperature to zero so rapidly that we simply used zero temperature quantum field theory. We were able to use the Lagrangian of conventional general relativity:

$$\mathcal{L} = \frac{1}{16\pi G} (R - 2\Lambda) \sqrt{-g} , \quad (1.2)$$

because our infrared mechanism is insensitive to the still unknown ultraviolet sector of quantum gravity. We assumed only that the scale of inflation $M \sim (\Lambda/G)^{1/4}$ is at least a few orders of magnitude below the Planck mass $M_{\text{Pl}} \sim G^{-(1/2)}$:

$$M \lesssim 10^{-3} M_{\text{Pl}} . \quad (1.3)$$

In this case ultraviolet modes should have plenty of time to reach their natural equilibria as they redshift down to scales at which the dynamics is described by quantum general relativity. Our mechanism can be shown to derive from modes whose physical wavelength is about the Hubble radius at the time that they contribute most strongly. It is also worth pointing out that our mechanism is an inherently quantum mechanical effect, deriving ultimately from the gravitational interaction between the zero point motions of the various modes. It in no way conflicts with the classical and semi-classical stability of locally de Sitter backgrounds [3].

We inferred the physical rate of expansion from the effective Hubble parameter:

$$H_{\text{eff}}(t) \equiv \frac{d}{dt} \ln(a) . \quad (1.4)$$

The first secular effect occurs at two loops and has the form:

$$H_{\text{eff}}(t) = H \left\{ 1 - \left(\frac{\kappa H}{4\pi} \right)^4 \left[\frac{1}{6} (Ht)^2 + (\text{subdominant}) \right] + O(\kappa^6) \right\} , \quad (1.5)$$

where $\kappa^2 \equiv 16\pi G$ is the usual loop counting parameter of quantum gravity and $3H^2 \equiv \Lambda$ is the bare Hubble constant. We were also able to show that the dominant contribution at ℓ loops has the form:

$$-\# (\kappa H)^{2\ell} (Ht)^\ell . \quad (1.6)$$

This permits the following estimate of the number of e-foldings needed for the extinction of inflation:

$$N \equiv Ht \sim (\kappa H)^{-2} \gtrsim 10^{12} . \quad (1.7)$$

Of course perturbation theory is no longer reliable when quantum corrections become of order one so the valid conclusion is that quantum gravitational effects slow the rate of inflation by an amount which becomes non-perturbatively large at late times.

This completes our discussion of why we undertook the project and what we got. A more complete discussion of the physical consequences can be found elsewhere [4]. The remainder of this paper is devoted to an explanation of how we obtained the result and why we believe it is accurate. Section 2 deals with basic issues of the formalism. Crucial points here are the distinction between “in”-“out” matrix elements and expectation values, the physical significance of our ultraviolet regularization, the demonstration that $H_{\text{eff}}(t)$ is independent of the choice of gauge, the reason why infrared logarithms are almost inevitable, and a derivation of our bound (1.6) for the dominant corrections at ℓ loops. Sections 3 and 4 deal with our specific process. Section 3 is devoted to the class of diagrams which involve only 3-point vertices, while Section 4 describes the dominant diagram which has a 4-point vertex and a 3-point vertex. Section 5 assembles the final result and discusses the many accuracy checks. We close the section, and the paper, with a brief consideration of the issues pertaining to the case of negative Λ .

2. Basic Issues

2.1 The Apparatus of Perturbation Theory.

We take the onset of inflation to be $t = 0$, and we work perturbatively around the classical background:

$$a_{\text{class}}(t) = \exp(Ht) . \quad (2.1)$$

It is simplest to perform the calculation in conformally flat coordinates, for which the invariant element of the background is:

$$-dt^2 + a_{\text{class}}^2(t) d\vec{x} \cdot d\vec{x} = \Omega^2(-du^2 + d\vec{x} \cdot d\vec{x}) , \quad (2.2a)$$

$$\Omega \equiv (Hu)^{-1} = \exp(Ht) . \quad (2.2b)$$

Note the temporal inversion and the fact that the onset of inflation at $t = 0$ corresponds to $u = H^{-1}$. Since $t \rightarrow \infty$ corresponds to $u \rightarrow 0^+$, and since the spatial coordinates of T^3 fall within the region, $-\frac{1}{2}H^{-1} < x^i \leq \frac{1}{2}H^{-1}$, the range of conformal coordinates is rather small. This is why a conformally invariant field — whose dynamics are locally the same as in flat space, except for ultraviolet regularization — cannot induce a big infrared effect.

Perturbation theory is organized most conveniently in terms of a “pseudo-graviton” field, $\psi_{\mu\nu}$, obtained by conformally re-scaling the metric:

$$g_{\mu\nu} \equiv \Omega^2 \tilde{g}_{\mu\nu} \equiv \Omega^2 (\eta_{\mu\nu} + \kappa\psi_{\mu\nu}) . \quad (2.3)$$

As usual, pseudo-graviton indices are raised and lowered with the Lorentz metric, and the loop counting parameter is $\kappa^2 \equiv 16\pi G$. After some judicious partial integrations the invariant part of the bare Lagrangian takes the following form [5]:

$$\begin{aligned} \mathcal{L}_{\text{inv}} = & \sqrt{-\tilde{g}} \tilde{g}^{\alpha\beta} \tilde{g}^{\rho\sigma} \tilde{g}^{\mu\nu} \Omega^2 \left[\frac{1}{2}\psi_{\alpha\rho,\mu} \psi_{\nu\sigma,\beta} - \frac{1}{2}\psi_{\alpha\beta,\rho} \psi_{\sigma\mu,\nu} + \frac{1}{4}\psi_{\alpha\beta,\rho} \psi_{\mu\nu,\sigma} \right. \\ & \left. - \frac{1}{4}\psi_{\alpha\rho,\mu} \psi_{\beta\sigma,\nu} \right] - \frac{1}{2}\sqrt{-\tilde{g}} \tilde{g}^{\rho\sigma} \tilde{g}^{\mu\nu} (\Omega^2)_{,\alpha} \psi_{\rho\sigma,\mu} \psi_{\nu}^{\alpha} . \end{aligned} \quad (2.4)$$

Gauge fixing is accomplished through the addition of $-\frac{1}{2}\eta^{\mu\nu}F_\mu F_\nu$, where [5]:

$$F_\mu \equiv \Omega \left(\psi_{\mu,\alpha}^\alpha - \frac{1}{2}\psi_{\alpha,\mu}^\alpha + 2\psi_\mu^\alpha (\ln \Omega)_{,\alpha} \right) . \quad (2.5)$$

The associated ghost Lagrangian is [5]:

$$\begin{aligned} \mathcal{L}_{\text{ghost}} = & -\Omega^2 \bar{\omega}^{\mu,\nu} \left[\tilde{g}_{\rho\mu} \partial_\nu + \tilde{g}_{\rho\nu} \partial_\mu + \tilde{g}_{\mu\nu,\rho} + 2\tilde{g}_{\mu\nu} (\ln \Omega)_{,\rho} \right] \omega^\rho \\ & + \left(\Omega^2 \bar{\omega}^\mu \right)_{,\mu} \eta^{\rho\sigma} \left[\tilde{g}_{\nu\rho} \partial_\sigma + \frac{1}{2}\tilde{g}_{\rho\sigma,\nu} + \tilde{g}_{\rho\sigma} (\ln \Omega)_{,\nu} \right] \omega^\nu . \end{aligned} \quad (2.6)$$

In our gauge the pseudo-graviton kinetic operator has the form:

$$D_{\mu\nu}{}^{\rho\sigma} \equiv \left[\frac{1}{2}\bar{\delta}_\mu^{(\rho} \bar{\delta}_\nu^{\sigma)} - \frac{1}{4}\eta_{\mu\nu} \eta^{\rho\sigma} - \frac{1}{2}t_\mu t_\nu t^\rho t^\sigma \right] D_A - t_{(\mu} \bar{\delta}_{\nu)}^{(\rho} t^{\sigma)} D_B + t_\mu t_\nu t^\rho t^\sigma D_C , \quad (2.7)$$

where parenthesized indices are symmetrized. Two notational conventions reflect the fact that the 0 direction is special. First, we define t_μ as:

$$t_\mu \equiv \eta_{\mu 0} = -\delta_\mu^0 . \quad (2.8a)$$

(Recall from (1.1) that our metric is spacelike.) Second, we define barred tensors to have their natural zero components nulled, for example:

$$\bar{\delta}_\nu^\mu \equiv \delta_\nu^\mu - \delta_0^\mu \delta_\nu^0 = \delta_\nu^\mu + t_\nu t^\mu . \quad (2.8b)$$

Note also that $D_A \equiv \Omega(\partial^2 + \frac{2}{u^2})\Omega$ is the kinetic operator for a massless, minimally coupled scalar and $D_B = D_C \equiv \Omega \partial^2 \Omega$ is the kinetic operator for a conformally coupled scalar.

The zeroth order action results in the following free field expansion [6]:

$$\psi_{\mu\nu}(u, \vec{x}) = \left(\begin{array}{c} \text{Zero} \\ \text{Modes} \end{array} \right) + H^3 \sum_{\lambda, \vec{k} \neq 0} \left\{ \Psi_{\mu\nu}(u, \vec{x}; \vec{k}, \lambda) a(\vec{k}, \lambda) + \Psi_{\mu\nu}^*(u, \vec{x}; \vec{k}, \lambda) a^\dagger(\vec{k}, \lambda) \right\} . \quad (2.9)$$

The spatial polarizations consist of ‘‘A’’ modes:

$$\Psi_{\mu\nu}(u, \vec{x}; \vec{k}, \lambda) = \frac{Hu}{\sqrt{2k}} \left(1 + \frac{i}{ku} \right) \exp \left[ik \left(u - \frac{1}{H} \right) + i\vec{k} \cdot \vec{x} \right] \epsilon_{\mu\nu}(\vec{k}, \lambda) \quad ; \quad \forall \lambda \in A \quad (2.10a)$$

while the space-time and purely temporal polarizations are associated, respectively, with “B” and “C” modes:

$$\Psi_{\mu\nu}\left(u, \vec{x}; \vec{k}, \lambda\right) = \frac{Hu}{\sqrt{2k}} \exp\left[ik\left(u - \frac{1}{H}\right) + i\vec{k} \cdot \vec{x}\right] \epsilon_{\mu\nu}(\vec{k}, \lambda) \quad ; \quad \forall \lambda \in B, C \quad (2.10b)$$

In LSZ reduction one would integrate against and contract into $\Psi_{\mu\nu}(u, \vec{x}; \vec{k}, \lambda)$ to insert an “in”-coming graviton of momentum \vec{k} and polarization λ ; the conjugate would be used to extract an “out”-going graviton with the same quantum numbers. The zero modes evolve as free particles with time dependences 1 and u^3 for the A modes, and u and u^2 for the B and C modes. Since causality decouples the zero modes shortly after the onset of inflation, they play no role in screening and we shall not trouble with them further.

We define $|0\rangle$ as the Heisenberg state annihilated by $a(\vec{k}, \lambda)$ — and the analogous ghost operators — at the onset of inflation. We can use this condition and expansion (2.9) to express the free pseudo-graviton propagator as a mode sum [7]:

$$i\left[{}_{\mu\nu}\Delta_{\rho\sigma}\right](x; x') \equiv \left\langle 0 \left| T \left\{ \psi_{\mu\nu}(x) \psi_{\rho\sigma}(x') \right\} \right| 0 \right\rangle_{\text{free}} \quad (2.11a)$$

$$= H^3 \sum_{\lambda, \vec{k} \neq 0} \left\{ \theta(u' - u) \Psi_{\mu\nu} \Psi'_{\rho\sigma*} + \theta(u - u') \Psi_{\mu\nu}^* \Psi'_{\rho\sigma} \right\} e^{-\epsilon \|\vec{k}\|} . \quad (2.11b)$$

Note that the convergence factor $e^{-\epsilon \|\vec{k}\|}$ serves as an ultraviolet mode cutoff. Although the resulting regularization is very convenient for this calculation, its failure to respect general coordinate invariance necessitates the use of non-invariant counterterms. These are analogous to the photon mass which must be added to QED when using a momentum cutoff. Just as in QED, these non-invariant counterterms do not affect long distance phenomena.

Because the propagator is only needed for small conformal coordinate separations, $\Delta x \equiv \|\vec{x}' - \vec{x}\|$ and $\Delta u \equiv u' - u$, the sum over momenta is well approximated as an integral whose lower limit is the momentum $k = H$ of the longest wavelength. When this

is done the pseudo-graviton propagator becomes [6]:

$$\int_H \frac{d^3k}{(2\pi)^3} \left\{ \frac{H^2 u u'}{2k} \exp\left[-ik|\Delta u| + i\vec{k} \cdot (\vec{x}' - \vec{x}) - \epsilon k\right] \left[2\delta_\mu^{(\rho} \delta_\nu^{\sigma)} - \eta_{\mu\nu} \eta^{\rho\sigma}\right] \right. \\ \left. + \frac{H^2(1 + ik|\Delta u|)}{2k^3} \exp\left[-ik|\Delta u| + i\vec{k} \cdot (\vec{x}' - \vec{x}) - \epsilon k\right] \left[2\bar{\delta}_\mu^{(\rho} \bar{\delta}_\nu^{\sigma)} - 2\bar{\eta}_{\mu\nu} \bar{\eta}^{\rho\sigma}\right] \right\} \quad (2.12a)$$

so that:

$$i\left[\mu\nu\Delta^{\rho\sigma}\right](x; x') \approx \frac{H^2}{8\pi^2} \left\{ \frac{2u'u}{\Delta x^2 - \Delta u^2 + 2i\epsilon|\Delta u| + \epsilon^2} \left[2\delta_\mu^{(\rho} \delta_\nu^{\sigma)} - \eta_{\mu\nu} \eta^{\rho\sigma}\right] \right. \\ \left. - \ln\left[H^2\left(\Delta x^2 - \Delta u^2 + 2i\epsilon|\Delta u| + \epsilon^2\right)\right] \left[2\bar{\delta}_\mu^{(\rho} \bar{\delta}_\nu^{\sigma)} - 2\bar{\eta}_{\mu\nu} \bar{\eta}^{\rho\sigma}\right] \right\} \quad (2.12b)$$

The same approximation gives the following result for the ghost propagator:

$$i\left[\mu\Delta_\nu\right](x; x') \approx \frac{H^2}{8\pi^2} \left\{ \frac{2u'u}{\Delta x^2 - \Delta u^2 + 2i\epsilon|\Delta u| + \epsilon^2} \eta_{\mu\nu} \right. \\ \left. - \ln\left[H^2\left(\Delta x^2 - \Delta u^2 + 2i\epsilon|\Delta u| + \epsilon^2\right)\right] \bar{\eta}_{\mu\nu} \right\} . \quad (2.13)$$

The decoupling between tensor indices and the functional dependence upon spacetime — and the simplicity of each — greatly facilitates calculations. It is convenient to identify as the “normal” and “logarithmic” propagator functions as $i\Delta_N$ and $i\Delta_L$ respectively:

$$i\Delta_N(x, x') \equiv \frac{H^2}{8\pi^2} \frac{2uu'}{\Delta x^2 - \Delta u^2 + 2i\epsilon|\Delta u| + \epsilon^2} , \quad (2.14a)$$

$$i\Delta_L(x, x') \equiv \frac{H^2}{8\pi^2} \ln\left[H^2\left(\Delta x^2 - \Delta u^2 + 2i\epsilon|\Delta u| + \epsilon^2\right)\right] . \quad (2.14b)$$

In this notation we can write the pseudo-graviton and ghost propagators as:

$$i\left[\mu\nu\Delta^{\rho\sigma}\right](x; x') = i\Delta_N(x; x') \left[2\delta_\mu^{(\rho} \delta_\nu^{\sigma)} - \eta_{\mu\nu} \eta^{\rho\sigma}\right] \\ - i\Delta_L(x; x') \left[2\bar{\delta}_\mu^{(\rho} \bar{\delta}_\nu^{\sigma)} - 2\bar{\eta}_{\mu\nu} \bar{\eta}^{\rho\sigma}\right] , \quad (2.15a)$$

$$i\left[\mu\Delta_\nu\right](x; x') = i\Delta_N(x, x') \eta_{\mu\nu} - i\Delta_L(x; x') \bar{\eta}_{\mu\nu} . \quad (2.15b)$$

2.2 “In”-“Out” Matrix Elements and the S-Matrix.

Perturbative quantum field theory is usually formulated to give “in”-“out” amplitudes and S-matrix elements. These quantities are not well suited for our study because they require specification of the vacuum at asymptotically early and late times, which is precisely what we wish to determine. However, they can at least be used to negate the hypothesis that the vacuum of an initially inflating universe suffers only perturbatively small corrections. The procedure is simply to assume the “in” and “out” vacua are both free de Sitter, and then do the computation. If the hypothesis is correct, the result should be free of infrared divergences.

What one actually finds is that both “in”-“out” amplitudes [1,2] and S-matrix elements [7] are infrared divergent. Since even 3-particle tree amplitudes are affected, there is no possibility for solving the problem by summing degenerate ensembles. There is simply nothing of lower order in perturbation theory that could cancel the problem.

Why this happens can be readily understood from the previous section. S-matrix elements consist of wavefunctions integrated against interaction vertices, which are linked by propagators. From (2.10a) we see that physical wavefunctions become constant at late times; while (2.14-15) shows that non-coincident propagators remain of order one as $u \rightarrow 0$. But (2.4) reveals that vertices blow up at late times. A more physical way of understanding the phenomenon is that although the *coordinate* momentum of a graviton is unchanged by time evolution, its *physical* momentum is redshifted to zero. Since all gravitons of fixed coordinate momentum approach the same physical momentum, their interaction becomes infinitely strong at late times.

The correct interpretation of these infrared divergences is that the “in” vacuum is infinitely far from the “out” vacuum. Stated differently, the vacuum of an initially inflating universe suffers non-perturbatively large corrections at late times. However, it does not

follow that these corrections must depend upon time in the same way that the “in”-“out” divergences depend upon some arbitrarily chosen infrared cutoff. To obtain a quantitative result one must actually follow the evolution.

2.3 How to Compute Expectation Values.

The perturbative rules for calculating expectation values of operators in field theory were developed by Schwinger [8] and have been adapted to our particular problem and initial conditions in [2]. They are quite similar to the usual rules for computing “in”-“out” matrix elements since the propagators and vertices utilized are simple variations of the usual ones. The main idea is to evolve forward from the initial state with the action functionally integrated over the dummy field $\psi_{\mu\nu}^{(+)}$ and, then, to evolve back to the initial state using the conjugate action functionally integrated over the dummy field $\psi_{\mu\nu}^{(-)}$.

The Feynman rules are simple. An external line may be chosen as either “+” or “-” but one does not sum over both possibilities. Vertices have either all “+” or all “-” lines, and one sums the two possibilities for each vertex. The “+” vertices are identical to those of the “in”-“out” formalism, while the “-” vertices are complex conjugated. Propagators can link fields of either sign. All four possibilities can be obtained from (2.12a-b) by effecting the following substitutions for the quantity $(\Delta x^2 - \Delta u + 2i\epsilon|\Delta u| + \epsilon^2)$ in (2.14):

$$(+ \ +) \quad \Longrightarrow \quad (\Delta x - |\Delta u| + i\epsilon) (\Delta x + |\Delta u| - i\epsilon) \ , \quad (2.16a)$$

$$(- \ +) \quad \Longrightarrow \quad (\Delta x - \Delta u + i\epsilon) (\Delta x + \Delta u - i\epsilon) \ , \quad (2.16b)$$

$$(+ \ -) \quad \Longrightarrow \quad (\Delta x - \Delta u - i\epsilon) (\Delta x + \Delta u + i\epsilon) \ , \quad (2.16c)$$

$$(- \ -) \quad \Longrightarrow \quad (\Delta x - |\Delta u| - i\epsilon) (\Delta x + |\Delta u| + i\epsilon) \ . \quad (2.16d)$$

Two properties of Schwinger’s formalism have significance for our computation. First, the expectation value of a Hermitian operator such as the metric must be real. Second, the interference between “+” and “-” vertices results in complete cancellation whenever

an interaction strays outside the past lightcone of the observation point. This means that no infrared regularization is needed. The infrared divergences of the “in”-“out” formalism come from interactions in the infinite future, and these drop out of “in”-“in” calculations. In their place one expects growth in the observation time.

2.4 Ultraviolet Regularization.

The simplest way of regulating the ultraviolet is by keeping the parameter ϵ non-zero in the “++” propagators (2.14-15) and their variations (2.16). Consideration of the mode sums (2.11) reveals ϵ^{-1} to be an exponential cutoff on the coordinate 3-momentum. This would not be a very natural technique for an “in”-“out” calculation because there is nothing unique about the $t = 0$ surface of simultaneity. However, this surface has a special significance in our modified “in”-“in” computation: it is where the initial state is defined, and it is the point at which interactions begin. In the context of expectation values, our method corresponds to weighting the usual Fock space inner product with a factor of $\exp(-\frac{1}{2}\epsilon\|\vec{k}\|)$ for each creation and annihilation operator. In other words, *time evolution is unaffected by our method, only the inner product on the initial value surface changes.*

The point just made is crucial because spurious time dependence can be made to reside on the ultraviolet regularization parameter. Consider, for example, a logarithmic divergence of the form $\ln(\epsilon)$. Had we instead regulated by replacing ϵ everywhere with ϵHu , then we might have claimed to see a secular infrared effect:

$$\ln(\epsilon Hu) = \ln(\epsilon) - Ht \tag{2.17}$$

which is in fact of purely ultraviolet origin. We emphasize that the possibility for this sort of delusion has nothing to do with the perturbative non-renormalizability of quantum general relativity. One can see it even in the flat space, massless ϕ^3 model which was our original paradigm for relaxation [2]. Nor does the phenomenon signify any fuzziness in the

distinction between infrared and ultraviolet. The unambiguous signal for an ultraviolet effect is propagators at or near coincidence.

The time dependence of the inflating background has led to much confusion about ultraviolet regularization. Some researchers have thought it more natural to employ a mode cutoff which is invariant with respect to the background geometry. (Note that this method is no more invariant than ours with respect to the full geometry.) This amounts to replacing our parameter ϵ with $\epsilon\sqrt{H^2uu'}$. One consequence is that the coincidence limit of an undifferentiated propagator which has been so regulated grows linearly in the co-moving time. By first taking the coincidence limit of our propagator and then replacing ϵ with ϵHu :

$$\begin{aligned} \left[{}_{\mu\nu}\Delta^{\rho\sigma}\right](x;x) &= \frac{H^2}{8\pi^2} \left\{ \frac{2u'u}{\epsilon^2} \left[2\delta_{\mu}^{(\rho} \delta_{\nu}^{\sigma)} - \eta_{\mu\nu} \eta^{\rho\sigma}\right] \right. \\ &\quad \left. - \ln\left[H^2\epsilon^2\right] \left[2\bar{\delta}_{\mu}^{(\rho} \bar{\delta}_{\nu}^{\sigma)} - 2\bar{\eta}_{\mu\nu} \bar{\eta}^{\rho\sigma}\right] \right\} \end{aligned} \quad (2.18a)$$

$$\begin{aligned} \longrightarrow \frac{H^2}{8\pi^2} \left\{ \frac{2}{H^2\epsilon^2} \left[2\delta_{\mu}^{(\rho} \delta_{\nu}^{\sigma)} - \eta_{\mu\nu} \eta^{\rho\sigma}\right] \right. \\ \left. + \left(2Ht - \ln\left[H^2\epsilon^2\right]\right) \left[2\bar{\delta}_{\mu}^{(\rho} \bar{\delta}_{\nu}^{\sigma)} - 2\bar{\eta}_{\mu\nu} \bar{\eta}^{\rho\sigma}\right] \right\}, \end{aligned} \quad (2.18b)$$

we see that this growth is identical to that displayed in (2.17), and hence of purely ultraviolet provenance. One gets the same result with background-invariant point splitting.

An erroneous argument is sometimes given that this spurious time dependence from the ultraviolet is actually a reliable effect from the infrared. One first notes that on \mathfrak{R}^3 the propagator would be our integral expression (2.12a), but without the lower bound at $k = H$. The second term of the integrand grows rapidly enough near $k = 0$ to give an infrared divergence. According to the fallacious argument, one should regulate this infrared divergence by cutting off the integration at $k = (uu')^{-\frac{1}{2}}$. Of course this replaces the factor of H^2 inside the logarithm term of our propagator with $(uu')^{-\frac{1}{2}}$, and one can see from (2.18a) that the coincidence limit then exhibits the same linear growth as (2.18b).

We stress that the introduction of a time dependent infrared cutoff prevents the propagator from even inverting the kinetic operator. The rationale behind the cutoff is that coordinate momenta smaller than $k = u^{-1}$ correspond to physical wavelengths which have redshifted beyond the Hubble radius and should therefore decouple. This is correct physics but faulty mathematics. Modes indeed decouple when their physical wavelengths redshift beyond the Hubble radius, but this is accomplished by the causality of interactions in Schwinger's formalism, not by the *ad hoc* imposition of an infrared cutoff on the naive mode sum. The mode sum is actually regulated by the physically motivated restriction of coherent de Sitter vacuum to a spatial patch of finite extent. For us this was the Hubble radius, but any value would serve. The key point is that the infrared cutoff on the free mode sum is not time dependent. The only time dependence which appears in the coincidence limit of the propagator got there through a poor choice of the ultraviolet regulator.

Motivated by the faulty argument — for which we emphasize that he bore no responsibility — Ford [9] proposed a very interesting relaxation mechanism of which ours is, in some ways, a mirror image.* Among other differences, the most important diagrams for Ford were those with a coincident propagator attached to two legs of the same vertex. These are precisely the least important ones for us.

2.5 The Threshold for a Late Time Effect.

We found it convenient to compute the amputated expectation value of the pseudo-graviton field and then attach the external line by solving an ordinary differential equation. The homogeneity and isotropy of the dynamics, and of our initial state, allow us to express the amputated 1-point function in terms of two functions of u :

$$D_{\mu\nu}^{\alpha\beta} \langle 0 | \kappa \psi_{\alpha\beta}(u, \vec{x}) | 0 \rangle = a(u) \bar{\eta}_{\mu\nu} + c(u) \delta_{\mu}^0 \delta_{\nu}^0 . \quad (2.19)$$

The full 1-point function must have the same form, although with different coefficient

* We thank M. B. Einhorn for bringing Ford's work to our attention.

functions:

$$\langle 0 | \kappa \psi_{\mu\nu}(u, \vec{x}) | 0 \rangle = A(u) \bar{\eta}_{\mu\nu} + C(u) \delta_{\mu}^0 \delta_{\nu}^0 . \quad (2.20)$$

Comparing these two expressions and taking account of the kinetic operator (2.7), we see that $A(u)$ and $C(u)$ can be expressed in terms of $a(u)$ and $c(u)$ using the retarded Green's functions for the massless, minimally coupled and conformally coupled scalars:

$$A(u) = -4 G_A^{\text{ret}}[a](u) + G_C^{\text{ret}}[3a + c](u) , \quad (2.21a)$$

$$C(u) = G_C^{\text{ret}}[3a + c](u) . \quad (2.21b)$$

Although it is simple to give integral expressions for these Greens functions, the more revealing form is to work them out for arbitrary powers of u [2]:

$$G_A^{\text{ret}}[u^{-4} (Hu)^{\zeta}](u) = \frac{H^2}{3\zeta(1 - \frac{1}{3}\zeta)} \left\{ (Hu)^{\zeta} - (1 - \frac{1}{3}\zeta) - \frac{1}{3}\zeta(Hu)^3 \right\} , \quad (2.22a)$$

$$G_C^{\text{ret}}[u^{-4} (Hu)^{\zeta}](u) = \frac{H^2}{2(1 - \zeta)(1 - \frac{1}{2}\zeta)} \left\{ -(Hu)^{\zeta} + 2(1 - \frac{1}{2}\zeta)Hu - (1 - \zeta)(Hu)^2 \right\} \quad (2.22b)$$

Note that $\zeta = 0$ constitutes a sort of threshold. For larger values of ζ the late time limits of $A(u)$ and $C(u)$ approach constants, whereas smaller values of ζ give functions which grow as u approaches zero.

To obtain $H_{\text{eff}}(t)$ we compare with the invariant element in co-moving coordinates

$$-dt^2 + a^2(t) d\vec{x} \cdot d\vec{x} = \Omega^2 \left\{ -[1 - C(u)] du^2 + [1 + A(u)] d\vec{x} \cdot d\vec{x} \right\} . \quad (2.23)$$

Substituting into the definition (1.4) gives a result which is true even beyond perturbation theory:

$$H_{\text{eff}}(t) = \frac{H}{\sqrt{1 - C(u)}} \left\{ 1 - \frac{\frac{1}{2}u \frac{d}{du} A(u)}{1 + A(u)} \right\} . \quad (2.24)$$

With relations (2.21) and (2.22), this shows that $a(u)$ and $c(u)$ must grow faster than u^{-4} if quantum corrections are to overwhelm the classical result of $H_{\text{eff}}(t) = H$ at late times.

2.6 Gauge Independence of $H_{\text{eff}}(t)$.

In demonstrating the gauge independence of $H_{\text{eff}}(t)$ it is useful to recall that any quantity can be made invariant by defining it in a unique coordinate system. In this case we can also exploit the homogeneity and isotropy of our special state, although we feel confident that a satisfactory definition of the effective Hubble constant could be found for more general initial states. Since $H_{\text{eff}}(t)$ was defined in co-moving coordinates, for a state whose scale factor obeys the initial conditions:

$$a(0) = 1 \quad , \quad \frac{da(0)}{dt} = H \quad ; \quad (2.25)$$

our first step in any new coordinate system would be to restore these conditions by performing an appropriate coordinate transformation. We can therefore limit ourselves to consideration of gauge changes $F_\mu \rightarrow F_\mu + \delta F_\mu$ which preserve homogeneity, isotropy, and the initial conditions. Any such change can be parametrized as follows:

$$\delta F_\mu = \delta_\mu^0 \Omega^{-1} \varphi(u) \quad , \quad (2.26)$$

where preserving the initial condition requires $\varphi(H^{-1}) = 0$.

Changing our gauge condition (2.5) by (2.26) induces the following 1-point interaction:

$$\delta \left(-\frac{1}{2} \int d^4x F_\mu \eta^{\mu\nu} F_\nu \right) = \int d^4x F_0 \Omega^{-1} \varphi(u) \quad (2.27a)$$

$$= \int d^4x \left\{ \psi_{00} \varphi_{,0} + \frac{1}{2} \psi \varphi_{,0} + \frac{2}{u} \psi_{00} \varphi \right\} \quad . \quad (2.27b)$$

The coefficient functions of the amputated 1-point function therefore acquire the following variations:

$$\delta a(u) = \frac{\kappa}{2} \frac{d}{du} \varphi(u) \quad , \quad \delta c(u) = \frac{\kappa}{2} \frac{d}{du} \varphi(u) + \frac{2\kappa}{u} \varphi(u) \quad . \quad (2.28)$$

Now consider variation by a general power, minus a constant to enforce the initial condition:

$$\varphi(u) = u^{-3} (Hu)^\zeta - H^3 \quad . \quad (2.29)$$

The induced variations on $a(u)$ and $c(u)$ are:

$$\delta a(u) = \frac{\kappa}{2} (\zeta - 3) u^{-4} (Hu)^\zeta , \quad (2.30a)$$

$$\delta c(u) = \frac{\kappa}{2} (\zeta + 1) u^{-4} (Hu)^\zeta - \frac{2\kappa H^3}{u} . \quad (2.30b)$$

The coefficient functions of the unamputated 1-point function suffer the following variations:

$$\delta A(u) = 2\kappa H^2 \left\{ -\frac{(Hu)^\zeta}{\zeta(\zeta-1)} + \frac{\zeta-3}{3\zeta} - \left(\frac{\zeta-3}{\zeta-1} \right) \frac{Hu}{2} + \frac{(Hu)^3}{6} \right\} , \quad (2.31a)$$

$$\delta C(u) = 2\kappa H^2 \left\{ -\frac{(Hu)^\zeta}{\zeta-1} - \left(\frac{\zeta-3}{\zeta-1} \right) \frac{Hu}{2} + \frac{(Hu)^3}{2} \right\} . \quad (2.31b)$$

From (2.24) we see that the variation of $H_{\text{eff}}(t)$ is:

$$\delta H_{\text{eff}}(t) = H \left\{ -\frac{1}{2} u \frac{d}{du} \delta A(u) + \frac{1}{2} \delta C(u) \right\} , \quad (2.32)$$

and substitution of (2.31) gives $\delta H_{\text{eff}}(t) = 0$. The proof is completed by noting that a general variation of the required form can be built by superposing terms of the form (2.29).

2.7 The Genesis of Infrared Logarithms.

It turns out that perturbative corrections to the amputated 1-point function can grow no faster than u^{-4} times powers of $\ln(Hu)$ [2,10]. Since we will need to extend the argument, it is useful to begin by restating it. Recall first that κ has the dimensions of length, while H goes like an inverse length, and the amputated 1-point function has the dimensions of an inverse length squared. Diagrams which contribute to the amputated 1-point function at ℓ loops can involve up to $2\ell - 1$ 3-point interactions and $3\ell - 2$ propagators. Each 3-point vertex contributes a constant factor of κH^{-2} , while each propagator contributes a factor of H^2 . Including the single factor of κ in our definition (2.19), we see that the ℓ -loop contribution consists of $\kappa^{2\ell} H^{2\ell-2}$ times a function of H , u and ϵ which has the dimensionality $(\text{length})^{-4}$.

Since the ultraviolet regularization parameter goes to zero after renormalization, we can ignore positive powers of ϵ . The constant H can enter through undifferentiated $i\Delta_L$, and through the limits of integration on the conformal time integrals. Neither can contribute negative powers of H . This is obvious for $i\Delta_L$. To see that factors of H from the limits cannot contribute negative powers, note that performing the spatial integrations leaves $2\ell - 2$ conformal time integrations of an integrand which falls off like $S^{-2\ell-6}$ if all the conformal times are scaled by the common factor S . Since the integrand can contain at most two isolated factors of u^{-1} , the conformal time integrations must converge even if the factors of H^{-1} in their upper limits are taken to infinity. Hence there can be no negative powers of H .

To complete the argument consider a dimension $(\text{length})^{-4}$ function of H , u and ϵ which contains no negative powers of H or positive powers of ϵ . We can write any such function as u^{-4} times a combination of the dimensionless parameters Hu and ϵu^{-1} . Since there can be no negative powers of the first parameter, or positive powers of the second, the strongest growth possible as $u \rightarrow 0^+$ is u^{-4} times powers of $\ln(Hu)$ and $\ln(\epsilon u^{-1}) = \ln(H\epsilon) - \ln(Hu)$.

Because the amputated 1-point function must grow faster than u^{-4} in order for there to be a significant effect at late times, the appearance of infrared logarithms is essential for our scheme of relaxation. The preceding argument can be extended to show that infrared logarithms are just about inevitable if one accepts that there are logarithmic ultraviolet divergences. Since ϵ is a dimensionful quantity, logarithmic ultraviolet divergences can only come in the form of $\ln(\epsilon u^{-1})$ and $\ln(H\epsilon)$. As before, there are just two sources of H dependence: an undifferentiated $i\Delta_L$ and the upper limits H^{-1} of the conformal time integrations. The latter cannot provide factors of $\ln(H)$ for the same reason it gives no negative powers of H : the conformal time integrands fall off rapidly enough for large conformal times to make them converge even when the upper limits become infinite. The logarithm part of an undifferentiated propagator can indeed provide a factor of $\ln(H)$, but

there are never enough such terms to pair with all the factors of $\ln(\epsilon)$. At ℓ loops one has to expect ℓ factors of $\ln(\epsilon)$ from ultraviolet divergences, but there is a maximum of $\ell - 1$ logarithms from undifferentiated $i\Delta_L$'s. * Hence at least one of the ultraviolet logarithms must come in the form $\ln(\epsilon u^{-1})$.

We emphasize that the association we have exploited between infrared logarithms and logarithmic ultraviolet divergences in no way implies that factors of $\ln(u)$ are of ultraviolet origin. Some of them originate as factors of $\ln(Hu)$ from the logarithm parts of undifferentiated propagators. ** The physical origin of such terms is the increasing correlation of the free graviton vacuum as inflation proceeds. This effect is the casual analog of the problem discussed in sub-section 2.4 when one assumes the existence of coherent de Sitter vacuum over an infinite surface of simultaneity.

Even the factors of $\ln(u)$ which originate as $\ln(\epsilon u^{-1})$ are infrared effects. They derive from the coherent superposition of interactions throughout the invariant volume of the past lightcone. In the absence of a mass, ultraviolet divergences must always be associated with the infrared in this way. See, for example, the result we obtained for massless, ϕ^3 theory in flat space [2].

2.8 A Bound on the Number of Infrared Logarithms.

We argued in the preceding sub-section that infrared logarithms are all but inevitable, and that they derive jointly from the infrared regions of loop integrals which harbor logarithmic ultraviolet divergences and from an undifferentiated $i\Delta_L$. However, we did not explain how many of the $\ell - 1$ undifferentiated propagator logarithms can go to reinforce the ℓ ultraviolet logarithms that one expects in an ℓ -loop diagram. The answer turns out

* See the end of sub-section 2.9 for a proof.

** The reader should not be misled by our argument that there are fewer intrinsic factors of $\ln(Hu)$ than of $\ln(\epsilon u^{-1})$. We noted this only to rule out the remote possibility that the two factors come in pairs so as to cancel the infrared logarithms: $\ln(\epsilon u^{-1}) + \ln(Hu) = \ln(H\epsilon)$. In fact the two sources of infrared logarithms tend to add.

to be “none:” there can be at most ℓ infrared logarithms at ℓ loops. All the undifferentiated factors of $i\Delta_L$ do is to sometimes make up the difference for diagrams which would otherwise contribute less than ℓ infrared logarithms.

To see why, consider the way a single undifferentiated propagator might enhance the number of infrared logarithms. There can be ℓ logarithmic ultraviolet divergences at ℓ loops so what we are looking for is:

$$\ln^\ell(\epsilon u^{-1}) \times \ln(Hu) = \ln^\ell(\epsilon u^{-1}) \times \ln(H) + \ln^\ell(\epsilon u^{-1}) \times \ln(u) . \quad (2.33)$$

In other words, if we replace the propagator in question with $\ln(H)$, the resulting diagram must contribute ℓ logarithmic ultraviolet divergences. But replacing a propagator by a constant cuts the leg and results in a diagram containing only $\ell - 1$ loops. Such a diagram can contribute at most $\ell - 1$ factors of $\ln(\epsilon u^{-1})$. Therefore, an undifferentiated $i\Delta_L$ cannot increase the number of infrared logarithms in an ℓ -loop diagram beyond ℓ .

It is worth mentioning that this argument applies to diagrams, not to portions of diagrams. However, the only practical way of performing the computation was to break each diagram up into many pieces. At two loops some of these pieces produce three infrared logarithms; it is only their sums which are limited to two. On the first run of this calculation we did not appreciate that the triple log terms must cancel. This argument was only discovered after noting what was to us then, a surprising and disturbing cancellation. In retrospect the cancellation stands as a powerful check on the consistency and accuracy of our work.

2.9 Comments on One and Two Loops.

The first quantum corrections to the amputated 1-point function are the one-loop graphs shown in Fig. 1. Since the external line has been amputated, there is no integration over the single interaction vertex at $x^\mu = (u, \vec{x})$. One obtains just the coincidence limit of a pseudo-graviton or ghost propagator, acted upon by the appropriate vertex operator. It

turns out that there can be no undifferentiated “logarithmic” parts $i\Delta_L$, but even if there were, they would only contribute factors of $\ln(H\epsilon)$. One needs to *integrate* something over a large invariant volume in order to see an effect. This is one way that our mechanism differs from Ford’s [9].



Fig. 1: One-loop contributions to the background geometry. Gravitons reside on wavy lines and ghosts on segmented lines.

The one-loop graphs of Fig. 1 contribute at most terms of order u^{-2} , which is well below the threshold for producing an effect at late times.

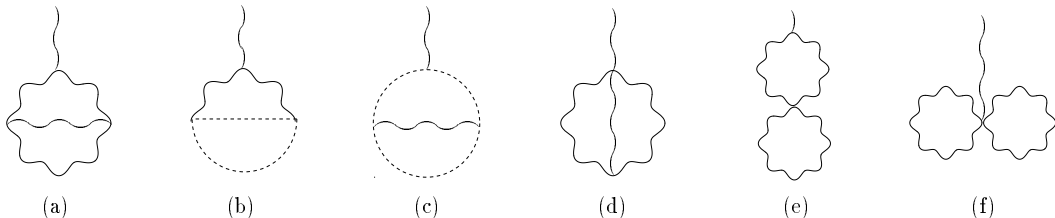


Fig. 2: Two-loop contributions to the background geometry. Gravitons reside on wavy lines and ghosts on segmented lines.

The graphs which contribute at two loops are displayed in Fig. 2. Diagram (2f) is another ultra-local coincidence limit, so it contributes no infrared logarithms. Diagram (2e) contains a single free interaction vertex, but the entire diagram is canceled by the counterterm needed to renormalize its coincident lower loop. Diagram (2d) also contains a single free interaction, and an undifferentiated $i\Delta_L$ allows it to contribute two infrared logarithms. We call this the “4-3” diagram because it consists of a 4-point and a 3-point vertex. What we call “3-3-3” diagrams are shown in (2a-c). They contain two free

interaction vertices and would give two infrared logarithms if the calculation were done in flat space. By the argument of the preceding sub-section we know that undifferentiated logarithms from the propagators do not change this.

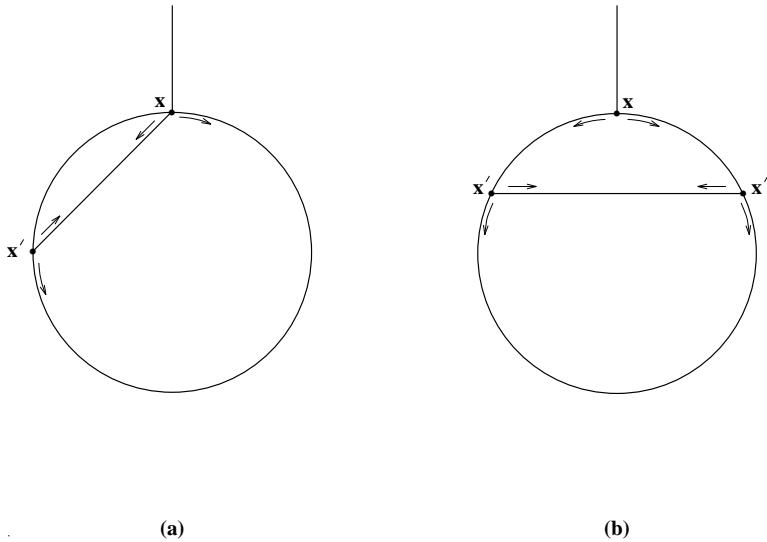


Fig. 3: In the 4-3 diagram (a) and the generic 3-3-3 diagram (b), solid lines can represent gravitons or ghosts and the arrows indicate the action of the vertex derivatives.

Fig. 3 is useful in understanding why two-loop contributions to the 1-point function have at most a single undifferentiated $i\Delta_L$. One can see from (2.4) and (2.6) that every interaction vertex contains two fields which are either differentiated or else contain a 0-index. From (2.15) one can see that a 0-index precludes coupling to the logarithm term in the propagator. We call a line which is either differentiated or forced to carry a 0-index, “contaminated.”

To treat the case for a general loop ℓ , note that a graph of this order can have $2\ell - 1$ 3-point vertices and $3\ell - 2$ internal propagators. One of the vertices is the external one, whose external leg may be contaminated, but the other vertices must each contribute two contaminated legs. This makes for a total number of either $4\ell - 3$ or $4\ell - 4$ contaminating factors (derivatives or 0-indices) to distribute among the $3\ell - 2$ internal propagators. The

smallest number of “spoiled” propagators is therefore $2\ell - 1$, leaving $\ell - 1$ which can harbor undifferentiated logarithms. The result is the same for ℓ -loop graphs constructed from higher point vertices because the number of contaminating factors falls by two for each internal line which is lost.

3. The 3–3–3 Diagrams

The three 3-3-3 diagram consists of an outer 3-point vertex joined to two freely integrated 3-point vertices (see Fig. 4).

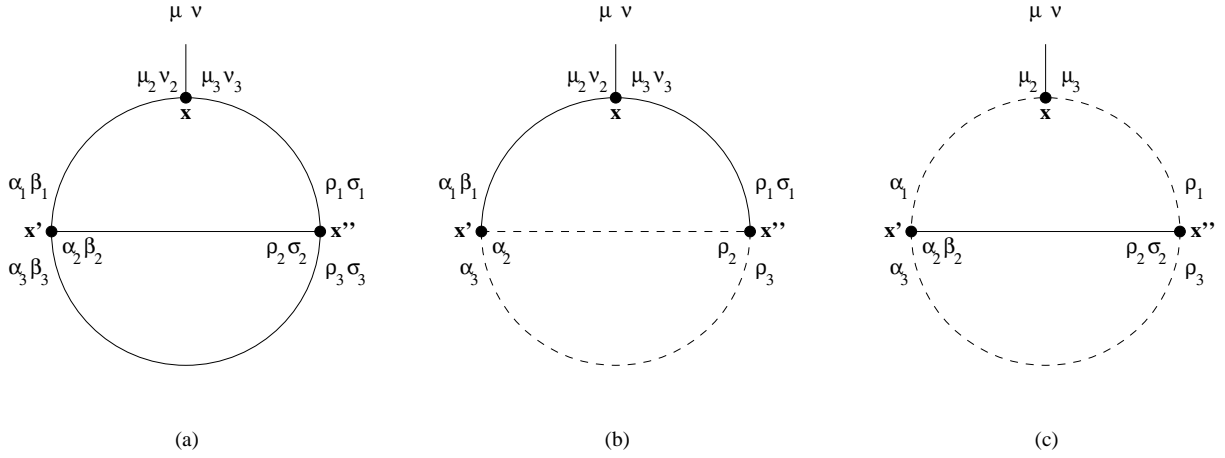


Fig. 4: The tensor structure of the 3-3-3 diagrams. Gravitons reside on solid lines and ghosts on segmented lines.

The fixed vertex is taken to be at $x^\mu = (u, \vec{x})$, and we can identify the locations of the two free vertices as $x'^\mu = (u', \vec{x}')$ and $x''^\mu = (u'', \vec{x}'')$. One can form three differences from these positions:

$$w^\mu \equiv (x - x')^\mu \quad , \quad y^\mu \equiv (x' - x'')^\mu \quad , \quad z^\mu \equiv (x'' - x)^\mu \quad . \quad (3.1)$$

The fixed vertex is taken to be of “+” type, and there are a total of four variations when each of the two free vertices is summed over “+” and “-”. These variations have no effect

until quite late in the reduction process because they control only the overall sign of the diagram and the order ϵ terms in the four propagators. However, since the variations interfere destructively whenever x'^{μ} or x''^{μ} is outside the rather small past lightcone of x^{μ} , we will make no error by extending the spatial integrations from T^3 to \mathfrak{R}^3 .

The Lorentz squares of the vectors (3.1) are understood to include terms of order ϵ according to the following scheme:

$$w^2 = (r' - d_w + i\epsilon) (r' + d_w - i\epsilon) \quad , \quad \vec{r}' \equiv \vec{x} - \vec{x}' \quad ; \quad (3.2a)$$

$$z^2 = (r'' - d_z + i\epsilon) (r'' + d_z - i\epsilon) \quad , \quad \vec{r}'' \equiv \vec{x}'' - \vec{x} \quad ; \quad (3.2b)$$

$$y^2 = (\|\vec{r}' + \vec{r}''\| - d_y + i\epsilon) (\|\vec{r}' + \vec{r}''\| + d_y - i\epsilon) \quad . \quad (3.2c)$$

Here $r' \equiv \|\vec{r}'\|$, $r'' \equiv \|\vec{r}''\|$, and the three d 's are conformal time differences which depend upon the four “ \pm ” variations. For example, when x'^{μ} is “+” and x''^{μ} is “-” we have:

$$d_w = |u' - u| \quad , \quad d_z = u - u'' \quad , \quad d_y = u' - u'' \quad . \quad (3.3)$$

We will eventually show that the order $u \leq u' \leq u'' \leq H^{-1}$ can be enforced, in which case the d 's have the form given in Table 1.

$V(x'), V(x'')$	d_w	d_z	d_y
+ , +	$u' - u$	$u'' - u$	$u'' - u'$
+ , -	$u' - u$	$u - u''$	$u' - u''$
- , +	$u - u'$	$u'' - u$	$u'' - u'$
- , -	$u - u'$	$u - u''$	$u' - u''$

Table 1: The values of the d 's for the four possible variations of the vertices at x' and x'' , assuming $u \leq u' \leq u'' \leq H^{-1}$.

The ghost-graviton interactions can be obtained from expression (2.6):

$$\begin{aligned} \mathcal{L}_{\text{ghost}}^{(3)} = & \kappa \Omega^2 \left\{ -\psi_{\mu\nu} \bar{\omega}^{\mu,\alpha} \omega^{\nu}_{,\alpha} - \psi_{\mu\nu} \bar{\omega}^{\alpha,\mu} \omega^{\nu}_{,\alpha} - \psi_{\mu\nu,\alpha} \bar{\omega}^{\mu,\nu} \omega^{\alpha} + \psi_{\mu\nu} \bar{\omega}^{\alpha}_{,\alpha} \omega^{\mu,\nu} \right. \\ & + \frac{1}{2} \psi_{,\mu} \bar{\omega}^{\alpha}_{,\alpha} \omega^{\mu} - \frac{2}{u} \psi_{\mu\nu} \bar{\omega}^{\mu,\nu} \omega^{\alpha} t_{\alpha} + \frac{1}{u} \psi \bar{\omega}^{\mu}_{,\mu} \omega^{\nu} t_{\nu} \\ & \left. + \frac{2}{u} \psi_{\mu\nu} \bar{\omega}^{\alpha} \omega^{\mu,\nu} t_{\alpha} + \frac{1}{u} \psi_{,\mu} \bar{\omega}^{\nu} \omega^{\mu} t_{\nu} + \frac{2}{u^2} \psi \bar{\omega}^{\mu} \omega^{\nu} t_{\mu} t_{\nu} \right\} \quad . \quad (3.4) \end{aligned}$$

(Recall that $t_\mu \equiv \eta_{\mu 0}$ and $\psi \equiv \eta^{\mu\nu} \psi_{\mu\nu}$.) The associated vertex operators $V_i^{\alpha_1\beta_1\mu\nu}$ are defined by the relation:

$$\mathcal{L}_{\text{ghost}}^i \equiv \eta_{\alpha_1\beta_1} \eta_{\alpha_2\alpha_3} V_i^{\alpha_1\beta_1\alpha_2\alpha_3}(x; \partial_1, \partial_2, \partial_3) \quad , \quad i = 1, \dots, 10 \quad ; \quad (3.5)$$

and are explicitly displayed in Table 2.

#	Vertex Operator	#	Vertex Operator
1	$-\eta^{\alpha_2(\alpha_1} \eta^{\beta_1)\alpha_3} \partial_2 \cdot \partial_3$	6	$\frac{1}{2}\eta^{\alpha_1\beta_1} \partial_2^{\alpha_2} \partial_1^{\alpha_3}$
2	$-\eta^{\alpha_3(\alpha_1} \partial_2^{\beta_1)} \partial_3^{\alpha_2}$	7	$\frac{1}{u}\eta^{\alpha_1\beta_1} \partial_2^{\alpha_2} t^{\alpha_3}$
3	$-\eta^{\alpha_2(\alpha_1} \partial_2^{\beta_1)} \partial_1^{\alpha_3}$	8	$\frac{2}{u}\eta^{\alpha_3(\alpha_1} \partial_3^{\beta_1)} t^{\alpha_2}$
4	$-\frac{2}{u}\eta^{\alpha_2(\alpha_1} \partial_2^{\beta_1)} t^{\alpha_3}$	9	$\frac{1}{u}\eta^{\alpha_1\beta_1} \partial_1^{\alpha_3} t^{\alpha_2}$
5	$\eta^{\alpha_3(\alpha_1} \partial_3^{\beta_1)} \partial_2^{\alpha_2}$	10	$\frac{2}{u^2}\eta^{\alpha_1\beta_1} t^{\alpha_2} t^{\alpha_3}$

Table 2: Vertex operators of ghost-pseudograviton interactions without the factor of $\kappa\Omega^2$.

We can read the graviton 3-point interaction off from expression (2.4):

$$\begin{aligned} \mathcal{L}_{\text{inv}}^{(3)} = \kappa \Omega^2 \left\{ \frac{1}{4}\psi \psi^{\alpha\beta,\mu} \psi_{\mu\alpha,\beta} - \psi^{\alpha\beta} \psi_{\alpha\mu,\nu} \psi^{\mu\nu}{}_{,\beta} - \frac{1}{2}\psi^{\alpha\beta} \psi_{\alpha\dot{\mu}}{}^{\dot{\nu}} \psi_{\beta\nu}{}^{,\dot{\mu}} \right. \\ - \frac{1}{4}\psi \psi_{,\mu} \psi^{\mu\nu}{}_{,\nu} + \frac{1}{2}\psi^{\alpha\beta} \psi_{\alpha\beta,\mu} \psi^{\mu\nu}{}_{,\nu} + \frac{1}{2}\psi^{\alpha\beta} \psi_{,\alpha} \psi_{\mu\beta}{}^{,\mu} + \frac{1}{2}\psi^{\alpha\beta} \psi_{\alpha\mu,\beta} \psi^{,\mu} \\ + \frac{1}{8}\psi \psi^{,\mu} \psi_{,\mu} - \frac{1}{2}\psi^{\alpha\beta} \psi_{\alpha\beta,\mu} \psi^{,\mu} - \frac{1}{4}\psi^{\alpha\beta} \psi_{,\alpha} \psi_{,\beta} \\ - \frac{1}{8}\psi \psi^{\alpha\beta,\mu} \psi_{\alpha\beta,\mu} + \frac{1}{2}\psi^{\alpha\beta} \psi_{\alpha\mu,\nu} \psi_{\beta}{}^{\mu,\nu} + \frac{1}{4}\psi^{\alpha\beta} \psi_{\mu\nu,\alpha} \psi^{\mu\nu}{}_{,\beta} \\ \left. - \frac{1}{2u}\psi \psi_{,\mu} \psi^{\mu\nu} t_\nu + \frac{1}{u}\psi^{\alpha\beta} \psi_{\alpha\beta,\mu} \psi^{\mu\nu} t_\nu + \frac{1}{u}\psi_{\alpha\mu} \psi^{,\alpha} \psi^{\mu\nu} t_\nu \right\} . \quad (3.6) \end{aligned}$$

It is worth noting that all but the last three terms can be checked against the previously published, flat space 3-point interactions [11] by merely omitting the factor of Ω^2 and regarding $\psi_{\mu\nu}$ as the graviton.

In deriving the associated vertex operators we must account for the indistinguishability of gravitons. This would ordinarily be accomplished by fully symmetrizing each interaction, which turns out to give 75 distinct terms. For the pure graviton diagram (4a) it is wasteful

to first sum over the $(75)^3 = 421,875$ possibilities for the three vertices and then divide by the symmetry factor of 4 to compensate for overcounting. The more efficient strategy is to symmetrize the vertices only on line #1 and then sum over the interchange of lines #2 and #3 for only the vertex at x''^μ , dispensing with the symmetry factor. One saves over a factor of 3 this way.

To obtain the partially symmetrized vertices one first takes any of the terms from (3.6) and permutes graviton #1 over the three possibilities. As an example, consider the first term in (3.6). Denoting graviton #1 by a breve, we obtain the following three terms:

$$\frac{1}{4} \kappa \Omega^2 \check{\psi} \psi^{\alpha\beta,\mu} \psi_{\mu\alpha,\beta} + \frac{1}{4} \kappa \Omega^2 \check{\psi}_{\mu\alpha,\beta} \psi \psi^{\alpha\beta,\mu} + \frac{1}{4} \kappa \Omega^2 \check{\psi}^{\alpha\beta,\mu} \psi_{\mu\alpha,\beta} \psi . \quad (3.7)$$

One then assigns the remaining two gravitons in each term as #2 and #3 in any way. For example, from (3.7) we could infer the following three vertex operators:

$$\frac{1}{4} \kappa \Omega^2 \eta^{\alpha_1\beta_1} \partial_3^{(\alpha_2} \eta^{\beta_2)(\alpha_3} \partial_2^{\beta_3)} , \quad (3.8a)$$

$$\frac{1}{4} \kappa \Omega^2 \eta^{\alpha_2\beta_2} \partial_1^{(\alpha_3} \eta^{\beta_3)(\alpha_1} \partial_3^{\beta_1)} , \quad (3.8b)$$

$$\frac{1}{4} \kappa \Omega^2 \eta^{\alpha_3\beta_3} \partial_2^{(\alpha_1} \eta^{\beta_1)(\alpha_2} \partial_1^{\beta_2)} . \quad (3.8c)$$

The 43 operators which comprise the full vertex are given in Table 3.

The various 3-3-3 diagrams can be written in terms of the vertex operators of Tables 2-3 and the propagators (2.15). The diagram of Fig. 4a has gravitons on both loops and results in the following expression:

$$\begin{aligned} & \kappa \int_u^{H^{-1}} du' \int d^3 r' \int_u^{H^{-1}} du'' \int d^3 r'' \sum_{i,j,k=1}^{43} \\ & V_i^{\mu\nu\mu_2\nu_2\mu_3\nu_3}(x; \partial_1, \partial_2, \partial_3) i \left[\mu_2\nu_2 \Delta_{\alpha_1\beta_1} \right] (x; x') i \left[\mu_3\nu_3 \Delta_{\rho_1\sigma_1} \right] (x; x'') \\ & \left\{ V_j^{\alpha_1\beta_1\alpha_2\beta_2\alpha_3\beta_3}(x'; \partial'_1, \partial'_2, \partial'_3) i \left[\alpha_2\beta_2 \Delta_{\rho_2\sigma_2} \right] (x'; x'') i \left[\alpha_3\beta_3 \Delta_{\rho_3\sigma_3} \right] (x'; x'') \right. \\ & \left. \left(V_k^{\rho_1\sigma_1\rho_2\sigma_2\rho_3\sigma_3}(x''; \partial''_1, \partial''_2, \partial''_3) + V_k^{\rho_1\sigma_1\rho_3\sigma_3\rho_2\sigma_2}(x''; \partial''_1, \partial''_3, \partial''_2) \right) \right\} . \quad (3.9a) \end{aligned}$$

#	Vertex Operator	#	Vertex Operator
1	$-\frac{1}{2u}\eta^{\alpha_1\beta_1}\eta^{\alpha_2\beta_2}\partial_2^{(\alpha_3}t^{\beta_3)}$	22	$\frac{1}{2}\eta^{\alpha_1(\alpha_2}\eta^{\beta_2)\beta_1}\partial_2^{(\alpha_3}\partial_3^{\beta_3)}$
2	$-\frac{1}{2u}\eta^{\alpha_2\beta_2}\eta^{\alpha_3\beta_3}\partial_3^{(\alpha_1}t^{\beta_1)}$	23	$\frac{1}{2}\eta^{\alpha_2(\alpha_3}\eta^{\beta_3)\beta_2}\partial_3^{(\alpha_1}\partial_1^{\beta_1)}$
3	$-\frac{1}{2u}\eta^{\alpha_3\beta_3}\eta^{\alpha_1\beta_1}\partial_1^{(\alpha_2}t^{\beta_2)}$	24	$\frac{1}{2}\eta^{\alpha_3(\alpha_1}\eta^{\beta_1)\beta_3}\partial_1^{(\alpha_2}\partial_2^{\beta_2)}$
4	$\frac{1}{u}\eta^{\alpha_1(\alpha_2}\eta^{\beta_2)\beta_1}\partial_2^{(\alpha_3}t^{\beta_3)}$	25	$\frac{1}{2}\partial_2^{(\alpha_1}\eta^{\beta_1)(\alpha_3}\partial_3^{\beta_3)}\eta^{\alpha_2\beta_2}$
5	$\frac{1}{u}\eta^{\alpha_2(\alpha_3}\eta^{\beta_3)\beta_2}\partial_3^{(\alpha_1}t^{\beta_1)}$	26	$\frac{1}{2}\partial_3^{(\alpha_2}\eta^{\beta_2)(\alpha_1}\partial_1^{\beta_1)}\eta^{\alpha_3\beta_3}$
6	$\frac{1}{u}\eta^{\alpha_3(\alpha_1}\eta^{\beta_1)\beta_3}\partial_1^{(\alpha_2}t^{\beta_2)}$	27	$\frac{1}{2}\partial_1^{(\alpha_3}\eta^{\beta_3)(\alpha_2}\partial_2^{\beta_2)}\eta^{\alpha_1\beta_1}$
7	$\frac{1}{u}t^{(\alpha_3}\eta^{\beta_3)(\alpha_1}\partial_2^{\beta_1)}\eta^{\alpha_2\beta_2}$	28	$\frac{1}{2}\partial_2^{(\alpha_1}\eta^{\beta_1)(\alpha_2}\partial_3^{\beta_2)}\eta^{\alpha_3\beta_3}$
8	$\frac{1}{u}t^{(\alpha_1}\eta^{\beta_1)(\alpha_2}\partial_3^{\beta_2)}\eta^{\alpha_3\beta_3}$	29	$\frac{1}{2}\partial_3^{(\alpha_2}\eta^{\beta_2)(\alpha_3}\partial_1^{\beta_3)}\eta^{\alpha_1\beta_1}$
9	$\frac{1}{u}t^{(\alpha_2}\eta^{\beta_2)(\alpha_3}\partial_1^{\beta_3)}\eta^{\alpha_1\beta_1}$	30	$\frac{1}{2}\partial_1^{(\alpha_3}\eta^{\beta_3)(\alpha_1}\partial_2^{\beta_1)}\eta^{\alpha_2\beta_2}$
10	$\frac{1}{4}\eta^{\alpha_1\beta_1}\partial_3^{(\alpha_2}\eta^{\beta_2)(\alpha_3}\partial_2^{\beta_3)}$	31	$\frac{1}{8}\eta^{\alpha_1\beta_1}\eta^{\alpha_2\beta_2}\eta^{\alpha_3\beta_3}\partial_2\cdot\partial_3$
11	$\frac{1}{4}\eta^{\alpha_2\beta_2}\partial_1^{(\alpha_3}\eta^{\beta_3)(\alpha_1}\partial_3^{\beta_1)}$	32	$\frac{1}{4}\eta^{\alpha_1\beta_1}\eta^{\alpha_2\beta_2}\eta^{\alpha_3\beta_3}\partial_3\cdot\partial_1$
12	$\frac{1}{4}\eta^{\alpha_3\beta_3}\partial_2^{(\alpha_1}\eta^{\beta_1)(\alpha_2}\partial_1^{\beta_2)}$	33	$-\frac{1}{2}\eta^{\alpha_1(\alpha_2}\eta^{\beta_2)\beta_1}\eta^{\alpha_3\beta_3}\partial_2\cdot\partial_3$
13	$-\partial_3^{(\alpha_1}\eta^{\beta_1)(\alpha_2}\eta^{\beta_2)(\alpha_3}\partial_2^{\beta_3)}$	34	$-\frac{1}{2}\eta^{\alpha_2(\alpha_3}\eta^{\beta_3)\beta_2}\eta^{\alpha_1\beta_1}\partial_3\cdot\partial_1$
14	$-\partial_1^{(\alpha_2}\eta^{\beta_2)(\alpha_3}\eta^{\beta_3)(\alpha_1}\partial_3^{\beta_1)}$	35	$-\frac{1}{2}\eta^{\alpha_3(\alpha_1}\eta^{\beta_1)\beta_3}\eta^{\alpha_2\beta_2}\partial_1\cdot\partial_2$
15	$-\partial_2^{(\alpha_3}\eta^{\beta_3)(\alpha_1}\eta^{\beta_1)(\alpha_2}\partial_1^{\beta_2)}$	36	$-\frac{1}{4}\partial_2^{(\alpha_1}\partial_3^{\beta_1)}\eta^{\alpha_2\beta_2}\eta^{\alpha_3\beta_3}$
16	$-\frac{1}{2}\partial_3^{(\alpha_2}\eta^{\beta_2)(\alpha_1}\eta^{\beta_1)(\alpha_3}\partial_2^{\beta_3)}$	37	$-\frac{1}{2}\partial_3^{(\alpha_2}\partial_1^{\beta_2)}\eta^{\alpha_3\beta_3}\eta^{\alpha_1\beta_1}$
17	$-\frac{1}{2}\partial_1^{(\alpha_3}\eta^{\beta_3)(\alpha_2}\eta^{\beta_2)(\alpha_1}\partial_3^{\beta_1)}$	38	$-\frac{1}{8}\eta^{\alpha_1\beta_1}\eta^{\alpha_2(\alpha_3}\eta^{\beta_3)\beta_2}\partial_2\cdot\partial_3$
18	$-\frac{1}{2}\partial_2^{(\alpha_1}\eta^{\beta_1)(\alpha_3}\eta^{\beta_3)(\alpha_2}\partial_1^{\beta_2)}$	39	$-\frac{1}{4}\eta^{\alpha_2\beta_2}\eta^{\alpha_3(\alpha_1}\eta^{\beta_1)\beta_3}\partial_3\cdot\partial_1$
19	$-\frac{1}{4}\eta^{\alpha_1\beta_1}\eta^{\alpha_2\beta_2}\partial_2^{(\alpha_3}\partial_3^{\beta_3)}$	40	$\frac{1}{2}\eta^{\alpha_1(\alpha_2}\eta^{\beta_2)(\alpha_3}\eta^{\beta_3)(\beta_1}\partial_2\cdot\partial_3$
20	$-\frac{1}{4}\eta^{\alpha_2\beta_2}\eta^{\alpha_3\beta_3}\partial_3^{(\alpha_1}\partial_1^{\beta_1)}$	41	$\eta^{\alpha_1(\alpha_2}\eta^{\beta_2)(\alpha_3}\eta^{\beta_3)(\beta_1}\partial_3\cdot\partial_1$
21	$-\frac{1}{4}\eta^{\alpha_3\beta_3}\eta^{\alpha_1\beta_1}\partial_1^{(\alpha_2}\partial_2^{\beta_2)}$	42	$\frac{1}{4}\partial_2^{(\alpha_1}\partial_3^{\beta_1)}\eta^{\alpha_2(\alpha_3}\eta^{\beta_3)\beta_2}$
		43	$\frac{1}{2}\partial_3^{(\alpha_2}\partial_1^{\beta_2)}\eta^{\alpha_3(\alpha_1}\eta^{\beta_1)\beta_3}$

Table 3: Partially symmetrized cubic pseudo-graviton vertex operators with vertex line #1 distinguished and without the factor of $\kappa\Omega^2$.

The diagram of Fig. 4b has a ghost inner loop and gives:

$$\begin{aligned}
& -\kappa \int_u^{H^{-1}} du' \int d^3 r' \int_u^{H^{-1}} du'' \int d^3 r'' \sum_{i=1}^{43} \sum_{j,k=1}^{10} \\
& V_i^{\mu\nu\mu_2\nu_2\mu_3\nu_3}(x; \partial_1, \partial_2, \partial_3) i[\mu_2\nu_2\Delta_{\alpha_1\beta_1}](x; x') i[\mu_3\nu_3\Delta_{\rho_1\sigma_1}](x; x'') \\
& \left\{ V_j^{\alpha_1\beta_1\alpha_2\alpha_3}(x'; \partial'_1, \partial'_2, \partial'_3) i[\alpha_2\Delta_{\rho_2}](x'; x'') i[\alpha_3\Delta_{\rho_3}](x'; x'') \right. \\
& \left. V_k^{\rho_1\sigma_1\rho_2\rho_3}(x''; \partial''_1, \partial''_2, \partial''_3) \right\} . \tag{3.9b}
\end{aligned}$$

And the diagram of Fig. 4c has ghosts on the outer legs and takes the form:

$$\begin{aligned}
& -\kappa \int_u^{H^{-1}} du' \int d^3 r' \int_u^{H^{-1}} du'' \int d^3 r'' \sum_{i,j,k=1}^{10} \\
& V_i^{\mu\nu\mu_2\mu_3}(x; \partial_1, \partial_2, \partial_3) i[\mu_2\Delta_{\alpha_1}](x; x') i[\mu_3\Delta_{\rho_1}](x; x'') \\
& \left\{ V_j^{\alpha_1\alpha_2\beta_2\alpha_3}(x'; \partial'_1, \partial'_2, \partial'_3) i[\alpha_2\beta_2\Delta_{\rho_2\sigma_2}](x'; x'') \right. \\
& \left. i[\alpha_3\Delta_{\rho_3}](x'; x'') V_k^{\rho_1\rho_2\sigma_2\rho_3}(x''; \partial''_1, \partial''_2, \partial''_3) \right\} . \tag{3.9c}
\end{aligned}$$

The meaning of the various derivatives is determined by the subscripts — indicating which propagator is being acted upon — and by the number of primes — telling with respect to which coordinate the derivative is being taken. For example, the derivative ∂'_2 of $V_j^{\alpha_1\beta_1\alpha_2\beta_2\alpha_3\beta_3}(x'; \partial'_1, \partial'_2, \partial'_3)$ in (3.9a) differentiates the propagator $i[\alpha_2\beta_2\Delta_{\rho_2\sigma_2}](x'; x'')$ with respect to x''^μ . The overall factor of κ in each expression is the one appearing in our definition (2.19) of the amputated 1-point function. The sign of (3.9a) is positive because each vertex comes with a factor of $+i$ and there is an additional factor of $+i$ from amputation:

$$D^{\mu\nu\kappa\lambda} i[\kappa\lambda\Delta_{\mu_1\nu_1}](x; x') = i \delta_{(\mu_1}^\mu \delta_{\nu_1)}^\nu \delta^{(4)}(x - x') . \tag{3.10}$$

Expressions (3.9b) and (3.9c) are negative on account of the same factors with the Fermi minus sign of their single ghost loops.

The various 3-3-3 diagrams were computed in six steps using the symbolic manipulation program Mathematica [12]. For diagrams (4a) and (4b) we first performed the

tensor algebra and acted the derivatives of the inner loop, then did the tensor algebra and derivatives of the outer loop and, finally, performed the integrations. The sums in diagram (4c) were short enough that we could do the contractions and act the derivatives for both loops at the same time. The tensor algebra was performed using FeynCalc [13] loaded in Mathematica.*

3.1 Inner Loop Tensor Algebra and Derivatives.

The inner loop is defined by the propagators which link x'^{μ} and x''^{μ} , and by the inner loop derivatives ∂'_{2-3} and ∂''_{2-3} . There are eight inner loop indices to contract in diagram (4a) and four in (4b), and there can be anywhere from zero to four inner loop derivatives to act. The outer derivatives, ∂'_1 and ∂''_1 are retained as free vector operators at this stage.

What one gets after contracting the inner loop indices and acting the inner loop derivatives is a series of scalar functions times the 4-index objects which we denote by the symbol, $\Pi_A^{\alpha_1\beta_1\rho_1\sigma_1}$. These are the 79 independent 4-index objects, with the appropriate symmetries, which can be formed from $\eta^{\mu\nu}$, y^{μ} , t^{μ} , and up to one of each outer derivative. It is useful to categorize the scalar functions by which, if any, contracted outer derivatives they possess. What remains are functions of u' , u'' and y^2 . We call these coefficient functions, $C_{mA}(u', u'', y^2)$, where the index m stands for which of the ten contracted external derivatives multiplies the function and the index A stands for which of the 79 4-index objects the combination multiplies. We therefore reach expressions of the following form for both (4a) and (4b):

$$\kappa \int_u^{H^{-1}} du' \int d^3 r' \int_u^{H^{-1}} du'' \int d^3 r'' \sum_{i=1}^{43} V_i^{\mu\nu\mu_2\nu_2\mu_3\nu_3}(x; \partial_1, \partial_2, \partial_3) \\ i \left[\mu_2\nu_2 \Delta_{\alpha_1\beta_1} \right] (x; x') i \left[\mu_3\nu_3 \Delta_{\rho_1\sigma_1} \right] (x; x'') \sum_{A=1}^{79} \Pi_A^{\alpha_1\beta_1\rho_1\sigma_1}$$

* It is not very efficient to use FeynCalc this way because most of the 2 megabytes memory of the program goes to define operations we never need. After completing the calculation we wrote a very short contraction program in collaboration with G. G. Huey which reproduces the tiny portion of FeynCalc we actually used.

$$\begin{aligned}
& \left\{ C_{1A} + t \cdot \partial'_1 C_{2A} + y \cdot \partial'_1 C_{3A} + t \cdot \partial''_1 C_{4A} + y \cdot \partial''_1 C_{5A} \right. \\
& \quad + (t \cdot \partial'_1) (t \cdot \partial''_1) C_{6A} + (t \cdot \partial'_1) (y \cdot \partial''_1) C_{7A} + (y \cdot \partial'_1) (t \cdot \partial''_1) C_{8A} \\
& \quad \left. + (y \cdot \partial'_1) (y \cdot \partial''_1) C_{9A} + \partial'_1 \cdot \partial''_1 C_{10A} \right\} . \tag{3.11}
\end{aligned}$$

What we call “the inner loop” part begins with the sum over A .

As an example, consider the contribution to the inner loop of (4a) from the vertex $j = k = 41$ of Table 3:

$$\begin{aligned}
(\text{inner})_{41,41} & \equiv \left\{ V_{41}^{\alpha_1 \beta_1 \alpha_2 \beta_2 \alpha_3 \beta_3} (x'; \partial'_1, \partial'_2, \partial'_3) i \left[\alpha_2 \beta_2 \Delta_{\rho_2 \sigma_2} \right] (x'; x'') i \left[\alpha_3 \beta_3 \Delta_{\rho_3 \sigma_3} \right] (x'; x'') \right. \\
& \quad \left. V_{41}^{\rho_1 \sigma_1 \rho_2 \sigma_2 \rho_3 \sigma_3} (x''; \partial''_1, \partial''_2, \partial''_3) \right\} \\
& = \kappa^2 \Omega'^2 \Omega''^2 \partial'_1 \cdot \partial'_3 \partial''_1 \cdot \partial''_3 \eta^{\alpha_1 (\alpha_2 \eta^{\beta_2} (\alpha_3 \eta^{\beta_3} (\beta_1 \eta^{\rho_1} (\rho_2 \eta^{\sigma_2} (\rho_3 \eta^{\sigma_3} (\sigma_1 \\
& \quad \left\{ i \Delta_{2N} \left[2 \eta_{\alpha_2 (\rho_2 \eta_{\sigma_2} \beta_2} - \eta_{\alpha_2 \beta_2} \eta_{\rho_2 \sigma_2} \right] \right. \\
& \quad \left. - i \Delta_{2L} \left[2 \bar{\eta}_{\alpha_2 (\rho_2 \bar{\eta}_{\sigma_2} \beta_2} - 2 \bar{\eta}_{\alpha_2 \beta_2} \bar{\eta}_{\rho_2 \sigma_2} \right] \right\} \\
& \quad \left\{ i \Delta_{3N} \left[2 \eta_{\alpha_3 (\rho_3 \eta_{\sigma_3} \beta_3} - \eta_{\alpha_3 \beta_3} \eta_{\rho_3 \sigma_3} \right] \right. \\
& \quad \left. - i \Delta_{3L} \left[2 \bar{\eta}_{\alpha_3 (\rho_3 \bar{\eta}_{\sigma_3} \beta_3} - 2 \bar{\eta}_{\alpha_3 \beta_3} \bar{\eta}_{\rho_3 \sigma_3} \right] \right\} . \tag{3.12}
\end{aligned}$$

After the contractions we obtain:

$$\begin{aligned}
(\text{inner})_{41,41} & = \kappa^2 \Omega'^2 \Omega''^2 \partial'_1 \cdot \partial'_3 \partial''_1 \cdot \partial''_3 \left\{ i \Delta_{2N} i \Delta_{3N} \left[2 \eta^{\alpha_1 \beta_1} \eta^{\rho_1 \sigma_1} + 2 \eta^{\alpha_1 (\rho_1 \eta^{\sigma_1} \beta_1)} \right] \right. \\
& \quad + \left(i \Delta_{2N} i \Delta_{3L} + i \Delta_{2L} i \Delta_{3N} \right) \left[-3 \eta^{\alpha_1 \beta_1} \eta^{\rho_1 \sigma_1} + \eta^{\alpha_1 (\rho_1 \eta^{\sigma_1} \beta_1)} \right. \\
& \quad \left. - 3 \eta^{\alpha_1 \beta_1} t^{\rho_1} t^{\sigma_1} - 3 t^{\alpha_1} t^{\beta_1} \eta^{\rho_1 \sigma_1} + 4 t^{(\alpha_1 \eta^{\beta_1} (\rho_1 t^{\sigma_1))} \right] \\
& \quad + i \Delta_{2L} i \Delta_{3L} \left[5 \eta^{\alpha_1 \beta_1} \eta^{\rho_1 \sigma_1} - 3 \eta^{\alpha_1 (\rho_1 \eta^{\sigma_1} \beta_1)} + 5 \eta^{\alpha_1 \beta_1} t^{\rho_1} t^{\sigma_1} \right. \\
& \quad \left. + 5 t^{\alpha_1} t^{\beta_1} \eta^{\rho_1 \sigma_1} - 6 t^{(\alpha_1 \eta^{\beta_1} (\rho_1 t^{\sigma_1))} + 2 t^{\alpha_1} t^{\beta_1} t^{\rho_1} t^{\sigma_1} \right] \left. \right\} . \tag{3.13}
\end{aligned}$$

At this stage we recognize six of the 4-index objects:

$$\Pi_1^{\alpha_1 \beta_1 \rho_1 \sigma_1} \equiv \eta^{\alpha_1 \beta_1} \eta^{\rho_1 \sigma_1} \quad , \quad \Pi_4^{\alpha_1 \beta_1 \rho_1 \sigma_1} \equiv t^{\alpha_1} t^{\beta_1} \eta^{\rho_1 \sigma_1} ; \tag{3.14a}$$

$$\Pi_2^{\alpha_1 \beta_1 \rho_1 \sigma_1} \equiv \eta^{\alpha_1 (\rho_1 \eta^{\sigma_1} \beta_1)} \quad , \quad \Pi_9^{\alpha_1 \beta_1 \rho_1 \sigma_1} \equiv t^{(\alpha_1 \eta^{\beta_1} (\rho_1 t^{\sigma_1))} ; \tag{3.14b}$$

$$\Pi_3^{\alpha_1\beta_1\rho_1\sigma_1} \equiv \eta^{\alpha_1\beta_1} t^{\rho_1} t^{\sigma_1} \quad , \quad \Pi_{13}^{\alpha_1\beta_1\rho_1\sigma_1} \equiv t^{\alpha_1} t^{\beta_1} t^{\rho_1} t^{\sigma_1} . \quad (3.14c)$$

There does not seem to be any point in giving the entire list of the 79 objects since we will not use them further. Dropping the indices and acting the derivatives gives:

$$\begin{aligned} (\text{inner})_{41,41} = \frac{\kappa^2}{2^6\pi^4} \left\{ \left(-\frac{32x\cdot\partial'_1 x\cdot\partial''_1}{x^8} + \frac{8\partial'_1\cdot\partial''_1}{x^6} + \frac{8x\cdot\partial'_1 t\cdot\partial''_1}{u''x^6} - \frac{8t\cdot\partial'_1 x\cdot\partial''_1}{u'x^6} + \frac{4t\cdot\partial'_1 t\cdot\partial''_1}{u'u''x^4} \right) [2\Pi_1 + 2\Pi_2] \right. \\ + \left[\left(-\frac{16x\cdot\partial'_1 x\cdot\partial''_1}{u'u''x^6} + \frac{4\partial'_1\cdot\partial''_1}{u'u''x^4} + \frac{4x\cdot\partial'_1 t\cdot\partial''_1}{u'u''x^4} - \frac{4t\cdot\partial'_1 x\cdot\partial''_1}{u'^2u''x^4} + \frac{2t\cdot\partial'_1 t\cdot\partial''_1}{u'^2u''x^2} \right) \ln(H^2x^2) \right. \\ \left. \left. + \left(-\frac{4\partial'_1\cdot\partial''_1}{u'u''x^4} + \frac{8x\cdot\partial'_1 x\cdot\partial''_1}{u'u''x^6} \right) \right] [-3\Pi_1 + \Pi_2 - 3\Pi_3 - 3\Pi_4 + 4\Pi_9] \right. \\ + \left(-\frac{2\partial'_1\cdot\partial''_1}{u'^2u''x^2} + \frac{4x\cdot\partial'_1 x\cdot\partial''_1}{u'^2u''x^4} \right) \ln(H^2x^2) \\ \left. \left. \left[5\Pi_1 - 3\Pi_2 + 5\Pi_3 + 5\Pi_4 - 6\Pi_9 + 2\Pi_{13} \right] \right\} , \quad (3.15) \end{aligned}$$

from which we recognize 27 non-zero coefficient functions. A few examples are:

$$C_{61}(u', u'', y^2) = -\frac{64}{y^8} - \frac{24}{u'u''y^6} + \frac{48\ln(H^2y^2)}{u'u''y^6} + \frac{20\ln(H^2y^2)}{u'^2u''y^4} , \quad (3.16a)$$

$$C_{82}(u', u'', y^2) = \frac{16}{u''y^6} + \frac{4\ln(H^2y^2)}{u'u''y^4} , \quad (3.16b)$$

$$C_{1013}(u', u'', y^2) = -\frac{4\ln(H^2y^2)}{u'^2u''y^2} . \quad (3.16c)$$

3.2 Outer Loop Tensor Algebra and Derivatives.

What we mean by the outer loop tensor algebra is the contractions over $\alpha_1, \beta_1; \rho_1, \sigma_1; \mu_{2-3}$ and ν_{2-3} . What we mean by the outer loop derivatives are $\partial'_1, \partial''_1$ and ∂_{2-3} . The single possible derivative on the external leg acts backwards on the entire expression, including the limits of integration. Only its 0-component survives:

$$\partial_1^\mu \longrightarrow t^\mu \partial_u . \quad (3.17)$$

The great advantage of the representation (3.11) we use for the inner loop is that it isolates the relatively simple dependence upon derivatives and indices from the very complicated coefficient functions $C_{mA}(u', u'', y^2)$. We can contract the indices and act the various derivatives for each coefficient function without having to worry about its functional form.

An additional simplification is that we can contract the external indices, μ and ν , into the two independent tensors — $\eta_{\mu\nu}$ and $t_\mu t_\nu$ — which survive the integrations. So the outer loop result can be expressed in terms of $2 \times (10 \times 79) = 1580$ outer coefficient functions:

$$\begin{aligned} \alpha_{mA}(u, u', u'', w^2, y^2, z^2; \partial_u) &\equiv \eta_{\mu\nu} \sum_{i=1}^{43} V_i^{\mu\nu\mu_2\nu_2\mu_3\nu_3}(x; \partial_1, \partial_2, \partial_3) \\ &\mathcal{D}_m(y, \partial'_1, \partial''_1) \Pi_A^{\alpha_1\beta_1\rho_1\sigma_1}(y, \partial'_1, \partial''_1) \\ &i\left[\mu_2\nu_2\Delta_{\alpha_1\beta_1}\right](x; x') \quad i\left[\mu_3\nu_3\Delta_{\rho_1\sigma_1}\right](x; x'') \quad , \quad (3.18a) \end{aligned}$$

$$\begin{aligned} \gamma_{mA}(u, u', u'', w^2, y^2, z^2; \partial_u) &\equiv t_\mu t_\nu \sum_{i=1}^{43} V_i^{\mu\nu\mu_2\nu_2\mu_3\nu_3}(x; \partial_1, \partial_2, \partial_3) \\ &\mathcal{D}_m(y, \partial'_1, \partial''_1) \Pi_A^{\alpha_1\beta_1\rho_1\sigma_1}(y, \partial'_1, \partial''_1) \\ &i\left[\mu_2\nu_2\Delta_{\alpha_1\beta_1}\right](x; x') \quad i\left[\mu_3\nu_3\Delta_{\rho_1\sigma_1}\right](x; x'') \quad . \quad (3.18b) \end{aligned}$$

The ten contracted derivatives $\mathcal{D}_m(y, \partial'_1, \partial''_1)$ are defined in expression (3.11). Because no derivative can appear more than once, the inner coefficient function C_{mA} is automatically zero for those combinations of m and A where either ∂'_1 or ∂''_1 appears in both the contracted derivative and the 4-index object, $\Pi_A^{\alpha_1\beta_1\rho_1\sigma_1}(y, \partial'_1, \partial''_1)$. This means that only 696 of the coefficients (3.18) were actually used, so of course only these were computed.

We should comment on how the outer coefficient functions (3.18) can be reduced to dependence upon only the three conformal times — u , u' , and u'' — and the three Lorentz squares of (3.2) — w^2 , y^2 and z^2 . First, one can re-express contractions of spatial vectors in terms of Lorentz contractions and 0-components:

$$\vec{a} \cdot \vec{b} = a \cdot b + a^0 b^0 \quad . \quad (3.19)$$

Second, contractions involving $t_\mu \equiv \eta_{\mu 0}$ can be expressed as follows:

$$t \cdot t = -1 \quad ; \quad (3.20a)$$

$$t \cdot w = u' - u \quad , \quad t \cdot y = u'' - u' \quad , \quad t \cdot z = u - u'' \quad . \quad (3.20b)$$

Finally, dot products between the three coordinate differences can always be expressed in terms of the Lorentz squares:

$$\begin{aligned}
w \cdot y &= \frac{1}{2}(-w^2 - y^2 + z^2) \ , \\
y \cdot z &= \frac{1}{2}(w^2 - y^2 - z^2) \ , \\
z \cdot w &= \frac{1}{2}(-w^2 + y^2 - z^2) \ .
\end{aligned} \tag{3.21}$$

Because the outer coefficient functions involve a sum over the 43 outer vertex operators, they often have lengthy expressions. One of reasonable size is γ_{113} :

$$\begin{aligned}
\gamma_{113}(u, u', u'', w^2, y^2, z^2; \partial_u) &= \frac{\kappa H^2}{2^6 \pi^4} \partial_u \left\{ \frac{12u'u''}{uw^2z^2} + \frac{8(u'-u)u'u''}{w^4z^2} - \frac{8u'(u''-u)u''}{w^2z^4} \right\} \\
&+ \frac{\kappa H^2}{2^6 \pi^4} \left\{ -\frac{3u'u''}{u^2w^2z^2} - \frac{10(u'-u)u'u''}{uw^4z^2} + \frac{22u'(u''-u)u''}{uw^2z^4} \right. \\
&\quad \left. - \frac{24(u'-u)u'(u''-u)u''}{w^4z^4} + \frac{6u'u''(-w^2+y^2-z^2)}{w^4z^4} \right\} \ . \tag{3.22}
\end{aligned}$$

Terms containing single factors of $\ln(H^2w^2)$ and/or $\ln(H^2z^2)$ can also appear but in these cases the outer loop coefficient functions are too lengthy to display. Note that the external leg derivative ∂_u is really still a free operator at this stage since it can also act on the u -dependence in the limits of the conformal time integrations.

The $i = 34$ contribution to α_{51} is in some ways more representative of what is involved in computing an outer loop coefficient function:

$$\begin{aligned}
\alpha_{51} &= \eta_{\mu\nu} V_{34}^{\mu\nu\mu_2\nu_2\mu_3\nu_3}(x; \partial_1, \partial_2, \partial_3) \mathcal{D}_5(y, \partial'_1, \partial''_1) \Pi_1^{\alpha_1\beta_1\rho_1\sigma_1}(y, \partial'_1, \partial''_1) \\
&\quad i \left[\mu_2\nu_2 \Delta_{\alpha_1\beta_1} \right](x; x') \quad i \left[\mu_3\nu_3 \Delta_{\rho_1\sigma_1} \right](x; x'') \\
&= -2\kappa \Omega^2 \eta^{\mu_2(\mu_3} \eta^{\nu_3)\nu_2} \partial_u \quad t \cdot \partial_3 \quad y \cdot \partial'_1 \eta^{\alpha_1\beta_1} \eta^{\rho_1\sigma_1} \\
&\quad \left\{ i\Delta_{2N} \left[2 \eta_{\mu_2(\alpha_1} \eta_{\beta_1)\nu_2} - \eta_{\mu_2\nu_2} \eta_{\alpha_1\beta_1} \right] \right. \\
&\quad \left. - i\Delta_{2L} \left[2 \bar{\eta}_{\mu_2(\alpha_1} \bar{\eta}_{\beta_1)\nu_2} - 2 \bar{\eta}_{\alpha_1\beta_1} \bar{\eta}_{\alpha_1\beta_1} \right] \right\} \\
&\quad \left\{ i\Delta_{3N} \left[2 \eta_{\mu_3(\rho_1} \eta_{\sigma_1)\nu_3} - \eta_{\mu_3\nu_3} \eta_{\rho_1\sigma_1} \right] \right.
\end{aligned}$$

$$- i\Delta_{3L} \left[2 \bar{\eta}_{\mu_3(\rho_1} \bar{\eta}_{\sigma_1)\nu_3} - 2 \bar{\eta}_{\mu_3\nu_3} \bar{\eta}_{\rho_1\sigma_1} \right] \} \quad (3.23a)$$

$$= - 2\kappa \Omega^2 \partial_u t \cdot \partial_3 y \cdot \partial_1'' \left\{ 16 i\Delta_{2N} i\Delta_{3N} \right. \\ \left. - 48 \left(i\Delta_{2N} i\Delta_{3L} + i\Delta_{2L} i\Delta_{3N} \right) + 48 i\Delta_{2L} i\Delta_{3L} \right\} \quad (3.23b)$$

$$= \frac{\kappa H^2}{2^6 \pi^4} \left\{ - \frac{256u'(u''-u')}{uw^2z^2} - \frac{256u'(u''-u)}{w^2z^4} + \frac{128u'u''(w^2-y^2-z^2)}{uw^2z^4} \right. \\ \left. - \frac{384u'(u''-u)(w^2-y^2-z^2)}{uw^2z^4} - \frac{512u'(u''-u)u''(w^2-y^2-z^2)}{w^2z^6} \right. \\ \left. + \partial_u \left[\frac{384(u''-u')}{u^2z^2} + \frac{384u'(u''-u)}{uz^4} - \frac{192u''(w^2-y^2-z^2)}{u^2z^4} \right] \right. \\ \left. + \frac{192(u''-u)(w^2-y^2-z^2)}{u^2z^4} + \frac{768(u''-u)u''(w^2-y^2-z^2)}{uz^6} \right] \ln(H^2w^2) \} . \quad (3.23c)$$

Note again that ∂_u is a free operator at this stage. It will eventually act on all u 's, including those in the limits of integration.

3.3 Re-Organization of the Integrals.

By adding to a generic integrand $I(x, x', x'')$ its reflection under $x''^\mu \leftrightarrow x'^{\mu}$, we can make the integrand symmetric. We can then enforce a canonical time ordering, $u \leq u' \leq u'' \leq H^{-1}$, by splitting the conformal time integrations into halves with u' before and after u'' , and changing variables:

$$\int_u^{H^{-1}} du' \int d^3r' \int_u^{H^{-1}} du'' \int d^3r'' I(x, x', x'') \\ = \frac{1}{2} \int_u^{H^{-1}} du' \int d^3r' \int_u^{H^{-1}} du'' \int d^3r'' \left[I(x, x', x'') + I(x, x'', x') \right] \quad (3.24a)$$

$$= \int_u^{H^{-1}} du' \int d^3r' \int_{u'}^{H^{-1}} du'' \int d^3r'' \left[I(x, x', x'') + I(x, x'', x') \right] . \quad (3.24b)$$

The advantage of ordering the conformal times is that the three d 's can be written without using absolute value symbols. With the ordering chosen, they are as given on Table 1.

The generic integrands for each 3-3-3 diagram can be obtained by contracting the integrands of expressions (3.9a-c) alternately with $\eta_{\mu\nu}$ (to give the α -contraction) and with $t_\mu t_\nu$ (to give the γ -contraction). We can express the integrands for diagrams (4a)

and (4b) by summing over the inner and outer loop coefficient functions:

$$\begin{aligned} & \begin{bmatrix} \alpha \\ \gamma \end{bmatrix} (u, u', u'', w^2, y^2, z^2; \partial_u) \\ &= \kappa \sum_{m=1}^{10} \sum_{A=1}^{79} \begin{bmatrix} \alpha \\ \gamma \end{bmatrix}_{mA} (u, u', u'', w^2, y^2, z^2; \partial_u) C_{mA}(u', u'', y^2) . \end{aligned} \quad (3.25)$$

The analogous integrands for diagram (4c) are simple enough to compute without distinguishing between inner and outer loop tensor algebra and derivatives. Performing the integrals gives each diagram's contribution to the α and γ contractions of the amputated 1-point function:

$$\begin{aligned} \begin{bmatrix} \alpha \\ \gamma \end{bmatrix} (u) &\equiv \int_u^{H^{-1}} du' \int d^3x' \int_{u'}^{H^{-1}} du'' \int d^3x'' \\ &\left\{ \begin{bmatrix} \alpha \\ \gamma \end{bmatrix} (u, u', u'', w^2, y^2, z^2, \partial_u) + \begin{bmatrix} \alpha \\ \gamma \end{bmatrix} (u, u'', u', z^2, y^2, w^2; \partial_u) \right\} . \end{aligned} \quad (3.26)$$

(Note that the free operator ∂_u acts *outside* the integrals.) And the diagram's contributions to the coefficients $a(u)$ and $c(u)$ of (2.19) are:

$$a(u) = \frac{1}{3} \left[\alpha(u) + \gamma(u) \right] , \quad (3.27a)$$

$$c(u) = \gamma(u) . \quad (3.27b)$$

It is useful to extract the universal constant factors which result from the initial κ , the three vertices, and the four propagators:

$$\kappa \times \left(\frac{\kappa}{H^2} \right)^3 \times \left(\frac{H^2}{2^3 \pi^2} \right)^4 = \frac{\kappa^4 H^2}{2^{12} \pi^8} . \quad (3.28)$$

It is also useful to split the various integrands up according to which, if any, of the three possible logarithms they contain. Recall from sub-section 2.9 that at most one logarithm from the propagators can survive differentiation. We therefore have four possibilities: a single factor of $\ln(H^2 w^2)$, a single factor of $\ln(H^2 y^2)$, a single factor of $\ln(H^2 z^2)$, or no logarithms at all. A final re-organization is to break the integrands up into monomials of

the three conformal times and the three Lorentz squares. What results is a dauntingly diverse series of integrals having the general form:

$$\# \frac{\kappa^4 H^2}{2^{12} \pi^8} (\partial_u)^{0,1} \int_u^{H^{-1}} du' \int_{u'}^{H^{-1}} du'' \frac{1}{(u)^i (u')^j (u'')^k} \int d^3 r' \int d^3 r'' \frac{\ln^{0,1} [H^2 (w^2, y^2, z^2)]}{(w^2)^\ell (y^2)^m (z^2)^n} . \quad (3.29)$$

The exponents of the various conformal times may be negative, and are always ≤ 2 . The exponents of the Lorentz squares may also be negative. Those for w^2 and z^2 can range from $+3$ to -2 , while the one for y^2 can range from $+6$ to -2 . It should also be noted that dimensional analysis constrains the sum $[i + j + k + 2(\ell + m + n)]$ to be either eleven, if there is an external ∂_u , or twelve if there is not.

3.4 The Angular Integrations.

When the vectors \vec{r}' and \vec{r}'' are written using a polar coordinate system in which the z axis of \vec{r}'' is along \vec{r}' , the three Lorentz squares have the following simple expressions:

$$w^2 = r'^2 - (d_w - i\epsilon)^2 = (r' - d_w + i\epsilon) (r' + d_w - i\epsilon) , \quad (3.30a)$$

$$z^2 = r''^2 - (d_z - i\epsilon)^2 = (r'' - d_z + i\epsilon) (r'' + d_z - i\epsilon) , \quad (3.30b)$$

$$y^2 = r'^2 - 2r'r'' \cos(\theta'') + r''^2 - (d_y - i\epsilon)^2 . \quad (3.30c)$$

Since the various integrands depend only on the \vec{r}'' zenith angle, we can perform the other angular integrations trivially:

$$\int_0^{2\pi} d\phi' \int_0^\pi d\theta' \sin(\theta') \int_0^{2\pi} d\phi'' = 8\pi^2 . \quad (3.31)$$

This factor is universal and we multiply it into the other universal factors (3.28). When there is no $\ln(H^2 y^2)$ and $m \neq 1$ the integral over θ'' gives:

$$\int_0^\pi d\theta'' \frac{\sin(\theta'')}{(y^2)^m} = \frac{-1}{2(m-1)r'r''} \left[r'^2 - 2r'r'' \cos(\theta'') + (r'')^2 - (d_y - i\epsilon)^2 \right]^{1-m} \quad (3.32a)$$

$$= \frac{-1}{2(m-1)r'r''} \left\{ \left[(r' + r'')^2 - (d_y - i\epsilon)^2 \right]^{1-m} - \left[(r' - r'')^2 - (d_y - i\epsilon)^2 \right]^{1-m} \right\} . \quad (3.32b)$$

When there is a $\ln(H^2 y^2)$ and $m \neq 1$ the integral over θ'' gives:

$$\begin{aligned} & \int_0^\pi d\theta'' \sin(\theta'') \frac{\ln(H^2 y^2)}{(y^2)^m} \\ &= \frac{-1}{2(m-1)r'r''} \left\{ \frac{\ln \left[\left((r' + r'')^2 - (d_y - i\epsilon)^2 \right) \right] + \frac{1}{m-1}}{\left[(r' + r'')^2 - (d_y - i\epsilon)^2 \right]^{m-1}} - \left(r'' \rightarrow -r'' \right) \right\} . \end{aligned} \quad (3.33)$$

When $m = 1$ one gets a new logarithm:

$$\int_0^\pi d\theta'' \sin(\theta'') \frac{1}{y^2} = \frac{-1}{2r'r''} \left\{ \ln \left[(r' + r'')^2 - (d_y - i\epsilon)^2 \right] - \left(r'' \rightarrow -r'' \right) \right\} , \quad (3.34a)$$

$$\int_0^\pi d\theta'' \sin(\theta'') \frac{\ln(H^2 y^2)}{y^2} = \frac{-1}{4r'r''} \left\{ \ln^2 \left[(r' + r'')^2 - (d_y - i\epsilon)^2 \right] - \left(r'' \rightarrow -r'' \right) \right\} \quad (3.34b)$$

In this case we always eliminate the extra logarithm by partially integrating on one of the radial variables or conformal times.

It is useful at this stage to absorb the lower limit of the angular integration — the $r'' \rightarrow -r''$ term in (3.32b), (3.33) and (3.34a-b) — into an extension in the ranges of the radial integrations. For the case of a $\ln(H^2 y^2)$ and $m \neq 1$ the extension goes as follows:

$$\begin{aligned} & \int_0^\infty dr' r'^2 \int_0^\infty dr'' r''^2 \frac{1}{(w^2)^\ell (z^2)^n} \times \frac{-1}{2(m-1)r'r''} \\ & \quad \left\{ \frac{\ln \left[H^2 \left((r' + r'')^2 - (d_y - i\epsilon)^2 \right) \right] + \frac{1}{m-1}}{\left[(r' + r'')^2 - (d_y - i\epsilon)^2 \right]^{m-1}} - \left(r'' \rightarrow -r'' \right) \right\} \\ &= -\frac{1}{2(m-1)} \int_0^\infty dr' r' \int_{-\infty}^\infty dr'' r'' \frac{\ln \left[H^2 \left((r' + r'')^2 - (d_y - i\epsilon)^2 \right) \right] + \frac{1}{m-1}}{(w^2)^\ell \left[(r' + r'')^2 - (d_y - i\epsilon)^2 \right]^{m-1} (z^2)^n} \end{aligned} \quad (3.35a)$$

$$= -\frac{1}{4(m-1)} \int_{-\infty}^\infty dr' r' \int_{-\infty}^\infty dr'' r'' \frac{\ln \left[H^2 \left((r' + r'')^2 - (d_y - i\epsilon)^2 \right) \right] + \frac{1}{m-1}}{(w^2)^\ell \left[(r' + r'')^2 - (d_y - i\epsilon)^2 \right]^{m-1} (z^2)^n} . \quad (3.35b)$$

The reduction is similar for the other cases.

We denote by Y^2 the combination of terms which descends from y^2 after performing the angular integrations and extending the radial ranges:

$$Y^2 \equiv (r' + r'')^2 - (d_y - i\epsilon)^2 = (r' + r'' - d_y + i\epsilon) (r' + r'' - d_y - i\epsilon) . \quad (3.36)$$

At this stage the answer is a long series of integrals of the form:

$$\# \frac{\kappa^4 H^2}{29\pi^6} (\partial_u)^{0,1} \int_u^{H^{-1}} du' \int_{u'}^{H^{-1}} du'' \frac{1}{(u)^i (u')^j (u'')^k} \int_{-\infty}^{\infty} dr' \int_{-\infty}^{\infty} dr'' Q \frac{\ln^{0,1} [H^2 (w^2, Y^2, z^2)]}{(w^2)^\ell (Y^2)^m (z^2)^n} . \quad (3.37)$$

where Q is a quadratic function of r' and r'' whose precise form depends upon what, if any, partial integrations were done to eliminate extra logarithms.

3.5 The Radial Integrations.

Since w^2 , z^2 and Y^2 factorize into products of linear functions of r' and r'' , the method of contours is especially effective. Note that the single possible logarithm can always be decomposed into a part which is analytic in the upper half plane and another part which is analytic in the lower half plane, for instance:

$$\ln(H^2 z^2) = \ln [H(r'' - d_z + i\epsilon)] + \ln [H(r'' + d_z - i\epsilon)] . \quad (3.38)$$

The factor of $(2\pi)^2$ which comes from the two contour integrations is universal and is multiplied in with the rest.

As an example, consider (3.35b) with $\ell = n = 1$ and $m = 2$:

$$\begin{aligned} & -\frac{1}{4} \int_{-\infty}^{\infty} dr' r' \int_{-\infty}^{\infty} dr'' r'' \frac{\ln(H^2 Y^2) + 1}{w^2 z^2 Y^2} \\ &= -\frac{\pi^2}{4} \frac{1}{(d_w + d_z + d_y - 3i\epsilon) (d_y - i\epsilon)} \\ &+ \frac{\pi^2}{4} \frac{d_y \ln [H(d_w + d_z + d_y - 3i\epsilon)] - (d_w + d_z) \ln [2H(d_y - i\epsilon)]}{(d_w + d_z + d_y - 3i\epsilon) (d_w + d_z - d_y - i\epsilon) (d_y - i\epsilon)} \\ &+ \frac{\pi^2}{4} \frac{d_y \ln [-H(d_w + d_z + d_y - 3i\epsilon)] - (d_w + d_z) \ln [-2H(d_y - i\epsilon)]}{(d_w + d_z + d_y - 3i\epsilon) (d_w + d_z - d_y - i\epsilon) (d_y - i\epsilon)} . \quad (3.39) \end{aligned}$$

Note that there is no pole for $d_y = d_w + d_z$; in this case the numerator vanishes as well as the denominator and the residue is finite. Note also that this integral can be differentiated with respect to d_w and d_z to give a generating function for integrals with higher ℓ and n

values. In fact only a handful of the radial integrations really need to be computed directly, although this was done anyway as a check on accuracy.

For large exponents the results can be quite a bit longer than (3.39). In the general case one also has to expect logarithms and inverse powers of $d_w - i\epsilon$ and $d_z - i\epsilon$. The form we reach after doing the radial integrations is a long sum of conformal time integrations of the following type:

$$\# \frac{\kappa^4 H^2}{2^7 \pi^4} (\partial_u)^{0,1} \int_u^{H^{-1}} du' \int_{u'}^{H^{-1}} du'' \frac{1}{(u)^i (u')^j (u'')^k} \frac{\ln^{0,1} \left[\pm H (2d_w - 2i\epsilon, 2d_z - 2i\epsilon, 2d_y - 2i\epsilon, d_w + d_z + d_y - 3i\epsilon) \right]}{(d_w - i\epsilon)^\zeta (d_z - i\epsilon)^\lambda (d_y - i\epsilon)^\xi (d_w + d_z + d_y - 3i\epsilon)^\sigma (d_w + d_z - d_y - i\epsilon)^\tau} . \quad (3.40)$$

3.6 The Conformal Time Integrations.

It is at this stage that the “ \pm ” variations of the vertices become important. One has to sum (3.40) over the four possibilities, with the d ’s assigned as in Table 1, and with a factor of -1 for each “ $-$ ” vertex. One can see from Table 1 that the three d ’s are always plus or minus the associated coordinate differences, for example, $d_z = \pm(u' - u)$. However, the two sums which can occur behave quite differently for the “ $++$ ” and “ $--$ ” variations:

$$d_w + d_z + d_y = \pm 2 (u'' - u) \quad , \quad d_w + d_z - d_y = \pm 2 (u' - u) \quad ; \quad (3.41a)$$

than for the “ $+ -$ ” and “ $- +$ ” variations:

$$d_w + d_z + d_y = \pm 2 (u'' - u') \quad , \quad d_w + d_z - d_y = 0 \quad . \quad (3.41b)$$

As noted above, apparent poles in at $d_y = d_w + d_z$ are always spurious. They are evaluated, for the “ $+ -$ ” and “ $- +$ ” variations, by first taking the limit $d_y \rightarrow d_w + d_z$, and then substituting for d_w and d_z from Table 1.

The obvious strategy at this point is to decompose the integrands by partial fractions. Because only single powers of logarithms arise, this will always suffice to reduce the result

to a single integral.* The remaining integral can also be decomposed by partial fractions, however, an integral of the form:

$$\int dx \frac{\ln(x-a)}{x-b} , \quad (3.42)$$

cannot be expressed in terms of elementary functions for $a \neq b$. When this occurs the strategy is to first extract any ultraviolet divergences by partial integration, then expand the logarithm and integrate termwise. Since we only require the leading order form as $u \rightarrow 0^+$, this is straightforward. Consider, for example, the following:

$$\int_u^{H^{-1}} du' \frac{\ln(Hu')}{u' - u - i\epsilon} = \ln(Hu') \ln[H(u' - u - i\epsilon)] \Big|_u^{H^{-1}} - \int_u^{H^{-1}} \frac{du'}{u'} \ln[H(u' - u)] \quad (3.43a)$$

$$= -\ln(Hu) \ln(-iH\epsilon) - \int_u^{H^{-1}} \frac{du'}{u'} \left[\ln(Hu') - \sum_{n=1}^{\infty} \frac{1}{n} \left(\frac{u}{u'}\right)^n \right] \quad (3.43b)$$

$$= -\ln(Hu) \ln(-iH\epsilon) + \frac{1}{2} \ln^2(Hu) + \sum_{n=1}^{\infty} \frac{1}{n^2} \left[1 - (Hu)^n \right] . \quad (3.43c)$$

Of course one can use these methods to perform the integrations in the original order and with the original variables of expression (3.40). We did it both ways and compared each term as a check on accuracy.

We have selected, as an example, the term which emerges from step 3 above in the form:

$$\# \frac{\kappa^4 H^2}{2^{12} \pi^8} \partial_u \int_u^{H^{-1}} du' \int_{u'}^{H^{-1}} \frac{du''}{u^2 u''} \int d^3 r' \int d^3 r'' \frac{\ln(H^2 y^2)}{w^2 y^4 z^2} . \quad (3.44)$$

It has already been shown that the integrations over \vec{r}' and \vec{r}'' give:

$$\begin{aligned} & \# \frac{1}{16} \frac{\kappa^4 H^2}{2^7 \pi^4} \partial_u \int_u^{H^{-1}} du' \int_{u'}^{H^{-1}} \frac{du''}{u^2 u''} \left\{ -\frac{1}{(d_w + d_z + d_y - 3i\epsilon)(d_y - i\epsilon)} \right. \\ & + \frac{d_y \ln[H(d_w + d_z + d_y - 3i\epsilon)] - (d_w + d_z) \ln[2H(d_y - i\epsilon)]}{(d_w + d_z + d_y - 3i\epsilon)(d_w + d_z - d_y - i\epsilon)(d_y - i\epsilon)} \\ & \left. + (H \rightarrow -H) \right\} . \quad (3.45) \end{aligned}$$

* Although sometimes not in terms of either u' or u'' .

If we neglect terms of order ϵ , the “++” and “+-” variations give the following expressions:

$$\begin{aligned} \# \frac{1}{16} \frac{\kappa^4 H^2}{27\pi^4} \partial_u \int_u^{H^{-1}} du' \int_{u'}^{H^{-1}} \frac{du''}{u^2 u''} \left\{ -\frac{1}{2} \frac{1}{(u'' - u' - i\epsilon)(u'' - u - i\epsilon)} \right. \\ \left. + \frac{1}{4} \frac{\ln[2H(u'' - u - i\epsilon)]}{(u'' - u - i\epsilon)(u' - u - i\epsilon)} - \frac{1}{4} \frac{\ln[2H(u'' - u' - i\epsilon)]}{(u'' - u - i\epsilon)(u'' - u' - i\epsilon)} \right. \\ \left. - \frac{1}{4} \frac{\ln[2H(u'' - u' - i\epsilon)]}{(u'' - u' - i\epsilon)(u' - u - i\epsilon)} + (H \rightarrow -H) \right\} , \end{aligned} \quad (3.46a)$$

$$-\# \frac{1}{16} \frac{\kappa^4 H^2}{27\pi^4} \partial_u \int_u^{H^{-1}} du' \int_{u'}^{H^{-1}} du'' \frac{\ln[-2H(u'' - u' + i\epsilon)] + (H \rightarrow -H)}{2 u^2 u'' (u'' - u' + i\epsilon)^2} . \quad (3.46b)$$

The “--” and “-+” variations can be obtained by complex conjugation of (3.46a) and (3.46b), respectively.

The first integral in the “++” variation (3.46a) has a simple result:

$$\begin{aligned} -\frac{1}{2u^2} \int_u^{H^{-1}} du' \int_{u'}^{H^{-1}} \frac{du''}{u''(u'' - u' - i\epsilon)(u'' - u - i\epsilon)} = \quad (3.47a) \\ \frac{1}{2u^3} \sum_{n=1}^{\infty} \frac{(Hu)^n - 1}{n^2} + \frac{1}{4u^3} \left\{ -\ln^2\left(\frac{-i\epsilon}{u}\right) + 2\ln(-iH\epsilon) \ln(1 - Hu) - \ln^2(1 - Hu) \right\} . \end{aligned}$$

Note how it illustrates the arguments given in sub-section 2.7 for the inevitability of infrared logarithms when an ℓ -loop graph contains ℓ logarithmic ultraviolet divergences. Nice as it is to have exact expressions, what we really want is an asymptotic expansion for late times ($u \rightarrow 0^+$):

$$-\frac{1}{2u^2} \int_u^{H^{-1}} du' \int_{u'}^{H^{-1}} \frac{du''}{u''(u'' - u' - i\epsilon)(u'' - u - i\epsilon)} = -\frac{\ln^2(Hu)}{4u^3} + O\left(\frac{\ln(Hu)}{u^3}\right) \quad (3.47b)$$

The asymptotic expansion for all of (3.46a) is:

$$\# \frac{\kappa^4 H^2}{27\pi^4} \partial_u \left\{ -\frac{1}{96} \frac{\ln^3(Hu)}{u^3} - \frac{1}{32} \left[\ln(2) + \frac{i\pi}{2} \right] \frac{\ln^2(Hu)}{u^3} + O\left(\frac{\ln(Hu)}{u^3}\right) \right\} . \quad (3.48a)$$

The analogous expansion for the “+-” variation (3.46b) is:

$$\# \frac{\kappa^4 H^2}{27\pi^4} \partial_u \left\{ -\frac{1}{32} \frac{\ln^2(Hu)}{u^3} + O\left(\frac{\ln(Hu)}{u^3}\right) \right\} . \quad (3.48b)$$

Summing these, along with the respective complex conjugates for the “--” and “-+” variations, gives:

$$\# \frac{\kappa^4 H^2}{2^7 \pi^4} \left\{ \frac{1}{16} \frac{\ln^3(Hu)}{u^4} + \text{Bigl} \left[\frac{7}{32} + \frac{3}{16} \ln(2) \right] \frac{\ln^2(Hu)}{u^4} + O\left(\frac{\ln(Hu)}{u^4}\right) \right\} . \quad (3.49)$$

Note the triple log terms. From the discussion of sub-section 2.8 we know that these cannot appear in the full result,* however, they *do* appear in pieces of it such as this example. An important check on accuracy is that the sum of all such triple log terms cancels.

Many, many terms such as (3.44) emerge from step 3. For example, the γ contraction of diagram (4a) — which is also diagram (2a) — consists of 842 terms whose integrands contain a factor of $\ln(H^2 y^2)$, 301 terms which contain $\ln(H^2 w^2)$, another 301 terms which contain $\ln(H^2 z^2)$, and 1663 terms which contain no logarithm at all. When all the 3-3-3 integrals are computed and the results summed, the totals are:

$$\alpha(u) = \frac{\kappa^4 H^2}{2^7 \pi^4} \left\{ \left[-492 + 234 + 216 \right] \frac{\ln^2(Hu)}{u^4} + O\left(\frac{\ln(Hu)}{u^4}\right) \right\} , \quad (3.50a)$$

$$\gamma(u) = \frac{\kappa^4 H^2}{2^7 \pi^4} \left\{ \left[+\frac{1157}{6} - \frac{400}{3} - 56 \right] \frac{\ln^2(Hu)}{u^4} + O\left(\frac{\ln(Hu)}{u^4}\right) \right\} . \quad (3.50b)$$

where the three numbers between the square brackets refer to the contributions from diagrams (2a), (2b) and (2c), respectively. Taking account of (3.27) this gives the following 3-3-3 contributions to the coefficient functions $a(u)$ and $c(u)$:

$$a_{333}(u) = \frac{\kappa^4 H^2}{2^7 \pi^4} \left\{ \left[-\frac{1795}{18} + \frac{302}{9} + \frac{160}{3} \right] \frac{\ln^2(Hu)}{u^4} + O\left(\frac{\ln(Hu)}{u^4}\right) \right\} , \quad (3.51a)$$

$$c_{333}(u) = \frac{\kappa^4 H^2}{2^7 \pi^4} \left\{ \left[+\frac{1157}{6} - \frac{400}{3} - 56 \right] \frac{\ln^2(Hu)}{u^4} + O\left(\frac{\ln(Hu)}{u^4}\right) \right\} . \quad (3.51b)$$

The results quoted above contain the contributions of some degenerate terms whose reduction is actually much more akin to that of diagram (2d), to be described in the next

* In fact the argument of 2.8 applies for the result from any triplet of vertex operators. We checked this explicitly for the triplet in which the x^μ vertex operator is #10 and the vertex operators at x'^μ and x''^μ are both #41. Step 3 in the reduction of this triplet gives 117 terms containing a factor of $\ln(H^2 y^2)$ and 77 terms with no logarithms.

section. These terms come from the action of two 0-component derivatives on the normal part (2.14a) of an outer leg propagator which connects two “+” vertices. The vertices can be either x^μ and x'^μ or x^μ and x''^μ . What such a double derivative really gives is:

$$\partial_0 \partial'_0 i\Delta_N(x; x') = \frac{H^2}{8\pi^2 \Delta x} \partial_0 \partial'_0 \left\{ \frac{u u'}{\Delta x - |\Delta u| + i\epsilon} + \frac{u u'}{\Delta x + |\Delta u| - i\epsilon} \right\} \quad (3.52a)$$

$$\begin{aligned} &= \frac{H^2}{8\pi^2 \Delta x} \left\{ \frac{1}{\Delta x - |\Delta u| + i\epsilon} + \frac{1}{\Delta x + |\Delta u| - i\epsilon} \right. \\ &\quad + \left[\theta(\Delta u) - \theta(-\Delta u) \right] \left[\frac{\Delta u}{(\Delta x - |\Delta u| + i\epsilon)^2} - \frac{\Delta u}{(\Delta x + |\Delta u| - i\epsilon)^2} \right] \\ &\quad - \frac{2 u u'}{(\Delta x - |\Delta u| + i\epsilon)^3} - \frac{2 u u'}{(\Delta x + |\Delta u| - i\epsilon)^3} \\ &\quad \left. - 2 \delta(\Delta u) \left[\frac{u^2}{(\Delta u + i\epsilon)^2} - \frac{u^2}{(\Delta x - i\epsilon)^2} \right] \right\} . \quad (3.52b) \end{aligned}$$

(Recall that $\Delta u \equiv u' - u$ and $\Delta x \equiv \|\vec{x}' - \vec{x}\|$.) The reduction procedure outlined in this section accounts for all but the terms proportional to $\delta(\Delta u)$. They are of order ϵ but sufficiently singular at $\vec{x} = \vec{x}'$ that the result is a spacetime delta function:*

$$-\frac{H^2 u^2}{4\pi^2} \frac{\delta(\Delta u)}{\Delta x} \left[\frac{1}{(\Delta u + i\epsilon)^2} - \frac{1}{(\Delta x - i\epsilon)^2} \right] = \frac{H^2 u^2}{\pi^2} \frac{i\epsilon \delta(\Delta u)}{(\Delta x^2 + \epsilon^2)^2} \quad (3.53a)$$

$$\longrightarrow \Omega^2 i \delta^4(x' - x) . \quad (3.53b)$$

Performing the now trivial integration over x'^μ causes the 3-3-3 diagram to degenerate to the 4-3 topology of diagram (2d). The reduction thereafter is the same as will be described in the next section. Of course delta function terms can happen whenever a propagator is doubly differentiated. They give 4-3 diagrams when either of the two outer leg propagators is affected; when one of the two inner propagators is affected the degenerate diagram has the topology of figure (2e) and fails to contribute to leading order for the same reason.

* Similar terms of order ϵ arise from the logarithm part of the propagator but they are not singular enough to survive in the unregulated limit.

4. The 4-3 Diagram

The 4-3 diagram consists of an outer 4-point vertex joined to a freely integrated 3-point vertex as shown in Fig. 5 below. From the discussion of sub-section 2.7 we see that this diagram can contribute at leading order when a factor of $\ln(Hu)$ from integrating the free interaction vertex combines with a factor of $\ln(Hu)$ from an undifferentiated propagator logarithm. The physical origin of the first logarithm is the growth in the invariant volume of the past lightcone, while the second logarithm comes from the increasing correlation of the free graviton vacuum of an inflating universe.

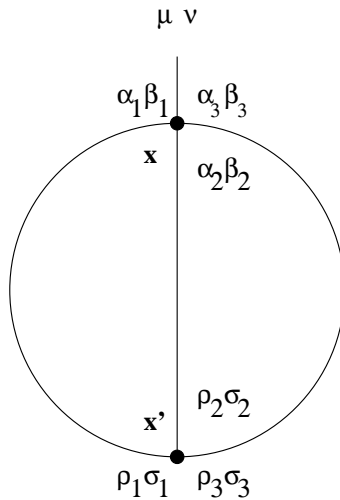


Fig. 5: The tensor structure of the 4-3 diagram.

The 4-3 diagram has an obvious 3-fold symmetry, corresponding to permutations of lines 1, 2 and 3. In computing such a highly symmetric diagram it is not efficient to fully symmetrize the vertex operators and then divide by the symmetry factor of 6. The better strategy is to symmetrize the 4-point vertex operator only on the external line, and then contract this partially symmetrized vertex operator, through propagators, into the fully symmetrized 3-point vertex operator.

We can read off the graviton 4-point interaction from expression (2.4):

$$\begin{aligned}
\mathcal{L}_{\text{inv}}^{(4)} = & \kappa^2 \Omega^2 \left\{ \frac{1}{32} \psi^2 \psi_{,\mu} \psi^{,\mu} - \frac{1}{16} \psi^2 \psi_{,\mu} \psi^{\mu\nu}{}_{,\nu} - \frac{1}{32} \psi^2 \psi_{\mu\nu,\alpha} \psi^{\mu\nu,\alpha} + \frac{1}{16} \psi^2 \psi_{\alpha\mu,\nu} \psi^{\alpha\nu,\mu} \right. \\
& - \frac{1}{8} \psi \psi^{\alpha\beta} \psi_{,\alpha} \psi_{,\beta} + \frac{1}{8} \psi \psi^{\alpha\beta} \psi^{\mu\nu}{}_{,\alpha} \psi_{\mu\nu,\beta} + \frac{1}{4} \psi \psi^{\alpha\beta} \psi_{\alpha\beta,\mu} \psi^{\mu\nu}{}_{,\nu} \\
& - \frac{1}{4} \psi \psi^{\alpha\beta} \psi_{\alpha\beta,\nu} \psi^{,\nu} + \frac{1}{4} \psi \psi^{\alpha\beta} \psi_{\alpha\mu,\nu} \psi_{\beta}{}^{\mu,\nu} - \frac{1}{4} \psi \psi^{\alpha\beta} \psi_{\alpha\dot{\mu}}{}^{,\nu} \psi_{\beta\nu}{}^{,\dot{\mu}} \\
& + \frac{1}{4} \psi \psi^{\alpha\beta} \psi_{\mu\alpha,\beta} \psi^{,\mu} + \frac{1}{4} \psi \psi^{\alpha\beta} \psi_{,\alpha} \psi_{\beta\nu}{}^{,\nu} - \frac{1}{2} \psi \psi^{\alpha\beta} \psi_{\alpha\mu,\nu} \psi^{\mu\nu}{}_{,\beta} \\
& - \frac{1}{16} \psi_{\beta}^{\alpha} \psi_{\alpha}^{\beta} \psi_{\mu,\gamma}^{\mu} \psi_{,\gamma} + \frac{1}{8} \psi_{\beta}^{\alpha} \psi_{\alpha}^{\beta} \psi_{,\mu} \psi^{\mu\nu}{}_{,\nu} + \frac{1}{16} \psi_{\beta}^{\alpha} \psi_{\alpha}^{\beta} \psi_{\mu\nu,\gamma} \psi^{\mu\nu,\gamma} \\
& - \frac{1}{8} \psi_{\beta}^{\alpha} \psi_{\alpha}^{\beta} \psi_{\gamma\nu,\mu} \psi^{\gamma\mu,\nu} + \frac{1}{4} \psi_{\beta}^{\alpha} \psi^{\beta\gamma} \psi_{,\alpha} \psi_{,\gamma} - \frac{1}{4} \psi_{\beta}^{\alpha} \psi^{\beta\gamma} \psi_{\mu\nu,\alpha} \psi^{\mu\nu}{}_{,\gamma} \\
& + \frac{1}{2} \psi_{\beta}^{\alpha} \psi^{\beta\gamma} \psi_{\alpha\gamma,\mu} \psi^{,\mu} - \frac{1}{2} \psi_{\beta}^{\alpha} \psi^{\beta\gamma} \psi_{\alpha\gamma,\mu} \psi^{\mu\nu}{}_{,\nu} + \frac{1}{2} \psi_{\beta}^{\alpha} \psi^{\beta\gamma} \psi_{\alpha\dot{\mu}}{}^{,\nu} \psi_{\gamma\nu}{}^{,\dot{\mu}} \\
& - \frac{1}{2} \psi_{\beta}^{\alpha} \psi^{\beta\gamma} \psi_{\alpha\mu,\nu} \psi_{\gamma}{}^{\mu,\nu} + \psi_{\beta}^{\alpha} \psi^{\beta\gamma} \psi_{\alpha\mu,\nu} \psi^{\mu\nu}{}_{,\gamma} - \frac{1}{2} \psi_{\beta}^{\alpha} \psi^{\beta\gamma} \psi_{,\alpha} \psi_{\gamma\nu}{}^{,\nu} \\
& - \frac{1}{2} \psi_{\beta}^{\alpha} \psi^{\beta\gamma} \psi^{,\nu} \psi_{\alpha\nu,\gamma} + \frac{1}{4} \psi^{\alpha\beta} \psi^{\mu\nu} \psi_{\alpha\beta,\gamma} \psi_{\mu\nu}{}^{,\gamma} - \frac{1}{2} \psi^{\alpha\beta} \psi^{\mu\nu} \psi_{\alpha\beta,\mu} \psi_{\nu\gamma}{}^{,\gamma} \\
& + \frac{1}{2} \psi^{\alpha\beta} \psi^{\mu\nu} \psi_{\alpha\beta,\mu} \psi_{,\nu} - \frac{1}{2} \psi^{\alpha\beta} \psi^{\mu\nu} \psi_{\alpha\mu,\nu} \psi_{,\beta} - \frac{1}{2} \psi^{\alpha\beta} \psi^{\mu\nu} \psi_{\alpha\gamma,\mu} \psi_{\beta\nu}{}^{,\gamma} \\
& - \frac{1}{2} \psi^{\alpha\beta} \psi^{\mu\nu} \psi_{\alpha\beta,\gamma} \psi_{\mu,\nu}^{\gamma} - \frac{1}{4} \psi^{\alpha\beta} \psi^{\mu\nu} \psi_{\alpha\mu,\gamma} \psi_{\beta\nu}{}^{,\gamma} + \psi^{\alpha\beta} \psi^{\mu\nu} \psi_{\alpha\mu,\gamma} \psi_{\beta\nu}{}^{,\gamma} \\
& + \frac{1}{2} \psi^{\alpha\beta} \psi^{\mu\nu} \psi_{\alpha\gamma,\mu} \psi_{\nu,\beta}^{\gamma} - \frac{1}{8u} \psi_{,\mu} \psi^2 \psi^{\mu\nu} t_{\nu} + \frac{1}{4u} \psi_{,\mu} \psi^{\alpha\beta} \psi_{\alpha\beta} \psi^{\mu\nu} t_{\nu} \\
& - \frac{1}{u} \psi_{,\mu}^{\alpha\beta} \psi_{\alpha\gamma} \psi_{\beta}^{\gamma} \psi^{\mu\nu} t_{\nu} - \frac{1}{u} \psi_{\mu}^{\alpha} \psi_{\alpha\beta} \psi^{,\beta} \psi^{\mu\nu} t_{\nu} + \frac{1}{2u} \psi_{,\mu}^{\alpha\beta} \psi_{\alpha\beta} \psi \psi^{\mu\nu} t_{\nu} \\
& \left. + \frac{1}{2u} \psi_{\alpha\mu} \psi^{,\alpha} \psi \psi^{\mu\nu} t_{\nu} - \frac{1}{u} \psi_{\gamma\mu} \psi_{\alpha\beta} \psi^{\alpha\beta,\gamma} \psi^{\mu\nu} t_{\nu} \right\} . \tag{4.1}
\end{aligned}$$

(Recall that $\psi \equiv \psi^{\mu}_{\mu}$ and $t_{\mu} \equiv \eta_{\mu 0}$.) Almost all of this ungainly expression can be checked against published results [11] by taking the flat space limit: $u = H^{-1} - t$ and $H \rightarrow 0$. The procedure for partially symmetrizing a vertex was described at the beginning of Section 3. As an example consider the final term in (4.1):

$$-\kappa^2 \Omega^2 \frac{1}{u} \psi_{\gamma\mu} \psi_{\alpha\beta} \psi^{\alpha\beta,\gamma} \psi^{\mu\nu} t_{\nu} . \tag{4.2}$$

If the indices μ and ν and the derivative ∂_u represent the distinguished line, a valid partial symmetrization of this interaction gives the following vertex operators:

$$-\kappa^2 \Omega^2 \frac{1}{u} \eta^{\mu(\alpha_2} \eta^{\beta_2)\nu} \partial_2^{(\alpha_1} \eta^{\beta_1)(\alpha_3} t^{\beta_3)} , \tag{4.3a}$$

$$-\kappa^2 \Omega^2 \frac{1}{u} \partial_2^{(\mu} \eta^{\nu)(\alpha_3} t^{\beta_3)} \eta^{\alpha_1(\alpha_2} \eta^{\beta_2)\beta_1} , \quad (4.3b)$$

$$-\kappa^2 \Omega^2 \frac{1}{u} \partial_u \eta^{\mu(\alpha_1} \eta^{\beta_1)\nu} t^{(\alpha_2} \eta^{\beta_2)(\alpha_3} t^{\beta_3)} , \quad (4.3c)$$

$$-\kappa^2 \Omega^2 \frac{1}{u} t^{(\mu} \eta^{\nu)(\alpha_1} \partial_3^{\beta_1)} \eta^{\alpha_2(\alpha_3} \eta^{\beta_3)\beta_2} . \quad (4.3d)$$

These are vertex operators $i = 127, \dots, 130$ in Table 4. The fully symmetrized cubic vertex operators are given in Table 5. They were obtained by interchanging legs 2 and 3 from the Table 3, but we have taken account of symmetries to reduce the $2 \times 43 = 86$ terms to only 75.

The unprimed vertex at x^μ is “+” type and we must sum the primed vertex over both “+” and “-” variations. Since the $(++)$ and $(+-)$ propagators are identical for $u' < u$, the relative minus sign between the two vertex assignments allows us to restrict the range of integration to $u \leq u' \leq H^{-1}$. In this region the $(+-)$ propagator is the complex conjugate of the $(++)$ one, so we can write the total contribution of the 4-3 diagram as twice the real part of the $(++)$ term:

$$\begin{aligned} \mathcal{T}_{43}^{\mu\nu} &\equiv a_{43}(u) \bar{\eta}^{\mu\nu} + c_{43}(u) t^\mu t^\nu \\ &= 2\text{Re} \left\{ -i\kappa \int_u^{H^{-1}} du' \int d^3x' \sum_{i=1}^{130} V_i^{\mu\nu\alpha_1\beta_1\alpha_2\beta_2\alpha_3\beta_3}(x; \partial_u, \partial_1, \partial_2, \partial_3) \right. \\ &\quad \left. i \left[\alpha_1\beta_1 \Delta_{\rho_1\sigma_1} \right](x; x') i \left[\alpha_2\beta_2 \Delta_{\rho_2\sigma_2} \right](x; x') i \left[\alpha_3\beta_3 \Delta_{\rho_3\sigma_3} \right](x; x') \right. \\ &\quad \left. \sum_{j=1}^{75} V_j^{\rho_1\sigma_1\rho_2\sigma_2\rho_3\sigma_3}(x'; \partial'_1, \partial'_2, \partial'_3) \right\} . \end{aligned} \quad (4.4)$$

The subscripts i and j refer to Tables 4 and 5 respectively. Recall that where each derivative acts is indicated by primes and subscripts. For example, the derivative ∂_3 in the 4-point vertex operator acts on the first argument of the propagator $i[{}_3\Delta_3](x; x')$. The derivative ∂_u acts on all u 's in the vertex and the three propagators.

The entire calculation was performed by computer using Mathematica [12] and FeynCalc [13]. The first step was to contract each pair of vertex operators into the three internal

propagator and write the results onto a file. The next step was to act the internal derivatives (∂_{1-3} and ∂'_{1-3}) and store the results for each pair of vertex operators. Selected vertex pairs were computed by hand to check the procedure.

i	Vertex Operator	i	Vertex Operator
1	$\frac{1}{8}\eta^{\mu\nu}\eta^{\alpha_1\beta_1}\partial_3^{(\alpha_2}\eta^{\beta_2)(\alpha_3}\partial_2^{\beta_3)}$	66	$\frac{1}{16}\partial_u\eta^{\mu\nu}\eta^{\alpha_1\beta_1}\eta^{\alpha_2\beta_2}\eta^{\alpha_3\beta_3}t\cdot\partial_3$
2	$\frac{1}{8}\partial_u\partial_3^{(\mu}\eta^{\nu)(\alpha_3}t^{\beta_3)}\eta^{\alpha_1\beta_1}\eta^{\alpha_2\beta_2}$	67	$-\frac{1}{8}\eta^{\mu(\alpha_1}\eta^{\beta_1)\nu}\eta^{\alpha_2\beta_2}\eta^{\alpha_3\beta_3}\partial_2\cdot\partial_3$
3	$-\frac{1}{4}\eta^{\mu(\alpha_1}\eta^{\beta_1)\nu}\partial_3^{(\alpha_2}\eta^{\beta_2)(\alpha_3}\partial_2^{\beta_3)}$	68	$-\frac{1}{8}\partial_u\eta^{\mu\nu}\eta^{\alpha_1(\alpha_2}\eta^{\beta_2)\beta_1}\eta^{\alpha_3\beta_3}t\cdot\partial_3$
4	$-\frac{1}{4}\partial_u\partial_3^{(\mu}\eta^{\nu)(\alpha_3}t^{\beta_3)}\eta^{\alpha_1(\alpha_2}\eta^{\beta_2)\beta_1}$	69	$\eta^{\mu(\alpha_1}\eta^{\beta_1)(\alpha_2}\eta^{\beta_2)(\nu}\eta^{\alpha_3\beta_3}\partial_2\cdot\partial_3$
5	$\eta^{\mu(\alpha_1}\partial_3^{\beta_1)}\partial_2^{(\alpha_3}\eta^{\beta_3)(\alpha_2}\eta^{\beta_2)(\nu}$	70	$\frac{1}{2}\partial_u\eta^{\mu(\alpha_1}\eta^{\beta_1)(\alpha_2}\eta^{\beta_2)(\nu}\eta^{\alpha_3\beta_3}t\cdot\partial_3$
6	$\partial_2^{(\mu}\eta^{\nu)(\alpha_1}\eta^{\beta_1)(\alpha_3}\eta^{\beta_3)(\alpha_2}\partial_3^{\beta_2)}$	71	$\frac{1}{2}\partial_u\eta^{\mu\nu}\eta^{\alpha_1(\alpha_2}\eta^{\beta_2)(\alpha_3}\eta^{\beta_3)(\beta_1}t\cdot\partial_3$
7	$\partial_u\eta^{\mu(\alpha_2}\eta^{\beta_2)(\alpha_1}\partial_3^{\beta_1)}t^{(\alpha_3}\eta^{\beta_3)(\nu}$	72	$\frac{1}{2}\partial_2^{(\mu}\eta^{\nu)(\alpha_1}\partial_3^{\beta_1)}\eta^{\alpha_2\beta_2}\eta^{\alpha_3\beta_3}$
8	$\partial_u\partial_3^{(\mu}\eta^{\nu)(\alpha_3}\eta^{\beta_3)(\alpha_1}\eta^{\beta_1)(\alpha_2}t^{\beta_2)}$	73	$\frac{1}{2}\partial_u\eta^{\mu\nu}t^{(\alpha_1}\eta^{\beta_1)(\alpha_2}\partial_3^{\beta_2)}\eta^{\alpha_3\beta_3}$
9	$\eta^{\mu(\alpha_1}\eta^{\beta_1)(\alpha_3}\partial_2^{\beta_3)}\partial_3^{(\alpha_2}\eta^{\beta_2)(\nu}$	74	$-\frac{1}{4}\eta^{\mu\nu}\eta^{\alpha_1(\alpha_2}\eta^{\beta_2)\beta_1}\eta^{\alpha_3\beta_3}\partial_2\cdot\partial_3$
10	$\partial_u\partial_3^{(\mu}\eta^{\nu)(\alpha_2}\eta^{\beta_2)(\alpha_1}\eta^{\beta_1)(\alpha_3}t^{\beta_3)}$	75	$-\frac{1}{4}\eta^{\mu(\alpha_2}\eta^{\beta_2)\nu}\eta^{\alpha_1\beta_1}\eta^{\alpha_3\beta_3}\partial_2\cdot\partial_3$
11	$-\frac{1}{2}\eta^{\mu\nu}\partial_3^{(\alpha_1}\eta^{\beta_1)(\alpha_2}\eta^{\beta_2)(\alpha_3}\partial_2^{\beta_3)}$	76	$-\frac{1}{4}\partial_u\eta^{\mu(\alpha_2}\eta^{\beta_2)\nu}\eta^{\alpha_1\beta_1}\eta^{\alpha_3\beta_3}t\cdot\partial_3$
12	$-\frac{1}{2}\partial_2^{(\mu}\eta^{\nu)(\alpha_3}\eta^{\beta_3)(\alpha_2}\partial_3^{\beta_2)}\eta^{\alpha_1\beta_1}$	77	$-\frac{1}{4}\partial_u\eta^{\mu\nu}\eta^{\alpha_1\beta_1}\eta^{\alpha_2(\alpha_3}\eta^{\beta_3)\beta_2}t\cdot\partial_3$
13	$-\frac{1}{2}\partial_u\eta^{\mu(\alpha_2}\partial_3^{\beta_2)}t^{(\alpha_3}\eta^{\beta_3)(\nu}\eta^{\alpha_1\beta_1}$	78	$-\frac{1}{8}\eta^{\mu\nu}\partial_2^{(\alpha_1}\partial_3^{\beta_1)}\eta^{\alpha_2\beta_2}\eta^{\alpha_3\beta_3}$
14	$-\frac{1}{2}\partial_u\partial_3^{(\mu}\eta^{\nu)(\alpha_3}\eta^{\beta_3)(\alpha_2}t^{\beta_2)}\eta^{\alpha_1\beta_1}$	79	$-\frac{1}{8}\partial_2^{(\mu}\partial_3^{\nu)}\eta^{\alpha_1\beta_1}\eta^{\alpha_2\beta_2}\eta^{\alpha_3\beta_3}$
15	$-\frac{1}{4}\eta^{\mu\nu}\partial_3^{(\alpha_2}\eta^{\beta_2)(\alpha_1}\eta^{\beta_1)(\alpha_3}\partial_2^{\beta_3)}$	80	$-\frac{1}{4}\partial_u\eta^{\mu\nu}\eta^{\alpha_1\beta_1}\eta^{\alpha_3\beta_3}\partial_3^{(\alpha_2}t^{\beta_2)}$
16	$-\frac{1}{4}\eta^{\mu(\alpha_2}\partial_3^{\beta_2)}\eta^{\alpha_1\beta_1}\partial_2^{(\alpha_3}\eta^{\beta_3)(\nu}$	81	$\frac{1}{2}\eta^{\mu(\alpha_2}\eta^{\beta_2)\nu}\partial_2^{(\alpha_1}\partial_3^{\beta_1)}\eta^{\alpha_3\beta_3}$
17	$-\frac{1}{2}\partial_u\partial_3^{(\mu}\eta^{\nu)(\alpha_2}\eta^{\beta_2)(\alpha_3}t^{\beta_3)}\eta^{\alpha_1\beta_1}$	82	$\frac{1}{2}\partial_2^{(\mu}\partial_3^{\nu)}\eta^{\alpha_1(\alpha_2}\eta^{\beta_2)\beta_1}\eta^{\alpha_3\beta_3}$
18	$\partial_2^{(\mu}\eta^{\nu)(\alpha_3}\eta^{\beta_3)(\alpha_1}\eta^{\beta_1)(\alpha_2}\partial_3^{\beta_2)}$	83	$\frac{1}{2}\partial_u\eta^{\mu(\alpha_1}\eta^{\beta_1)\nu}\partial_3^{(\alpha_2}t^{\beta_2)}\eta^{\alpha_3\beta_3}$
19	$\eta^{\mu(\alpha_2}\eta^{\beta_2)(\alpha_1}\partial_3^{\beta_1)}\partial_2^{(\alpha_3}\eta^{\beta_3)(\nu}$	84	$\frac{1}{2}\partial_u\eta^{\mu\nu}\partial_3^{(\alpha_1}t^{\beta_1)}\eta^{\alpha_2(\alpha_3}\eta^{\beta_3)\beta_2}$
20	$\partial_u\eta^{\mu(\alpha_1}\eta^{\beta_1)(\alpha_3}t^{\beta_3)}\partial_3^{(\alpha_2}\eta^{\beta_2)(\nu}$	85	$\frac{1}{2}\eta^{\mu(\alpha_3}\eta^{\beta_3)\nu}\eta^{\alpha_1(\alpha_2}\eta^{\beta_2)\beta_1}\partial_2\cdot\partial_3$
21	$\partial_u\partial_3^{(\mu}\eta^{\nu)(\alpha_2}\eta^{\beta_2)(\alpha_3}\eta^{\beta_3)(\alpha_1}t^{\beta_1)}$	86	$\frac{1}{2}\partial_u\eta^{\mu(\alpha_2}\eta^{\beta_2)\nu}\eta^{\alpha_1(\alpha_3}\eta^{\beta_3)\beta_1}t\cdot\partial_3$
22	$\partial_2^{(\mu}\eta^{\nu)(\alpha_3}\eta^{\beta_3)(\alpha_2}\eta^{\beta_2)(\alpha_1}\partial_3^{\beta_1)}$	87	$-\frac{1}{16}\eta^{\mu\nu}\eta^{\alpha_1\beta_1}\eta^{\alpha_2(\alpha_3}\eta^{\beta_3)\beta_2}\partial_2\cdot\partial_3$

Table 4: The partially symmetrized quartic pseudo-graviton vertex operators $V_i^{\mu\nu\alpha_1\beta_1\alpha_2\beta_2\alpha_3\beta_3}$ without the factor of $\kappa^2\Omega^2$.

i	Vertex Operator	i	Vertex Operator
23	$\partial_u \eta^{\mu(\alpha_2} \partial_3^{\beta_2)} t^{(\alpha_1} \eta^{\beta_1)(\alpha_3} \eta^{\beta_3)(\nu}$	88	$-\frac{1}{16} \partial_u \eta^{\mu(\alpha_3} \eta^{\beta_3)\nu} \eta^{\alpha_1 \beta_1} \eta^{\alpha_2 \beta_2} t \cdot \partial_3$
24	$-\frac{1}{8} \eta^{\mu\nu} \eta^{\alpha_1 \beta_1} \eta^{\alpha_2 \beta_2} \partial_2^{(\alpha_3} \partial_3^{\beta_3)}$	89	$\frac{1}{8} \eta^{\mu(\alpha_1} \eta^{\beta_1)\nu} \eta^{\alpha_2(\alpha_3} \eta^{\beta_3)\beta_2} \partial_2 \cdot \partial_3$
25	$-\frac{1}{16} \partial_u \eta^{\mu\nu} \eta^{\alpha_1 \beta_1} \eta^{\alpha_2 \beta_2} \partial_3^{(\alpha_3} t^{\beta_3)}$	90	$\frac{1}{8} \partial_u \eta^{\mu(\alpha_3} \eta^{\beta_3)\nu} \eta^{\alpha_1(\alpha_2} \eta^{\beta_2)\beta_1} t \cdot \partial_3$
26	$-\frac{1}{16} \partial_u \partial_3^{(\mu} t^{\nu)} \eta^{\alpha_1 \beta_1} \eta^{\alpha_2 \beta_2} \eta^{\alpha_3 \beta_3}$	91	$-\eta^{\mu(\alpha_1} \eta^{\beta_1)(\alpha_3} \eta^{\beta_3)(\alpha_2} \eta^{\beta_2)(\nu} \partial_2 \cdot \partial_3$
27	$\frac{1}{4} \eta^{\mu(\alpha_1} \eta^{\beta_1)\nu} \eta^{\alpha_2 \beta_2} \partial_2^{(\alpha_3} \partial_3^{\beta_3)}$	92	$-\partial_u \eta^{\mu(\alpha_2} \eta^{\beta_2)(\alpha_1} \eta^{\beta_1)(\alpha_3} \eta^{\beta_3)(\nu} t \cdot \partial_3$
28	$\frac{1}{8} \partial_u \eta^{\mu\nu} \eta^{\alpha_1(\alpha_2} \eta^{\beta_2)\beta_1} \partial_3^{(\alpha_3} t^{\beta_3)}$	93	$-\frac{1}{2} \partial_2^{(\mu} \eta^{\nu)(\alpha_1} \partial_3^{\beta_1)} \eta^{\alpha_2(\alpha_3} \eta^{\beta_3)\beta_2}$
29	$\frac{1}{8} \partial_u \partial_3^{(\mu} t^{\nu)} \eta^{\alpha_1(\alpha_2} \eta^{\beta_2)\beta_1} \eta^{\alpha_3 \beta_3}$	94	$-\frac{1}{2} \partial_u \eta^{\mu(\alpha_3} \eta^{\beta_3)\nu} t^{(\alpha_1} \eta^{\beta_1)(\alpha_2} \partial_3^{\beta_2)}$
30	$-\eta^{\mu(\alpha_1} \eta^{\beta_1)(\alpha_2} \eta^{\beta_2)(\nu} \partial_2^{(\alpha_3} \partial_3^{\beta_3)}$	95	$\frac{1}{4} \eta^{\mu\nu} \eta^{\alpha_1(\alpha_2} \eta^{\beta_2)(\alpha_3} \eta^{\beta_3)(\beta_1} \partial_2 \cdot \partial_3$
31	$-\frac{1}{2} \partial_u \eta^{\mu(\alpha_1} \eta^{\beta_1)(\alpha_2} \eta^{\beta_2)(\nu} \partial_3^{(\alpha_3} t^{\beta_3)}$	96	$\frac{1}{4} \eta^{\mu(\alpha_2} \eta^{\beta_2)(\alpha_3} \eta^{\beta_3)(\nu} \eta^{\alpha_1 \beta_1} \partial_2 \cdot \partial_3$
32	$-\frac{1}{2} \partial_u \partial_3^{(\mu} t^{\nu)} \eta^{\alpha_1(\alpha_2} \eta^{\beta_2)(\alpha_3} \eta^{\beta_3)(\beta_1}$	97	$\frac{1}{2} \partial_u \eta^{\mu(\alpha_2} \eta^{\beta_2)(\alpha_3} \eta^{\beta_3)(\nu} \eta^{\alpha_1 \beta_1} t \cdot \partial_3$
33	$-\frac{1}{2} \partial_2^{(\mu} \eta^{\nu)(\alpha_1} \eta^{\beta_1)(\alpha_3} \partial_3^{\beta_3)} \eta^{\alpha_2 \beta_2}$	98	$\frac{1}{8} \eta^{\mu\nu} \partial_2^{(\alpha_1} \partial_3^{\beta_1)} \eta^{\alpha_2(\alpha_3} \eta^{\beta_3)\beta_2}$
34	$-\frac{1}{2} \eta^{\mu(\alpha_1} \partial_3^{\beta_1)} \partial_2^{(\alpha_2} \eta^{\beta_2)(\nu} \eta^{\alpha_3 \beta_3}$	99	$\frac{1}{8} \partial_2^{(\mu} \partial_3^{\nu)} \eta^{\alpha_1 \beta_1} \eta^{\alpha_2(\alpha_3} \eta^{\beta_3)\beta_2}$
35	$-\frac{1}{2} \partial_u \eta^{\mu\nu} t^{(\alpha_1} \eta^{\beta_1)(\alpha_2} \eta^{\beta_2)(\alpha_3} \partial_3^{\beta_3)}$	100	$\frac{1}{4} \partial_u \eta^{\mu(\alpha_3} \eta^{\beta_3)\nu} \partial_3^{(\alpha_2} t^{\beta_2)} \eta^{\alpha_1 \beta_1}$
36	$-\frac{1}{2} \partial_u t^{(\mu} \eta^{\nu)(\alpha_2} \eta^{\beta_2)(\alpha_1} \partial_3^{\beta_1)} \eta^{\alpha_3 \beta_3}$	101	$-\frac{1}{2} \eta^{\mu(\alpha_2} \eta^{\beta_2)(\alpha_1} \eta^{\beta_1)(\alpha_3} \eta^{\beta_3)(\nu} \partial_2 \cdot \partial_3$
37	$-\frac{1}{2} \eta^{\mu(\alpha_1} \partial_2^{\beta_1)} \partial_3^{(\alpha_2} \eta^{\beta_2)(\nu} \eta^{\alpha_3 \beta_3}$	102	$-\frac{1}{2} \partial_u \eta^{\mu(\alpha_1} \eta^{\beta_1)(\alpha_3} \eta^{\beta_3)(\alpha_2} \eta^{\beta_2)(\nu} t \cdot \partial_3$
38	$-\frac{1}{2} \partial_2^{(\mu} \eta^{\nu)(\alpha_1} \eta^{\beta_1)(\alpha_2} \partial_3^{\beta_2)} \eta^{\alpha_3 \beta_3}$	103	$-\frac{1}{2} \eta^{\mu(\alpha_2} \eta^{\beta_2)(\alpha_3} \eta^{\beta_3)(\nu} \partial_2^{(\alpha_1} \partial_3^{\beta_1)}$
39	$-\frac{1}{2} \partial_u \eta^{\mu\nu} \partial_3^{(\alpha_2} \eta^{\beta_2)(\alpha_1} \eta^{\beta_1)(\alpha_3} t^{\beta_3)}$	104	$-\frac{1}{2} \partial_2^{(\mu} \partial_3^{\nu)} \eta^{\alpha_1(\alpha_2} \eta^{\beta_2)(\alpha_3} \eta^{\beta_3)(\beta_1}$
40	$-\frac{1}{2} \partial_u \partial_1^{(\mu} \eta^{\nu)(\alpha_2} \eta^{\beta_2)(\alpha_3} t^{\beta_3)} \eta^{\alpha_1 \beta_1}$	105	$-\partial_u \eta^{\mu(\alpha_2} \eta^{\beta_2)(\alpha_3} \eta^{\beta_3)(\nu} \partial_3^{(\alpha_1} t^{\beta_1)}$
41	$\frac{1}{4} \eta^{\mu\nu} \eta^{\alpha_1(\alpha_2} \eta^{\beta_2)\beta_1} \partial_2^{(\alpha_3} \partial_3^{\beta_3)}$	106	$-\frac{1}{4u} \eta^{\mu\nu} \eta^{\alpha_1 \beta_1} \eta^{\alpha_2 \beta_2} \partial_2^{(\alpha_3} t^{\beta_3)}$
42	$\frac{1}{4} \eta^{\mu(\alpha_2} \eta^{\beta_2)\nu} \eta^{\alpha_1 \beta_1} \partial_2^{(\alpha_3} \partial_3^{\beta_3)}$	107	$-\frac{1}{8u} \partial_u \eta^{\mu\nu} \eta^{\alpha_1 \beta_1} \eta^{\alpha_2 \beta_2} t^{\alpha_3} t^{\beta_3}$
43	$\frac{1}{4} \partial_u \eta^{\mu(\alpha_2} \eta^{\beta_2)\nu} \eta^{\alpha_1 \beta_1} \partial_3^{(\alpha_3} t^{\beta_3)}$	108	$-\frac{1}{8u} t^{(\mu} \partial_3^{\nu)} \eta^{\alpha_1 \beta_1} \eta^{\alpha_2 \beta_2} \eta^{\alpha_3 \beta_3}$
44	$\frac{1}{4} \partial_u \partial_3^{(\mu} t^{\nu)} \eta^{\alpha_1 \beta_1} \eta^{\alpha_2(\alpha_3} \eta^{\beta_3)\beta_2}$	109	$\frac{1}{2u} \eta^{\mu(\alpha_1} \eta^{\beta_1)\nu} \eta^{\alpha_2 \beta_2} \partial_2^{(\alpha_3} t^{\beta_3)}$

Table 4: (continued from previous page)

i	Vertex Operator	i	Vertex Operator
45	$\frac{1}{4}\eta^{\mu\nu} \partial_2^{(\alpha_1 \eta^{\beta_1})(\alpha_3 \partial_3^{\beta_3})} \eta^{\alpha_2\beta_2}$	110	$\frac{1}{4u}\eta^{\mu\nu} \eta^{\alpha_1(\alpha_2 \eta^{\beta_2})\beta_1} t^{\alpha_3} t^{\beta_3}$
46	$\frac{1}{4}\partial_2^{(\mu \eta^\nu)(\alpha_3 \partial_3^{\beta_3})} \eta^{\alpha_1\beta_1} \eta^{\alpha_2\beta_2}$	111	$\frac{1}{4u}t^{(\mu \partial_3^\nu)} \eta^{\alpha_1(\alpha_2 \eta^{\beta_2})\beta_1} \eta^{\alpha_3\beta_3}$
47	$\frac{1}{4}\partial_u \eta^{\mu\nu} \eta^{\alpha_1\beta_1} t^{(\alpha_2 \eta^{\beta_2})(\alpha_3 \partial_3^{\beta_3})}$	112	$-\frac{2}{u}\eta^{(\mu)(\alpha_1 \eta^{\beta_1})(\alpha_2 \eta^{\beta_2})(\nu \partial_2^{(\alpha_3} t^{\beta_3)})}$
48	$\frac{1}{4}\partial_u t^{(\mu \eta^\nu)(\alpha_2 \partial_3^{\beta_2})} \eta^{\alpha_1\beta_1} \eta^{\alpha_3\beta_3}$	113	$-\frac{1}{u}\partial_u \eta^{(\mu)(\alpha_1 \eta^{\beta_1})(\alpha_2 \eta^{\beta_2})(\nu t^{\alpha_3} t^{\beta_3})}$
49	$\frac{1}{4}\eta^{\mu\nu} \partial_3^{(\alpha_1 \eta^{\beta_1})(\alpha_3 \partial_2^{\beta_3})} \eta^{\alpha_2\beta_2}$	114	$-\frac{1}{u}t^{(\mu \partial_3^\nu)} \eta^{\alpha_1(\alpha_2 \eta^{\beta_2})(\alpha_3 \eta^{\beta_3})(\beta_1)}$
50	$\frac{1}{4}\partial_3^{(\mu \eta^\nu)(\alpha_3 \partial_2^{\beta_3})} \eta^{\alpha_1\beta_1} \eta^{\alpha_2\beta_2}$	115	$-\frac{1}{u}\partial_2^{(\mu \eta^\nu)(\alpha_1 \eta^{\beta_1})(\alpha_3 t^{\beta_3})} \eta^{\alpha_2\beta_2}$
51	$\frac{1}{4}\partial_u \eta^{\mu\nu} \eta^{\alpha_1\beta_1} \partial_3^{(\alpha_2 \eta^{\beta_2})(\alpha_3 t^{\beta_3})}$	116	$-\frac{1}{u}\eta^{(\mu)(\alpha_1 \partial_2^{\beta_1})} t^{(\alpha_3 \eta^{\beta_3})(\nu \eta^{\alpha_2\beta_2})}$
52	$\frac{1}{4}\partial_u \partial_3^{(\mu \eta^\nu)(\alpha_2 t^{\beta_2})} \eta^{\alpha_1\beta_1} \eta^{\alpha_3\beta_3}$	117	$-\frac{1}{u} \partial_u \eta^{\mu\nu} t^{(\alpha_1 \eta^{\beta_1})(\alpha_2 \eta^{\beta_2})(\alpha_3 t^{\beta_3})}$
53	$-\frac{1}{2}\eta^{\mu(\alpha_2 \eta^{\beta_2})\nu} \partial_2^{(\alpha_1 \eta^{\beta_1})(\alpha_3 \partial_3^{\beta_3})}$	118	$-\frac{1}{u}t^{(\mu \eta^\nu)(\alpha_1 \eta^{\beta_1})(\alpha_2 \partial_3^{\beta_2})} \eta^{\alpha_3\beta_3}$
54	$-\frac{1}{2}\partial_2^{(\mu \eta^\nu)(\alpha_3 \partial_3^{\beta_3})} \eta^{\alpha_1(\alpha_2 \eta^{\beta_2})\beta_1}$	119	$\frac{1}{2u}\eta^{\mu\nu} \eta^{\alpha_1(\alpha_2 \eta^{\beta_2})\alpha_1} \partial_2^{(\alpha_3} t^{\beta_3)}$
55	$-\frac{1}{2}\partial_u \eta^{\mu(\alpha_1 \eta^{\beta_1})\nu} t^{(\alpha_2 \eta^{\beta_2})(\alpha_3 \partial_3^{\beta_3})}$	120	$\frac{1}{2u}\eta^{\mu(\alpha_2 \eta^{\beta_2})\nu} \eta^{\alpha_1\beta_1} \partial_2^{(\alpha_3} t^{\beta_3)}$
56	$-\frac{1}{2}\partial_u t^{(\mu \eta^\nu)(\alpha_2 \partial_3^{\beta_2})} \eta^{\alpha_1(\alpha_3 \eta^{\beta_3})\beta_1}$	121	$\frac{1}{2u}\partial_u \eta^{\mu(\alpha_2 \eta^{\beta_2})\nu} \eta^{\alpha_1\beta_1} t^{\alpha_3} t^{\beta_3}$
57	$-\frac{1}{2}\eta^{\mu(\alpha_2 \eta^{\beta_2})\nu} \partial_3^{(\alpha_1 \eta^{\beta_1})(\alpha_3 \partial_2^{\beta_3})}$	122	$\frac{1}{2u}t^{(\mu \partial_3^\nu)} \eta^{\alpha_1\beta_1} \eta^{\alpha_2(\alpha_3 \eta^{\beta_3})\beta_2}$
58	$-\frac{1}{2}\partial_3^{(\mu \eta^\nu)(\alpha_3 \partial_2^{\beta_3})} \eta^{\alpha_1(\alpha_2 \eta^{\beta_2})\beta_1}$	123	$\frac{1}{2u}\eta^{\mu\nu} \partial_2^{(\alpha_1 \eta^{\beta_1})(\alpha_3 t^{\beta_3})} \eta^{\alpha_2\beta_2}$
59	$-\frac{1}{2}\partial_u \eta^{\mu(\alpha_1 \eta^{\beta_1})\nu} \partial_3^{(\alpha_2 \eta^{\beta_2})(\alpha_3 t^{\beta_3})}$	124	$\frac{1}{2u}\partial_2^{(\mu \eta^\nu)(\alpha_3 t^{\beta_3})} \eta^{\alpha_1\beta_1} \eta^{\alpha_2\beta_2}$
60	$-\frac{1}{2}\partial_u \partial_2^{(\mu \eta^\nu)(\alpha_3 t^{\beta_3})} \eta^{\alpha_1(\alpha_2 \eta^{\beta_2})\beta_1}$	125	$\frac{1}{2u}\partial_u \eta^{\mu\nu} \eta^{\alpha_1\beta_1} t^{(\alpha_2 \eta^{\beta_2})(\alpha_3 t^{\beta_3})}$
61	$-\frac{1}{2}\partial_2^{(\mu \eta^\nu)(\alpha_3 \eta^{\beta_3})(\alpha_1 \partial_3^{\beta_1})} \eta^{\alpha_2\beta_2}$	126	$\frac{1}{2u}t^{(\mu \eta^\nu)(\alpha_2 \partial_3^{\beta_2})} \eta^{\alpha_1\beta_1} \eta^{\alpha_3\beta_3}$
62	$-\frac{1}{2}\partial_3^{(\mu \eta^\nu)(\alpha_3 \eta^{\beta_3})(\alpha_1 \partial_2^{\beta_1})} \eta^{\alpha_2\beta_2}$	127	$-\frac{1}{u}\eta^{\mu(\alpha_2 \eta^{\beta_2})\nu} \partial_2^{(\alpha_1 \eta^{\beta_1})(\alpha_3 t^{\beta_3})}$
63	$-\frac{1}{2}\partial_u \eta^{\mu\nu} t^{(\alpha_1 \eta^{\beta_1})(\alpha_3 \eta^{\beta_3})(\alpha_2 \partial_3^{\beta_2})}$	128	$-\frac{1}{u}\partial_2^{(\mu \eta^\nu)(\alpha_3 t^{\beta_3})} \eta^{\alpha_1(\alpha_2 \eta^{\beta_2})\beta_1}$
64	$-\frac{1}{2}\partial_u \eta^{(\mu)(\alpha_1 t^{\beta_1})} \partial_3^{(\alpha_2 \eta^{\beta_2})(\nu \eta^{\alpha_3\beta_3})}$	129	$-\frac{1}{u}\partial_u \eta^{\mu(\alpha_1 \eta^{\beta_1})\nu} t^{(\alpha_2 \eta^{\beta_2})(\alpha_3 t^{\beta_3})}$
65	$\frac{1}{16}\eta^{\mu\nu} \eta^{\alpha_1\beta_1} \eta^{\alpha_2\beta_2} \eta^{\alpha_3\beta_3} \partial_2 \cdot \partial_3$	130	$-\frac{1}{u}t^{(\mu \eta^\nu)(\alpha_1 \partial_3^{\beta_1})} \eta^{\alpha_2(\alpha_3 \eta^{\beta_3})\beta_2}$

Table 4: (continued from previous page)

j	Vertex Operator	j	Vertex Operator
1	$-\frac{1}{2u'}\eta^{\rho_1\sigma_1}\eta^{\rho_2\sigma_2}\partial_2^{(\rho_3}t^{\sigma_3)}$	39	$-\frac{1}{4}\eta^{\rho_2\sigma_2}\eta^{\rho_3(\rho_1}\eta^{\sigma_1)\sigma_3}\partial_3\cdot\partial_1$
2	$-\frac{1}{2u'}\eta^{\rho_2\sigma_2}\eta^{\rho_3\sigma_3}\partial_3^{(\rho_1}t^{\sigma_1)}$	40	$\eta^{\rho_1)(\rho_2}\eta^{\sigma_2)(\rho_3}\eta^{\sigma_3)(\sigma_1}\partial_2\cdot\partial_3$
3	$-\frac{1}{2u'}\eta^{\rho_3\sigma_3}\eta^{\rho_1\sigma_1}\partial_1^{(\rho_2}t^{\sigma_2)}$	41	$\eta^{\rho_1)(\rho_2}\eta^{\sigma_2)(\rho_3}\eta^{\sigma_3)(\sigma_1}\partial_3\cdot\partial_1$
4	$\frac{1}{u'}\eta^{\rho_1(\rho_2}\eta^{\sigma_2)\sigma_1}\partial_2^{(\rho_3}t^{\sigma_3)}$	42	$\frac{1}{2}\partial_2^{(\rho_1}\partial_3^{\sigma_1)}\eta^{\rho_2(\rho_3}\eta^{\sigma_3)\sigma_2}$
5	$\frac{1}{u'}\eta^{\rho_2(\rho_3}\eta^{\sigma_3)\sigma_2}\partial_3^{(\rho_1}t^{\sigma_1)}$	43	$\frac{1}{2}\partial_3^{(\rho_2}\partial_1^{\sigma_2)}\eta^{\rho_3(\rho_1}\eta^{\sigma_1)\sigma_3}$
6	$\frac{1}{u'}\eta^{\rho_3(\rho_1}\eta^{\sigma_1)\sigma_3}\partial_1^{(\rho_2}t^{\sigma_2)}$	44	$-\frac{1}{2u'}\eta^{\rho_1\sigma_1}\eta^{\rho_3\sigma_3}\partial_3^{(\rho_2}t^{\sigma_2)}$
7	$\frac{1}{u'}t^{(\rho_3}\eta^{\sigma_3)(\rho_1}\partial_2^{\sigma_1)}\eta^{\rho_2\sigma_2}$	45	$-\frac{1}{2u'}\eta^{\rho_3\sigma_3}\eta^{\rho_2\sigma_2}\partial_2^{(\rho_1}t^{\sigma_1)}$
8	$\frac{1}{u'}t^{(\rho_1}\eta^{\sigma_1)(\rho_2}\partial_3^{\sigma_2)}\eta^{\rho_3\sigma_3}$	46	$-\frac{1}{2u'}\eta^{\rho_2\sigma_2}\eta^{\rho_1\sigma_1}\partial_1^{(\rho_3}t^{\sigma_3)}$
9	$\frac{1}{u'}t^{(\rho_2}\eta^{\sigma_2)(\rho_3}\partial_1^{\sigma_3)}\eta^{\rho_1\sigma_1}$	47	$\frac{1}{u'}\eta^{\rho_1(\rho_3}\eta^{\sigma_3)\sigma_1}\partial_3^{(\rho_2}t^{\sigma_2)}$
10	$\frac{1}{2}\eta^{\rho_1\sigma_1}\partial_3^{(\rho_2}\eta^{\sigma_2)(\rho_3}\partial_2^{\sigma_3)}$	48	$\frac{1}{u'}\eta^{\rho_3(\rho_2}\eta^{\sigma_2)\sigma_3}\partial_2^{(\rho_1}t^{\sigma_1)}$
11	$\frac{1}{2}\eta^{\rho_2\sigma_2}\partial_1^{(\rho_3}\eta^{\sigma_3)(\rho_1}\partial_3^{\sigma_1)}$	49	$\frac{1}{u'}\eta^{\rho_2(\rho_1}\eta^{\sigma_1)\sigma_2}\partial_1^{(\rho_3}t^{\sigma_3)}$
12	$\frac{1}{2}\eta^{\rho_3\sigma_3}\partial_2^{(\rho_1}\eta^{\sigma_1)(\rho_2}\partial_1^{\sigma_2)}$	50	$\frac{1}{u'}\partial_3^{(\rho_1}\eta^{\sigma_1)(\rho_2}t^{\sigma_2)}\eta^{\rho_3\sigma_3}$
13	$-\partial_3^{(\rho_1}\eta^{\sigma_1)(\rho_2}\eta^{\sigma_2)(\rho_3}\partial_2^{\sigma_3)}$	51	$\frac{1}{u'}\partial_2^{(\rho_3}\eta^{\sigma_3)(\rho_1}t^{\sigma_1)}\eta^{\rho_2\sigma_2}$
14	$-\partial_1^{(\rho_2}\eta^{\sigma_2)(\rho_3}\eta^{\sigma_3)(\rho_1}\partial_3^{\sigma_1)}$	52	$\frac{1}{u'}\partial_1^{(\rho_2}\eta^{\sigma_2)(\rho_3}t^{\sigma_3)}\eta^{\rho_1\sigma_1}$
15	$-\partial_2^{(\rho_3}\eta^{\sigma_3)(\rho_1}\eta^{\sigma_1)(\rho_2}\partial_1^{\sigma_2)}$	53	$-\partial_2^{(\rho_1}\eta^{\sigma_1)(\rho_3}\eta^{\sigma_3)(\rho_2}\partial_3^{\sigma_2)}$
16	$-\partial_3^{(\rho_2}\eta^{\sigma_2)(\rho_1}\eta^{\sigma_1)(\rho_3}\partial_2^{\sigma_3)}$	54	$-\partial_1^{(\rho_3}\eta^{\sigma_3)(\rho_2}\eta^{\sigma_2)(\rho_1}\partial_2^{\sigma_1)}$
17	$-\partial_1^{(\rho_3}\eta^{\sigma_3)(\rho_2}\eta^{\sigma_2)(\rho_1}\partial_3^{\sigma_1)}$	55	$-\partial_3^{(\rho_2}\eta^{\sigma_2)(\rho_1}\eta^{\sigma_1)(\rho_3}\partial_1^{\sigma_3)}$
18	$-\partial_2^{(\rho_1}\eta^{\sigma_1)(\rho_3}\eta^{\sigma_3)(\rho_2}\partial_1^{\sigma_2)}$	56	$-\frac{1}{4}\eta^{\rho_1\sigma_1}\eta^{\rho_3\sigma_3}\partial_2^{(\rho_2}\partial_3^{\sigma_2)}$
19	$-\frac{1}{4}\eta^{\rho_1\sigma_1}\eta^{\rho_2\sigma_2}\partial_2^{(\rho_3}\partial_3^{\sigma_3)}$	57	$-\frac{1}{4}\eta^{\rho_3\sigma_3}\eta^{\rho_2\sigma_2}\partial_1^{(\rho_1}\partial_2^{\sigma_1)}$

Table 5: The fully symmetrized cubic pseudo-graviton vertex operators $V_j^{\rho_1\sigma_1\rho_2\sigma_2\rho_3\sigma_3}$ without the factor of $\kappa\Omega'^2$.

j	Vertex Operator	j	Vertex Operator
20	$-\frac{1}{4}\eta^{\rho_2\sigma_2}\eta^{\rho_3\sigma_3}\partial_3^{(\rho_1}\partial_1^{\sigma_1)}$	58	$-\frac{1}{4}\eta^{\rho_2\sigma_2}\eta^{\rho_1\sigma_1}\partial_3^{(\rho_3}\partial_1^{\sigma_3)}$
21	$-\frac{1}{4}\eta^{\rho_3\sigma_3}\eta^{\rho_1\sigma_1}\partial_1^{(\rho_2}\partial_2^{\sigma_2)}$	59	$\frac{1}{2}\eta^{\rho_1(\rho_3}\eta^{\sigma_3)\sigma_1}\partial_2^{(\rho_2}\partial_3^{\sigma_2)}$
22	$\frac{1}{2}\eta^{\rho_1(\rho_2}\eta^{\sigma_2)\sigma_1}\partial_2^{(\rho_3}\partial_3^{\sigma_3)}$	60	$\frac{1}{2}\eta^{\rho_3(\rho_2}\eta^{\sigma_2)\sigma_3}\partial_1^{(\rho_1}\partial_2^{\sigma_1)}$
23	$\frac{1}{2}\eta^{\rho_2(\rho_3}\eta^{\sigma_3)\sigma_2}\partial_3^{(\rho_1}\partial_1^{\sigma_1)}$	61	$\frac{1}{2}\eta^{\rho_2(\rho_1}\eta^{\sigma_1)\sigma_2}\partial_3^{(\rho_3}\partial_1^{\sigma_3)}$
24	$\frac{1}{2}\eta^{\rho_3(\rho_1}\eta^{\sigma_1)\sigma_3}\partial_1^{(\rho_2}\partial_2^{\sigma_2)}$	62	$\frac{1}{2}\partial_3^{(\rho_1}\eta^{\sigma_1)(\rho_2}\partial_2^{\sigma_2)}\eta^{\rho_3\sigma_3}$
25	$\frac{1}{2}\partial_2^{(\rho_1}\eta^{\sigma_1)(\rho_3}\partial_3^{\sigma_3)}\eta^{\rho_2\sigma_2}$	63	$\frac{1}{2}\partial_2^{(\rho_3}\eta^{\sigma_3)(\rho_1}\partial_1^{\sigma_1)}\eta^{\rho_2\sigma_2}$
26	$\frac{1}{2}\partial_3^{(\rho_2}\eta^{\sigma_2)(\rho_1}\partial_1^{\sigma_1)}\eta^{\rho_3\sigma_3}$	64	$\frac{1}{2}\partial_1^{(\rho_2}\eta^{\sigma_2)(\rho_3}\partial_3^{\sigma_3)}\eta^{\rho_1\sigma_1}$
27	$\frac{1}{2}\partial_1^{(\rho_3}\eta^{\sigma_3)(\rho_2}\partial_2^{\sigma_2)}\eta^{\rho_1\sigma_1}$	65	$\frac{1}{2}\partial_2^{(\rho_3}\eta^{\sigma_3)(\rho_1}\partial_3^{\sigma_1)}\eta^{\rho_2\sigma_2}$
28	$\frac{1}{2}\partial_2^{(\rho_1}\eta^{\sigma_1)(\rho_2}\partial_3^{\sigma_2)}\eta^{\rho_3\sigma_3}$	66	$\frac{1}{2}\partial_1^{(\rho_2}\eta^{\sigma_2)(\rho_3}\partial_2^{\sigma_3)}\eta^{\rho_1\sigma_1}$
29	$\frac{1}{2}\partial_3^{(\rho_2}\eta^{\sigma_2)(\rho_3}\partial_1^{\sigma_3)}\eta^{\rho_1\sigma_1}$	67	$\frac{1}{2}\partial_3^{(\rho_1}\eta^{\sigma_1)(\rho_2}\partial_1^{\sigma_2)}\eta^{\rho_3\sigma_3}$
30	$\frac{1}{2}\partial_1^{(\rho_3}\eta^{\sigma_3)(\rho_1}\partial_2^{\sigma_1)}\eta^{\rho_2\sigma_2}$	68	$\frac{1}{4}\eta^{\rho_1\sigma_1}\eta^{\rho_2\sigma_2}\eta^{\rho_3\sigma_3}\partial_1\cdot\partial_2$
31	$\frac{1}{4}\eta^{\rho_1\sigma_1}\eta^{\rho_2\sigma_2}\eta^{\rho_3\sigma_3}\partial_2\cdot\partial_3$	69	$-\frac{1}{2}\eta^{\rho_1(\rho_3}\eta^{\sigma_3)\sigma_1}\eta^{\rho_2\sigma_2}\partial_2\cdot\partial_3$
32	$\frac{1}{4}\eta^{\rho_1\sigma_1}\eta^{\rho_2\sigma_2}\eta^{\rho_3\sigma_3}\partial_3\cdot\partial_1$	70	$-\frac{1}{2}\eta^{\rho_3(\rho_2}\eta^{\sigma_2)\sigma_3}\eta^{\rho_1\sigma_1}\partial_1\cdot\partial_2$
33	$-\frac{1}{2}\eta^{\rho_1(\rho_2}\eta^{\sigma_2)\sigma_1}\eta^{\rho_3\sigma_3}\partial_2\cdot\partial_3$	71	$-\frac{1}{2}\eta^{\rho_1(\rho_2}\eta^{\sigma_2)\sigma_1}\eta^{\rho_3\sigma_3}\partial_3\cdot\partial_1$
34	$-\frac{1}{2}\eta^{\rho_2(\rho_3}\eta^{\sigma_3)\sigma_2}\eta^{\rho_1\sigma_1}\partial_3\cdot\partial_1$	72	$-\frac{1}{2}\eta^{\rho_1\sigma_1}\eta^{\rho_2\sigma_2}\partial_1^{(\rho_3}\partial_2^{\sigma_3)}$
35	$-\frac{1}{2}\eta^{\rho_3(\rho_1}\eta^{\sigma_1)\sigma_3}\eta^{\rho_2\sigma_2}\partial_1\cdot\partial_2$	73	$-\frac{1}{4}\eta^{\rho_1(\rho_2}\eta^{\sigma_2)\sigma_1}\eta^{\rho_3\sigma_3}\partial_1\cdot\partial_2$
36	$-\frac{1}{2}\partial_2^{(\rho_1}\partial_3^{\sigma_1)}\eta^{\rho_2\sigma_2}\eta^{\rho_3\sigma_3}$	74	$\eta^{\rho_1)(\rho_2}\eta^{\sigma_2)(\rho_3}\eta^{\sigma_3)(\sigma_1}\partial_1\cdot\partial_2$
37	$-\frac{1}{2}\partial_3^{(\rho_2}\partial_1^{\sigma_2)}\eta^{\rho_3\sigma_3}\eta^{\rho_1\sigma_1}$	75	$\frac{1}{2}\partial_1^{(\rho_3}\partial_2^{\sigma_3)}\eta^{\rho_1(\rho_2}\eta^{\sigma_2)\sigma_1}$
38	$-\frac{1}{4}\eta^{\rho_1\sigma_1}\eta^{\rho_2(\rho_3}\eta^{\sigma_3)\sigma_2}\partial_2\cdot\partial_3$		

Table 5: (continued from previous page)

As an example, consider the contraction of the $i = 1$ and $j = 10$ vertex operators:

$$\begin{aligned}
& -i\kappa V_1^{\mu\nu\alpha_1\beta_1\alpha_2\beta_2\alpha_3\beta_3}(x; \partial_u, \partial_1, \partial_2, \partial_3) i\left[\alpha_1\beta_1\Delta_{\rho_1\sigma_1}\right](x; x') i\left[\alpha_2\beta_2\Delta_{\rho_2\sigma_2}\right](x; x') \\
& i\left[\alpha_3\beta_3\Delta_{\rho_3\sigma_3}\right](x; x') V_{10}^{\rho_1\sigma_1\rho_2\sigma_2\rho_3\sigma_3}(x'; \partial'_1, \partial'_2, \partial'_3) \\
& = -\frac{i}{16} \kappa^4 \Omega^2 \Omega'^2 \eta^{\mu\nu} \eta^{\alpha_1\beta_1} \partial_3^{(\alpha_2} \eta^{\beta_2)(\alpha_3} \partial_2^{\beta_3)} \eta^{\rho_1\sigma_1} \partial_3^{(\rho_2} \eta^{\sigma_2)(\rho_3} \partial_2^{\sigma_3)} \\
& \quad \left\{ i\Delta_{1N} \left[2\eta_{\alpha_1(\rho_1} \eta_{\sigma_1)\beta_1} - \eta_{\alpha_1\beta_1} \eta_{\rho_1\sigma_1} \right] - i\Delta_{1L} \left[2\bar{\eta}_{\alpha_1(\rho_1} \bar{\eta}_{\sigma_1)\beta_1} - \bar{\eta}_{\alpha_1\beta_1} \bar{\eta}_{\rho_1\sigma_1} \right] \right\} \\
& \quad \left\{ i\Delta_{2N} \left[2\eta_{\alpha_2(\rho_2} \eta_{\sigma_2)\beta_2} - \eta_{\alpha_2\beta_2} \eta_{\rho_2\sigma_2} \right] - i\Delta_{2L} \left[2\bar{\eta}_{\alpha_2(\rho_2} \bar{\eta}_{\sigma_2)\beta_2} - 2\bar{\eta}_{\alpha_2\beta_2} \bar{\eta}_{\rho_2\sigma_2} \right] \right\} \\
& \quad \left\{ i\Delta_{3N} \left[2\eta_{\alpha_3(\rho_3} \eta_{\sigma_3)\beta_3} - \eta_{\alpha_3\beta_3} \eta_{\rho_3\sigma_3} \right] - i\Delta_{3L} \left[2\bar{\eta}_{\alpha_3(\rho_3} \bar{\eta}_{\sigma_3)\beta_3} - 2\bar{\eta}_{\alpha_3\beta_3} \bar{\eta}_{\rho_3\sigma_3} \right] \right\} \quad (4.5a)
\end{aligned}$$

$$\begin{aligned}
& = -\frac{i}{4} \kappa^4 \Omega^2 \Omega'^2 \eta^{\mu\nu} \left(-2 i\Delta_{1N} + 3 i\Delta_{1L} \right) \\
& \quad \left\{ \left[4\partial_2 \cdot \partial'_2 \partial_3 \cdot \partial'_3 - 2\partial_2 \cdot \partial'_3 \partial_3 \cdot \partial'_2 + 2\partial_2 \cdot \partial_3 \partial'_2 \cdot \partial'_3 \right] i\Delta_{2N} i\Delta_{3N} \right. \\
& \quad + \left[-2\bar{\partial}_2 \cdot \bar{\partial}'_2 \partial_3 \cdot \partial'_3 + 3\bar{\partial}_2 \cdot \bar{\partial}'_3 \bar{\partial}_3 \cdot \bar{\partial}'_2 - 3\bar{\partial}_2 \cdot \bar{\partial}_3 \bar{\partial}'_2 \cdot \bar{\partial}'_3 \right] i\Delta_{2N} i\Delta_{3L} \\
& \quad + \left[-2\partial_2 \cdot \partial'_2 \bar{\partial}_3 \cdot \bar{\partial}'_3 + 3\bar{\partial}_2 \cdot \bar{\partial}'_3 \bar{\partial}_3 \cdot \bar{\partial}'_2 - 3\bar{\partial}_2 \cdot \bar{\partial}_3 \bar{\partial}'_2 \cdot \bar{\partial}'_3 \right] i\Delta_{2L} i\Delta_{3N} \\
& \quad \left. + \left[\bar{\partial}_2 \cdot \bar{\partial}'_2 \bar{\partial}_3 \cdot \bar{\partial}'_3 - 4\bar{\partial}_2 \cdot \bar{\partial}'_3 \bar{\partial}_3 \cdot \bar{\partial}'_2 + 5\bar{\partial}_2 \cdot \bar{\partial}_3 \bar{\partial}'_2 \cdot \bar{\partial}'_3 \right] i\Delta_{2L} i\Delta_{3L} \right\} \quad (4.5b)
\end{aligned}$$

$$\begin{aligned}
& = \frac{-i\kappa^4 H^2}{29\pi^6 u^2 u'^2} \eta^{\mu\nu} \left\{ \left[24 \frac{t \cdot w^4}{w^8} + 24 \frac{u^2 t \cdot w^2}{w^8} - 336 \frac{uu' t \cdot w^2}{w^8} + 24 \frac{u'^2 t \cdot w^2}{w^8} - 48 \frac{u t \cdot w}{w^6} - 24 \frac{u^2}{w^6} \right. \right. \\
& \quad \left. \left. + 48 \frac{u' t \cdot w}{w^6} - 96 \frac{uu'}{w^6} - 24 \frac{u'^2}{w^6} + 24 \frac{1}{w^4} \right] \ln(H^2 w^2) \right. \\
& \quad \left. + \left[-32 \frac{uu' t \cdot w^4}{w^{10}} - 32 \frac{u^3 u' t \cdot w^2}{w^{10}} + 448 \frac{u^2 u'^2 t \cdot w^2}{w^{10}} - 32 \frac{uu'^3 t \cdot w^2}{w^{10}} + 64 \frac{u^2 u' t \cdot w}{w^8} \right. \right. \\
& \quad \left. \left. + 32 \frac{u^3 u'}{w^8} - 64 \frac{uu'^2 t \cdot w}{w^8} + 128 \frac{u^2 u'^2}{w^8} + 32 \frac{uu'^3}{w^8} - 32 \frac{uu'}{w^6} \right] \right\} . \quad (4.5c)
\end{aligned}$$

Note that we have dropped the order ϵ terms in derivatives of w^2 :

$$\frac{\partial}{\partial x^\mu} w^2 = 2 w_\mu - 2i \epsilon t_\mu \longrightarrow 2 w_\mu . \quad (4.6)$$

The neglected terms affect ultraviolet divergences but not the infrared terms of interest.

The next step is to perform the spatial integrations. The angular integrations give a factor of 4π and the radial integral was done by the method of contours. When no

logarithm is present we obtain:

$$\begin{aligned} \int d^3 x' \frac{1}{w^{2N}} &= 2\pi \int_{-\infty}^{\infty} dr \frac{r^2}{(r - w_0 + i\epsilon)^N (r + w_0 - i\epsilon)^N} \\ &= 8\pi^2 i \frac{(-1)^{N-1} (2N - 5)!!}{2^{N+1} (N - 1)!} \left(\frac{1}{w_0 - i\epsilon} \right)^{2N-3}. \end{aligned} \quad (4.7a)$$

The logarithm gives:

$$\begin{aligned} \int d^3 x' \frac{\ln(H^2 w^2)}{w^{2N}} &= 2\pi^2 \int_{-\infty}^{\infty} dr \frac{r^2 \ln[H^2(r - w_0 + i\epsilon)(r + w_0 - i\epsilon)]}{(r - w_0 + i\epsilon)^N (r + w_0 - i\epsilon)^N} \\ &= 8\pi^2 i \frac{(-1)^{N-1} (2N - 5)!!}{2^{N+1} (N - 1)!} \left\{ \ln[2H(w_0 - i\epsilon)] + \ln[-2H(w_0 - i\epsilon)] \right\} \left(\frac{1}{w_0 - i\epsilon} \right)^{2N-3} \\ &\quad + \frac{8\pi^2 i (-1)^N}{2^{2N-1} (N - 1)!} \sum_{k=1}^{N-1} \frac{(2N - 2 - k)! [2N - 2 - k - k^2]}{k (N - 1 - k)! (2N - 2 - k)(2N - 3 - k)} \left(\frac{1}{w_0 - i\epsilon} \right)^{2N-3}. \end{aligned} \quad (4.7b)$$

The case of $N = 2$ has to be treated specially:

$$\int d^3 x' \frac{1}{w^4} = -8\pi^2 i \frac{1}{8} \frac{1}{w_0 - i\epsilon}, \quad (4.8a)$$

$$\int d^3 x' \frac{\ln(H^2 w^2)}{w^4} = -8\pi^2 i \frac{1}{8} \left(\frac{\ln[2H(w_0 - i\epsilon)] + \ln[-2H(w_0 - i\epsilon)]}{w_0 - i\epsilon} + \frac{1}{w_0 - i\epsilon} \right). \quad (4.8b)$$

Performing the spatial integrations for our $i = 1, j = 10$ vertex pair gives:

$$\begin{aligned} &-i\kappa \int d^3 x' V_1^{\mu\nu\alpha_1\beta_1\alpha_2\beta_2\alpha_3\beta_3}(x; \partial_u, \partial_1, \partial_2, \partial_3) i[\alpha_1\beta_1 \Delta_{\rho_1\sigma_1}](x; x') i[\alpha_2\beta_2 \Delta_{\rho_2\sigma_2}](x; x') \\ &\quad i[\alpha_3\beta_3 \Delta_{\rho_3\sigma_3}](x; x') V_{10}^{\rho_1\sigma_1\rho_2\sigma_2\rho_3\sigma_3}(x'; \partial'_1, \partial'_2, \partial'_3) \\ &= \frac{\kappa^4 H^2}{2^6 \pi^4 u^2 u'^2} \eta^{\mu\nu} \left\{ -3 \frac{\ln[2H(u' - u - i\epsilon)] + \ln[-2H(u' - u - i\epsilon)]}{u' - u - i\epsilon} - \frac{7}{2} \frac{1}{u' - u - i\epsilon} \right. \\ &\quad \left. + \frac{15}{8} \frac{u' u}{(u' - u - i\epsilon)^3} - \frac{7}{16} \frac{u'^2 u^2}{(u' - u - i\epsilon)^5} \right\}. \end{aligned} \quad (4.9)$$

The final step is to integrate over the conformal time of the free vertex. The integrand always consists of a numerator — which may contain a pair of logarithms — and a denominator — which contains up to two powers of u' , and up to seven powers of $u' - u - i\epsilon$. Decomposing the denominator by partial fractions results in four distinct terms requiring

special attention: $(u' - u - i\epsilon)$, u' , u'^2 and $(u' - u - i\epsilon)^k$ for $k > 1$. When the pair of logarithms is present the four denominators give:

$$\begin{aligned}
\text{(i)} \quad & \int_u^{H^{-1}} \frac{du'}{u'-u-i\epsilon} \left\{ \ln \left[2H(u' - u - i\epsilon) \right] + \ln \left[-2H(u' - u - i\epsilon) \right] \right\} \quad (4.10) \\
& = \frac{1}{2} \left\{ \ln^2 \left[2H(u' - u - i\epsilon) \right] + \ln^2 \left[-2H(u' - u - i\epsilon) \right] \right\} \Big|_u^{H^{-1}} \\
& \longrightarrow \ln^2 \left[2(1 - Hu) \right] - \ln^2(2H\epsilon) + i\pi \ln \left[2(1 - Hu) \right] - \frac{1}{4}\pi^2 \quad ,
\end{aligned}$$

$$\begin{aligned}
\text{(ii)} \quad & \int_u^{H^{-1}} \frac{du'}{u'} \left\{ \ln \left[2H(u' - u - i\epsilon) \right] + \ln \left[-2H(u' - u - i\epsilon) \right] \right\} \quad (4.11) \\
& \longrightarrow \left\{ \ln^2(2Hu') + i\pi \ln(Hu') + 2 \sum_{k=1}^{\infty} \frac{1}{k^2} \left(\frac{u}{u'} \right)^k \right\} \Big|_u^{H^{-1}} \\
& = -2 \ln(2) \ln(Hu) - \ln^2(Hu) - i\pi \ln(Hu) + 2 \left[Hu\Phi(Hu, 2, 1) - \zeta(2) \right] \quad ,
\end{aligned}$$

$$\begin{aligned}
\text{(iii)} \quad & \int_u^{H^{-1}} \frac{du'}{u'^2} \left\{ \ln \left[2H(u' - u - i\epsilon) \right] + \ln \left[-2H(u' - u - i\epsilon) \right] \right\} \quad (4.12) \\
& \longrightarrow \left\{ -\frac{2}{u'} \ln(2Hu') - \frac{i\pi}{u'} + 2 \frac{u'-u}{u'u} \ln \left[1 - \frac{u}{u'} \right] \right\} \Big|_u^{H^{-1}} \\
& = \frac{2}{u} \ln(Hu) + \frac{2}{u} (1 - Hu) \left\{ \frac{i}{2}\pi + \ln \left[2(1 - Hu) \right] \right\} \quad ,
\end{aligned}$$

$$\begin{aligned}
\text{(iv)} \quad & \int_u^{H^{-1}} \frac{du'}{(u'-u-i\epsilon)^k} \left\{ \ln \left[2H(u' - u - i\epsilon) \right] + \ln \left[-2H(u' - u - i\epsilon) \right] \right\} \quad (4.13) \\
& = -\frac{1}{k-1} \frac{1}{(u'-u-i\epsilon)^{k-1}} \left\{ \ln \left[2H(u' - u - i\epsilon) \right] + \ln \left[-2H(u' - u - i\epsilon) \right] + \frac{2}{k-1} \right\} \Big|_u^{H^{-1}} \\
& \longrightarrow \frac{2}{k-1} \left(\frac{i}{\epsilon} \right)^{k-1} \left[\ln(2H\epsilon) + \frac{1}{k-1} \right] - \frac{2}{k-1} \left(\frac{H}{1-Hu} \right)^{k-1} \left\{ \ln \left[2(1 - Hu) \right] + \frac{i}{2}\pi + \frac{1}{k-1} \right\} \quad ,
\end{aligned}$$

where $\Phi(z, s, v)$ is the special function [14]:

$$\Phi(z, s, v) \equiv \sum_{n=0}^{\infty} \frac{z^n}{(v+n)^s} \quad . \quad (4.14)$$

and the arrow indicates the leading infinitesimal ϵ contributions. When no logarithms are present the integrals are simple enough that we give only the small ϵ forms:

$$\text{(i)} \quad \int_u^{H^{-1}} \frac{du'}{u' - u - i\epsilon} \longrightarrow \ln(1 - Hu) - \ln(H\epsilon) + \frac{i}{2}\pi \quad , \quad (4.15)$$

$$(ii) \int_u^{H^{-1}} \frac{du'}{u'} = -\ln(Hu) , \quad (4.16)$$

$$(iii) \int_u^{H^{-1}} \frac{du'}{u'^2} = \frac{1}{u}(1-Hu) , \quad (4.17)$$

$$(iv) \int_u^{H^{-1}} \frac{du'}{(u'-u-i\epsilon)^k} \rightarrow \frac{1}{k-1} \left\{ \left(\frac{i}{\epsilon}\right)^{k-1} - \left(\frac{H}{1-Hu}\right)^{k-1} \right\} . \quad (4.18)$$

We can now complete the reduction of the contribution from the $i = 1, j = 10$ vertex pair:

$$\begin{aligned} \mathcal{T}_{1,10}^{\mu\nu} = \frac{\kappa^4 H^2}{26\pi^4} \eta^{\mu\nu} \left\{ \left\{ -6 \ln^2(Hu) + \left[\frac{35}{4} - 12 \ln 2 \right] \ln(Hu) + 19(1-Hu) + \frac{3}{2}\pi^2 \right. \right. \\ + 12 \left[\zeta(2) - Hu\Phi(Hu, 2, 1) \right] - \frac{13}{4} \ln \left[2(1-Hu) \right] - 6 \ln^2 \left[2(1-Hu) \right] \\ + \frac{13}{4} \ln(2H\epsilon) + 6 \ln^2(2H\epsilon) \left. \right\} \frac{1}{u^4} + \frac{15}{4} \left(\frac{H}{1-Hu} \right) \frac{1}{u^3} \\ - \frac{15}{8} \left[\left(\frac{H}{1-Hu} \right)^2 + \frac{1}{\epsilon^2} \right] \frac{1}{u^2} + \frac{3}{8} \left[- \left(\frac{H}{1-Hu} \right)^4 + \frac{1}{\epsilon^4} \right] \left. \right\} . \quad (4.19) \end{aligned}$$

It is worth noting that the coefficient of the leading term for late times — $-6 u^{-4} \ln^2(Hu)$ — is opposite to that of the double logarithmic ultraviolet divergence — $+6 u^{-4} \ln^2(2H\epsilon)$. This is in sharp contrast to 3-3-3 contributions such as (3.47a) where an undifferentiated propagator logarithm is not involved. Then the leading infrared contribution has *the same* sign as the double logarithmic ultraviolet divergence.

The same sign phenomenon of (3.47a) was explained in sub-section 2.7. The parameter ϵ has dimensions of length so it can only appear in the combinations $H\epsilon$ or ϵu^{-1} . The dimensionality of the conformal time integrands shows that they converge even if the upper limit, H^{-1} , diverges, so the only factors of $\ln(H)$ can come from the single possible undifferentiated propagator logarithm. When no such logarithm is present any double logarithmic ultraviolet divergence must take the form:

$$\ln^2(\epsilon u^{-1}) = \ln^2(H\epsilon) - 2 \ln(H\epsilon) \ln(Hu) + \ln^2(Hu) . \quad (4.20)$$

One can understand why the opposite relation prevails in all 4-3 contributions by the need to avoid overlapping divergences. The 4-3 diagram contains only two vertices so its

ultraviolet divergences must be primitive; there cannot be any non-local sub-divergences such as $\ln(H\epsilon) \ln(Hu)$. The possibility of $\ln^2(H\epsilon)$ is ruled out because no factors of $\ln(H)$ can come from the limits of integration; the only $\ln(H)$ can come from the single possible undifferentiated propagator logarithm. So we are left with just one dimensionally consistent double ultraviolet logarithm:

$$\ln^2(H\epsilon) - \ln^2(Hu) = \ln^2(\epsilon) + 2 \ln(\epsilon) \ln(H) - 2 \ln(H) \ln(u) - \ln^2(u) . \quad (4.21)$$

Although the tensor algebra and derivatives of the 4-3 diagram are only marginally simpler than that of the most complicated 3-3-3 diagram (2a), the number of terms they produce is much smaller. There are just 39 integrands which contain $\ln(H^2w^2)$ and only 57 which have no logarithm. We have also seen that the integrals are simple enough for exact results to be obtained. Although we did this, we report just the leading results here:

$$a_{43}(u) = \frac{\kappa^4 H^2}{2^6 \pi^4} \left\{ -\frac{13}{3} \frac{\ln^2(Hu)}{u^4} + O\left(\frac{\ln(Hu)}{u^4}\right) \right\} , \quad (4.22a)$$

$$c_{43}(u) = \frac{\kappa^4 H^2}{2^6 \pi^4} \left\{ +2 \frac{\ln^2(Hu)}{u^4} + O\left(\frac{\ln(Hu)}{u^4}\right) \right\} . \quad (4.22b)$$

5. Epilogue

We can now assemble the results from the various diagrams of Fig. 2. Combining (3.51) with (4.22) gives the following coefficient functions for the amputated 1-point function (2.19):

$$a(u) = H^{-2} \left(\frac{\kappa H}{4\pi u}\right)^4 \left\{ \left(-\frac{1795}{9} + \frac{604}{9} + \frac{320}{3} - \frac{52}{3}\right) \ln^2(Hu) + O(\ln(Hu)) \right\} + O(\kappa^6) \quad (5.1a)$$

$$c(u) = H^{-2} \left(\frac{\kappa H}{4\pi u}\right)^4 \left\{ \left(+\frac{1157}{3} - \frac{800}{3} - 112 + 8\right) \ln^2(Hu) + O(\ln(Hu)) \right\} + O(\kappa^6) \quad (5.1b)$$

The four numbers in each of these expressions represent the respective contributions from diagrams (2a), (2b), (2c) and (2d). As explained in sub-section 2.9, diagram (2e) can only contribute a single factor of $\ln(Hu)$ and diagram (2f) cannot contribute any.

Attaching the retarded Green's functions discussed in sub-section 2.5 gives the coefficient functions for the full 1-point function (2.20):

$$A(u) = \left(\frac{\kappa H}{4\pi u}\right)^4 \left\{ \left(+\frac{7180}{81} - \frac{2416}{81} - \frac{1280}{27} + \frac{208}{27} \right) \ln^3(Hu) + O(\ln^2(Hu)) \right\} + O(\kappa^6) \quad (5.2a)$$

$$C(u) = \left(\frac{\kappa H}{4\pi u}\right)^4 \left\{ \left(+\frac{319}{6} + \frac{49}{3} - 52 + 11 \right) \ln^2(Hu) + O(\ln(Hu)) \right\} + O(\kappa^6) . \quad (5.2b)$$

None of the four coefficient functions given above is free of gauge dependence. The physical, gauge independent observable is the combination (2.24) which gives the effective Hubble constant. Our result for it is:

$$H_{\text{eff}}(t) = H \left\{ 1 - \left(\frac{\kappa H}{4\pi}\right)^4 \left[\left(+\frac{4309}{54} - \frac{1649}{27} - \frac{172}{9} + \frac{5}{9} \right) (Ht)^2 + O(Ht) \right] + O(\kappa^6) \right\} \quad (5.3a)$$

$$= H \left\{ 1 - \left(\frac{\kappa H}{4\pi}\right)^4 \left[\frac{1}{6} (Ht)^2 + O(Ht) \right] + O(\kappa^6) \right\} . \quad (5.3b)$$

Although we have given the contribution from each diagram in (5.3a), only the sum (5.3b) is really physical and gauge independent. Still, it is worth pointing out that the pure graviton diagrams — (2a) and (2d) — act to slow inflation while the ghost diagrams — (2b) and (2c) — contribute in the opposite sense.

The physical significance of our result has been discussed elsewhere [4] but two points should be mentioned here. First, we get a *reduction* in the effective Hubble constant due to the negative energy of the gravitational interaction between the zero point motions of gravitons.* This tendency ought to persist to all orders in perturbation theory. Second, recall from sub-section 2.8 that at most ℓ infrared logarithms can appear at ℓ loops. This means that the ℓ -loop contribution to the bracketed term in (5.3b) is at most:

$$-\# (\kappa H)^{2\ell} (Ht)^\ell . \quad (5.4)$$

* The induced stress-energy is that of negative vacuum energy, to leading order, because causality restricts the gravitational interaction to the constant Hubble volume. The induced energy density is therefore independent of the true volume of the inflating universe, so the total energy is just $E = V\rho$ and the pressure is $p = -\partial E/\partial V = -\rho$.

The bound is quite likely to be saturated because one can form higher loop graphs by attaching the 2-loop tadpole we have computed. But one in any case obtains the following estimate for the number of e-foldings needed to end rapid inflation:

$$N = Ht \sim (\kappa H)^{-2} . \quad (5.5)$$

This is $\gtrsim 10^{12}$ for inflation at the GUT scale or below, which is more than enough to explain the homogeneity and isotropy of the observed universe. If the unknown numerical coefficients in (5.4) fall off less rapidly than ℓ^{-1} then the end of rapid inflation is likely to be quite abrupt because all orders will become strong at once. This augurs well for reheating.

We turn now to a discussion of accuracy. The strongest checks on the consistency of our basic formalism and the accuracy of our implementation are provided by the one-loop self-energy. This quantity was relatively simple to obtain [15] because technical considerations compelled us to compute the inner loops of diagrams (2a) and (2b) before doing the outer loop contractions and acting the outer loop derivatives. We checked that the one-loop self-energy has the appropriate reflection symmetry, that it obeys the Ward identity, and that it agrees, for $H \rightarrow 0$ at fixed t , with the flat space self-energy obtained by Capper [16] in the same gauge. Since we used only partially symmetrized vertices and then interchanged lines where necessary, reflection symmetry is a non-trivial test of our programs for the tensor algebra. It also checks the programs for taking derivatives because the order of differentiation breaks manifest reflection symmetry. The Ward identity tests the apparatus of gauge fixing, our solutions for the ghost and graviton propagators, and the 3-point interaction vertices. It also provides a powerful independent check of the tensor algebra and derivative programs. In addition to giving further independent tests for all these things, the flat space limit checks the overall factor and the sign.

One of the major complications in computing diagram (2a) was that the number of

intermediate expressions becomes prohibitive if one attempts to perform the tensor algebra all at once, even for a single “trio” of vertex operators.* This is why we first did the inner loop tensor algebra and acted the inner loop derivatives for each pair of inner loop vertices, then summed the results and projected the lengthy total onto a basis formed from products of the 79 independent 4-index objects and the 10 possible contracted outer leg derivatives. Each basis element with a non-zero coefficient was contracted into the outer loop propagators and the outer vertex operators, and the various outer loop derivatives were acted. Then the inner loop coefficients were multiplied and the results summed.

The cumbersome nature of this procedure caused us much anxiety and we devised a number of ways to check it. First, a program was written to check the inner loop projection by simply summing the product of each basis element with its coefficient and then comparing with the original expression. Second, the outer loop tensor algebra and derivative programs were based on the same scheme as those which were so effectively checked by the Ward identity, and of course we used the same stored expressions for the vertices and propagators. Third, it was not too time consuming to perform all the tensor algebra at once for a single “trio” of vertex operators. This was done for the case where the vertex operator at x^μ is #10 in Table 3, and where those at x'^μ and x''^μ are both #41. The derivatives were then acted (using a different program from the usual one) and the result compared with what our standard programs give. The same calculation was performed by hand as an additional check.

Diagram (2b) was computed using the same programs as for (2a), so its accuracy is checked by that of (2a). An additional test was provided by the fact that no undifferentiated propagator logarithms can come from ghost lines.* We checked that the integrands

* The problem is that expanding the four propagators gives $6^4 = 1296$ terms, each of which involves a contraction over 16 indices.

* To see this note that the 10 vertices of Table 2 have either a factor of ∂_2 or a factor of t^{α_2} — which accesses only the normal part of the propagator.

for (2b) are indeed free of $\ln(H^2y^2)$, and that those of diagram (2c) are free of either $\ln(H^2w^2)$ or $\ln(H^2z^2)$.

Our greatest worry was the complicated integrations of 3-3-3 diagrams. We checked these a number of ways. First, we did a large number of examples by hand. Second, the two authors wrote independent integration schemes. The first of these did each radial integration independently by the method of contours and changed variables as necessary so that only the final conformal time integration needed to be expanded. This program also computed the four “ \pm ” variations separately. The second program did the radial integrals by differentiating generating functions. The conformal time integrations were carried out in the standard order, expanding whenever necessary. This second program also added the “ \pm ” variations of the integrands before evaluating the integral. We ran the two programs for each of the thousands of terms and then scanned the results to make sure they agreed.

One of the strongest checks on the accuracy of the 3-3-3 diagrams derives from our proof in sub-section 2.8 that each “trio” of vertices for each of the 3-3-3 diagrams must be free of triple log terms — $u^{-4} \ln^3(Hu)$. As mentioned there, and as we saw explicitly in (3.49), this is *not* true for each of the integrands which emerge from step 3 of our reduction procedure. Yet when the results from integrating the thousands of distinct integrands were summed, the triple logs cancelled for each diagram. We also checked that our programs show this cancellation separately for the previously mentioned 10-41-41 vertex triad.

We fretted long about how to check the 4-3 diagram (2d). Of course it is partially checked by the 3-3-3 diagrams by virtue of the fact that all use the same stored expression for the graviton propagator, and since their tensor algebra and derivative action programs are based on the same scheme. One of our big worries was the different vertices. We checked the fully symmetrized 3-point vertex by having the computer symmetrize the partially symmetrized vertex of Table 3. We also wrote a program in which the computer produces fully symmetrized 3-point and 4-point vertex operators from the respective interaction

Lagrangians (3.6) and (4.1). These were compared directly with our stored expression for the symmetrized 3-point vertex; of course we had to (computer) symmetrize our 4-point vertex before comparing it.

As an additional check on the 4-3 diagram, we compared the output from our programs with a hand computation of the result for vertex operator #1 at x^μ and #10 at x'^μ . It is also worth pointing out that the 4-3 integrations are vastly simpler than those of the 3-3-3 diagrams. In fact only the single term (4.11) can contribute at leading order.

Finally, there is the fact that the result is plausible. Quantum gravity is not on-shell finite at one loop when the cosmological constant is non-zero [17], so one has to expect ultraviolet divergences of the form $\ln^2(\epsilon)$ at two loops. Since ϵ has dimensions of length, logarithms of it must come in the form $\ln(\epsilon u^{-1})$ and $\ln(H\epsilon)$. We showed in sub-section 2.7 that only a single factor of $\ln(H)$ can occur, so there must be at least one $\ln(u)$, and we can think of no reason why two should not occur. The reason why these infrared logarithms act to slow inflation is that they represent the negative gravitational interaction energy between the zero point motions of gravitons. At the risk of putting too much faith in gauge-dependent results one can even understand that pure graviton diagrams should act to slow inflation, and that the ghost diagrams should diminish this effect.*

There is also a good physical interpretation for infrared logarithms. The up to two powers of $\ln(Hu)$ that derive from integrating factors of u'^{-1} and u''^{-1} represent the invariant volume of the past lightcone as viewed from the observation point [2]. The single $\ln(Hu)$ which can come from an undifferentiated propagator logarithm represents the ever-increasing correlation of the free graviton vacuum in an inflating universe. It has long been known that the assumption of correlated de Sitter vacuum over an infinite surface of simultaneity leads to a divergence in the propagator. (This was first proved by Allen

* The near cancellation between the two classes is perhaps explicable from the fact that the gauge fixed graviton field carries eight unphysical modes and only two physical ones. At two loops this means roughly $10^2 = 100$ mode pairs of which the ghost loops must remove all but $2^2 = 4$.

and Folacci [18]. See also [7] and the references cited therein.) Infrared logarithms are the causal manifestation of this effect when one approaches an infinite surface of simultaneity by inflating a finite patch of correlated de Sitter vacuum.

In sum, the procedure we used should work, it gives a reasonable result, and every care has been taken to ensure accuracy. However, we do not wish this discussion to convey a false sense of infallibility. We have been schooled in humility by the disconcerting experience of detecting errors even after the final one seemed to have been expunged. It must be stressed that this was an enormously complicated piece of work. Only one other two-loop result has ever been obtained in quantum gravity [19], and it was confined to the ultraviolet divergent part of the on-shell effective action for zero cosmological constant. We feel very strongly that computer calculations on this scale should be regarded as experiments whose results require independent verification before they can be completely trusted. We would be happy to cooperate with anyone wishing to undertake even a partial check.

We conclude by briefly discussing a perturbative issue which demands further study: the case of a negative cosmological constant. This is interesting in its own right and because it may have relevance to the period after rapid inflation has ended, when an energetically favored phase transition would be expected to generate a negative effective cosmological constant. Two qualitative questions are of great importance: are there strong infrared effects from quantum gravity? and, do they tend to resist the contraction of spacetime?

Careful consideration of the effect for positive cosmological constant leads to the conclusion that it derives from the combination of three features:

- (1) Propagators which do not oscillate or fall off over large temporal separations;
- (2) An interaction of dimension three;
- (3) The fact that the invariant volume of the past lightcone increases without bound.

The last two are certainly true as well for a negative cosmological constant. In fact the

causal structure of anti-de Sitter space allows one to access spatial infinity after only a finite amount of time. The non-trivial issue is the propagator. The usual prescription for defining what happens at spatial infinity is to impose reflective boundary conditions [20]. These are enforced mathematically by a negative image source at the antipodal point, so they make propagators fall off too rapidly to give a big infrared effect.

We believe that reflective boundary conditions are reasonable for Euclidean anti-de Sitter space because its antipodal points are not part of the manifold. However, the antipodal points of the Minkowski signature formalism are on the manifold. In this case the use of reflective boundary conditions implies the physical absurdity that every source of stress energy has an antipodal anti-source. It is not reasonable to suppose a man is forbidden to shake his fist (which generates gravitational radiation) without the cooperation of someone of the other side of the Universe.

The more sensible boundary conditions seem to be transmissive, in which information is allowed to flow to spatial infinity without hindrance. These do not lead to a globally well-posed initial value problem, but they do make physical sense locally. The propagator associated with this condition does not fall off rapidly enough to preclude a large infrared effect. It should also be noted that arguments in the literature about the stability of supergravity or superstrings on an anti de Sitter background are based on reflective boundary conditions.*

It is very much more difficult to determine whether quantum gravity makes a negative Λ universe collapse slower or faster. Local considerations compel us to the view that gravitational interaction energy should still be negative. However, the fact that the sign of the dimension three coupling changes makes it hard to say what this does. (Note that the 1-point function is odd in the 3-point vertex.) An additional complication is that we can no longer count on the induced stress tensor to be that of pure vacuum energy. That

* We are indebted to I. Antoniadis for bringing this point to our attention.

it came out this way for the case of positive cosmological constant derives from the finite causal horizon of de Sitter space, which means that the gravitational interaction energy density must be independent of the true volume. This is not true for anti-de Sitter space. And it is worth recalling that inflation is driven by the negative pressure of a positive cosmological constant; the positive energy density serves as a drag on expansion. So it is conceivable that negative Λ quantum gravity induces a negative energy density, while still resisting contraction by virtue of generating less than an equal and opposite pressure.

ACKNOWLEDGEMENTS

We wish to give special thanks to T. J. M. Zouros for the use of his SUN SPARC station, and to S. Deser for his encouragement and support during this project. We have profited from conversations with I. Antoniadis, C. Bachas and J. Iliopoulos. One of us (RPW) thanks the University of Crete and the Theory Group of FO.R.T.H. for their hospitality during the execution of this project. This work was partially supported by DOE contract 86-ER40272, by NSF grant 94092715 and by EEC grant 933582.

REFERENCES

- [1] N. C. Tsamis and R. P. Woodard, *Phys. Lett.* **B1993** (1993) 351.
- [2] N. C. Tsamis and R. P. Woodard, *Ann. Phys.* **238** (1995) 1.
- [3] S. Deser and L. F. Abbott, *Nucl. Phys.* **B195** (1982) 76.
P. Ginsparg and M. J. Perry, *Nucl. Phys.* **B222** (1983) 245.
- [4] N. C. Tsamis and R. P. Woodard, *Nucl. Phys.* **B474** (1996) 235.
- [5] N. C. Tsamis and R. P. Woodard, *Commun. Math. Phys.* **162** (1994) 217.
- [6] N. C. Tsamis and R. P. Woodard, *Phys. Lett.* **B269** (1992) 269.
- [7] N. C. Tsamis and R. P. Woodard, *Class. Quantum Grav.* **11** (1994) 2969
- [8] J. Schwinger, *J. Math. Phys.* **2** (1961) 407; *Particles, Sources and Fields* (Addison-Wesley, Reading, MA, 1970).
- [9] L. H. Ford, *Phys. Rev.* **D31** (1985) 710.
- [10] A. D. Dolgov, M. B. Einhorn and V. I. Zakharov, *Phys. Rev.* **D52** (1995) 717.
- [11] B. S. DeWitt, *Phys. Rev.* **162** (1967) 1239.
F. A. Berends and R. Gastmans, *Nucl. Phys.* **B88** (1975) 99.
- [12] S. Wolfram, *Mathematica, 2nd edition* (Addison-Wesley, Redwood City, CA, 1991).
- [13] R. Mertig, *Guide to FeynCalc 1.0*, University of Würzburg preprint, March 1992.
- [14] I. S. Gradshteyn and I. M. Ryzhik, *Table of Integrals, Series, and Products, 4th edition* (Academic Press, New York, 1965) pp. 1075 – 1076.
- [15] N. C. Tsamis and R. P. Woodard, *Phys. Rev.* **D15** (1996) 2621.
- [16] D. M. Capper, *J. Phys.* **A13** (1980) 199.
- [17] S. Deser and P. van Nieuwenhuizen, *Phys. Rev.* **D10** (1974) 401.

- [18] B. Allen and A. Folacci, *J. Math. Phys.* **32** (1991) 2828.
- [19] M. Goroff and A. Sagnotti, *Phys. Lett.* **B160** (1986) 81; *Nucl. Phys.* **B266** (1986) 709.
- [20] S. J. Avis, C. J. Isham and D. Storey, *Phys. Rev.* **D18** (1978) 3565.